GENE EXPRESSION ANALYSIS OF SQUAMOUS CELL CARCINOMA OF THE OESOPHAGUS USING A NOVEL REAL TIME PCR PROBE SYSTEM

BY

NEELAM MALIK

A dissertation submitted in partial fulfilment of the requirements for the degree of

MASTER OF MEDICAL SCIENCE

Pfizer Molecular Biology Research Facility
Nelson R Mandela School of Medicine
University of KwaZulu-Natal
Durban
South Africa

This thesis is dedicated to:

My father, Razak. A great man, whose love continues to reach us despite his absence.

Zohra, my wonderful mother, for her unwavering support, love and sacrifice.

DECLARATION

The experimental work presented in this thesis represents the original work of the author and has not been submitted to any other university. Where use was made of the work of others, it has been duly acknowledged in the text.

The research described in this study was carried out at the Pfizer Molecular Biology Research Facility, Nelson R. Mandela School of Medicine, University of KwaZulu-Natal, Durban, South Africa, with supervision by Professor R.J. Pegoraro of the Medicine Research Laboratory and Professor P.K. Ramdial of the Department of Anatomical Pathology.

Neelam Malik

June 2008

Professor R.J. Pegoraro
(Supervisor)

Professor P.K. Ramdial
(Co-supervisor)

ACKNOWLEDGEMENTS

I would like to thank the following people:

Professor W.A. Sturm, Professor R.J. Pegoraro, Professor P.K. Ramdial and Professor P. Moodley for their encouragement, invaluable advice, compassion, patience and help through trying and difficult times. Thank you for your kindness.

Tonya Esterhuizen for her help with statistics, Siva Danaviah for the use of her equipment, Michelle Tarin for her help with the bioinformatics and Salem Karwa for his help with histopathology.

I would especially like to convey my heartfelt gratitude to the following people:

My sister and brothers- Naazneen, Nadeem and Nawaaz**,** for their endless love that helped me through the challenges I faced.

My family- Naila and Muhammad**,** who have given me so much love, care and support so that I never felt alone. Shireen, Shabir, Waadabapu, Amina masi, Sameer and Shakil for their encouragement, love and advice.

My dearest friends for their love, laughter, tears, support and strength:

Mark, Raves, Zack, Tipsy, Saz, Candice, Sally, Marta, Suj, Shams, Max and Mantha.

ETHICAL APPROVAL

Ethical approval was granted for this study by the Biomedical Research Ethics Committee, University of KwaZulu-Natal (UKZN), Durban, South Africa. Reference: H147/04.

ABSTRACT

Squamous cell carcinoma of the oesophagus (OSCC) is a common malignancy that occurs with high frequency in certain parts of the world, including South Africa. The aetiology of OSCC has remained unclear although many studies suggest that it is caused by a combination of variable risk factors. Recent reports implicate a variety of genetic factors in the carcinogenesis of OSCC but their involvement is yet to be defined.

The aim of this study was to examine in oesophageal tumour samples, the relative expression of the genes for vascular endothelial growth factor (*VEGF),* human epidermal growth factor receptor 1 and 2 *(HER1* and *HER2)* and matrix metalloproteinase 2 (*MMP2*), all of which have been implicated in carcinogenesis.

A novel universal probe library (UPL) system and real time PCR technology was used to detect gene expression. The relative expression of the four genes was standardized using the gene for a non-regulated reference protein, glyceraldehyde-3-phosphate dehydrogenase (GAPDH). The UPL detection system with real time PCR was compared to the conventional SYBR Green I system, based on *VEGF* expression. Quantification of real time PCR was evaluated by two methods, namely the standard curve method and the Pfaffl model, which is based on PCR efficiencies. Two groups of patients were analysed in this study following a retrospective histological assessment of sampling methods, which demonstrated the discordant classification of eight sample pairs. Group A comprised the original 30 patient cohort while Group B comprised the resulting 22 patient cohort after the removal of discordant sample pairs.

Evaluation of mRNA gene expression using the standard curve method combined with either the UPL system or the SYBR Green I system deduced that all four genes studied were upregulated in oesophageal tumours. Upregulation of *VEGF* in sample groups A and B was by factors of 3.6 (A) and 4 (B) using the UPL system, and by factors of 3 (A; $p = 0.001$) and 4 (B; $p = 0.001$) using SYBR Green I. The *HER1* gene was upregulated by a factor of 2.9 in both A and B groups ($p = 0.003$), the *HER2* gene by factors of 2.6 (A) and 1.9 (B), and the *MMP2* gene by a factor of 1.7 (both A and B), all using the UPL system. Assessment using the Pfaffl model combined with either the UPL or SYBR Green I system showed upregulation of all genes by the following factors: 2.8 in group A ($p = 0.001$) and 3.4 in group B ($p = 0.001$) for *VEGF* (UPL), 4.8 (A) and 6.6 (B) for *VEGF* (SYBR Green I), 3.2 (A; $p = 0.001$) and 4.0 (B) for *HER1* (UPL), 3.6 (A; $p = 0.001$) and 4.0 (B) for *HER2* (UPL), and finally 1.4 (A; $p = 0.001$) and 1.1 (B; $p = 0.001$) for *MMP2* (UPL).

Correlation analyses of mRNA expression of the *VEGF*, *HER1* and *MMP2* genes in oesophageal tumours showed strong gene inter-relationship associations: 79.8% for *VEGF* and *MMP2*, 86.4% for *HER1* and *VEGF*, and 88.8% for *HER1* and *MMP2*. With respect to clinical features, overexpression of *VEGF* was related to gender (group A, $p = 0.012$; group B, $p = 0.044$) and race ($p = 0.044$), as well as an increased depth of tumour invasion ($p = 0.046$). Overexpression of *HER2* was also related to race ($p = 0.015$), while overexpression of the *MMP2* gene was related to patients that did not have lymphatic node metastasis ($p = 0.030$). Furthermore, a larger tumour size was associated with an increased mitotic rate ($p = 0.043$) and increased necrosis ($p = 0.043$). Anaplasia was

associated with an increased depth of tumour invasion ($p = 0.015$) while perineurial invasion was influenced by gender ($p = 0.041$).

It was concluded that the UPL system using real time PCR technology is a robust and reliable method for the detection of gene expression. The UPL system and SYBR Green I system demonstrated similar detection abilities, but the UPL system showed equal or better performance and specificity compared with the SYBR Green I system. The Pfaffl model was found to combine simple, precise ease of performance with the production of rapid and reliable results. The overexpression of *VEGF*, *HER1*, *HER2* and *MMP2* genes in oesophageal tumours implicates a possible role in both the tumourigenesis of OSCC and the pathophysiology of tumour growth and spread. The positive correlations between clinicopathological factors, such as gender and race, to gene expression suggest a multi-factorial aetiology of OSCC. Further large scale and in-depth gene expression studies, combined with clinicopathological analyses are necessary for a better understanding of OSCC carcinogenesis. The identification of prognostic biomarkers and novel therapeutic targets may ultimately lead to improved diagnosis, treatment and prognosis of OSCC.

TABLE OF CONTENTS

LIST OF TABLES

LIST OF FIGURES

LIST OF APPENDICES

ABBREVIATIONS

˚C	Degrees Centigrade
µg	Microgram
µl	Microlitre
AJCC	American Joint Committee on Cancer
APC	Adenomatous Polyposis Coli gene
AR	Amphiregulin
Bcl-2	B-cell Lymphoma 2
BLAST	Basic Local Alignment Search Tool
Bp	Base pairs
BRCA-1	*Breast Cancer gene-1*
CDKI	Cyclin Dependent Kinase Inhibitors
CDKs	Cyclin Dependent Kinases
cDNA	Complimentary DNA
CIS	Carcinoma In Situ
CP	Crossing Point
Ct	Cycle threshold
CT	Computer Tomography
CYP2E1	Cytochrome P4502E1
Da	Dalton
DEPC	Diethyl pyrocarbonate
DNA	Deoxyribonucliec acid
dNTPs	Deoxyribonucleotide triphosphate
E	PCR Efficiency
ECM	Extracellular Matrix
EGF	Epidermal Growth Factor
EGFR	Epidermal Growth Factor Receptor
G0	Gap phase 0
GAPDH	Glyceraldehyde-3-phosphate dehydrogenase
GST	Glutathione S-transferase
H&E	Hematoxylin and Eosin
HCL	Hydrogen Chloride
HER	Human Epidermal Growth Factor Receptor

HPF	High Power Fields
Hybprobes	Hybridisation probes
IALCH	Inkosi Albert Luthuli Central Hospital
KCL	Potassium Chloride
kDa	KiloDalton
KZN	KwaZulu-Natal
LNA	Locked Nucleic Acid
LNM	Lymph Node Metastasis
M	Mitosis
MAPK	Mitogen Activated Protein Kinase
$MgCl_2$	Magnesium Chloride
MMP2	Matrix Metalloproteinase 2
mmol/l	Millimoles per litre
MRC	Medical Research Council
mRNA	Messenger RNA
MRT	Magnetic Resonance Tomography
MW	Molecular Weight
NCBI	National Center for Biotechnology Information
ng	Nanogram
nm	Nanometer
Nmol/l	Nanomoles per litre
OSCC	Oesophageal Squamous Cell Carcinoma
PCR	Polymerase Chain reaction
PDGF	Platelet-Derived Growth Factor
PET	Positron Emission Tomography
PGF	Placenta Growth Factor
PNI	Perineurial Invasion
pT	Tumour stage
Rb	Retinoblastoma
RefSeq	Reference Sequence
REST©	Relative Expression Software Tool
RNA	Ribonucleic acid
rRNA	Ribosomal RNA
RTK	Receptor Tyrosine Kinase

S	Synthesis
TGF-α	Transforming Growth Factor alpha
TIMP	Tissue inhibitors of metalloproteinase
Tm	Melting temperature
TNM	Tumour node metastasis
UICC	Union Internationale Contre le Cancer
UPL	Universal Probe Library
UV	Ultraviolet
VEGF	Vascular Endothelial Growth Factor
VEGFR	Vascular Endothelial Growth Factor Receptor
VPF	Vascular Permeability Factor

Chapter 1: Literature review

1.1 Oesophageal cancer

Worldwide, oesophageal cancer is the eighth most common cancer and occurs as two main aetiologically unrelated subtypes, namely, oesophageal squamous cell carcinoma (OSCC) and adenocarcinoma (World Health Organisation, 1997). Adenocarcinoma is more common in developed countries and is primarily associated with gastric reflux and Barrett's oesophagus. In contrast, OSCC is generally more prevalent in developing countries and is associated mainly with smoking, alcohol consumption and other factors (World Health Organisation, 1997). Variations in the incidence and aetiological features of OSCC suggest that specific environmental, geographical and lifestyle risk factors may play an important role in the aetiology of OSCC.

1.1.1 Epidemiology and Trends

1.1.1.1 Geographical

The incidence of OSCC shows distinct variations in its geographical distribution. It occurs at very high frequencies in areas such as the Linxian district in China, parts of Iraq and Iran, particular regions in South Africa, South America, East and Central Africa (Lam, 2000; Yang, 1980; Sitas, 1992). Endemic regions for OSCC are those that display a high incidence of the disease relative to other parts of the world with as much as a 500-fold difference in incidence between these areas (Parkin et al., 1988).

Prior to the 1950s, OSCC was rarely reported in South Africa (Isaacson, 1982). Thereafter, studies reported an increase in the number of oesophageal cancer cases diagnosed in the Black population, including the Zulu people of the Natal region (now KwaZulu-Natal) (Dlamini and Bhoola, 2005; Higginson and Oettle, 1960; Isaacson, 1982; Schonland and Bradshaw, 1969). The Transkei region in South Africa is often seen as the epicenter of OSCC in Africa and has one of the highest incidences in the world (357.2 per 100,000 for people aged between 35 and 64) (Doll, 1969). The disease has now reached epidemic proportions in the Transkei and Ciskei regions of South Africa, presenting a serious health burden to the country (Sammon, 2007)**.** Oesophageal squamous cell carcinoma is predominantly diagnosed in urban populations of the western world, but in China, Iran and South Africa it is mainly found in the rural population suggesting evidence of a socio-economic bias in poorer countries (Rose, 1973). This may be due to dietary, lifestyle and environmental risk factors that are common to these subpopulations.

1.1.1.2 Race and Gender

Oesophageal squamous cell carcinoma demonstrates distinct ethnic variations, with Black populations having a higher incidence of the disease compared with Caucasians. Numerous cultural and lifestyle factors have been attributed to these differences but the underlying cause is not clear (Duranceau et al., 1998). Gender also impacts on the incidence of OSCC. Men have a higher incidence of the disease compared to women. The worldwide incidence, per 100,000 population, lies between 2.5 and 5.0 for men and 1.5 and 2.5 for women (Parkin et al., 1988). In South Africa, OSCC is the most commonly occurring cancer in Black males and the third most common in Black females (MRC, 2001).

1.1.2 Aetiology

The aetiology of oesophageal cancer remains unclear. Evidence suggests that OSCC has a multi-factorial aetiology arising from a combination of associated risk factors (Blot, 1994). These risk factors are briefly discussed below.

1.1.3 Risk factors

1.1.3.1 Tobacco

Tobacco is a well recognised oesophageal carcinogen when used in any form e.g. cigarettes, cigars, pipe tobacco, chewing tobacco and snuff. Tobacco is associated with non-endemic oesophageal cancer worldwide, with the risk increasing in proportion to use (Yu et al., 1988). In endemic areas of South Africa, such as KwaZulu-Natal (KZN) and Transkei, studies have shown a significant association of tobacco usage, both duration and amount, with OSCC (Bradshaw and Schonland, 1969; Sammon, 1992; van Rensburg et al., 1985). Cigarette smokers are also reported to have a 5-10 fold higher risk for oesophageal cancer compared to non-smokers (Blot and Mclaughlin, 1999). In the urban Black population of Soweto, South Africa, the relative risk of cigarette smoke for OSCC was found to be higher with the use of hand-rolled cigarettes in comparison to commercial cigarettes (Segal et al., 1988). With cessation of smoking, the risk of OSCC has been shown to decrease substantially within 5-10 years (Blot and Mclaughlin, 1999). Tobacco tars and cigarette smoke contain many chemical carcinogens including aromatic amines, haloethers, lactones, N-nitriso compounds, polycyclic aromatic hydrocarbons and peroxy compounds (Hoffman et al., 1976).

1.1.3.2 Alcohol

Excessive use of alcohol has been observed as an independent risk factor for OSCC, with the highest risk being associated with consumption of spirits rather than wine or beer (Blot and Mclaughlin, 1999; Tuyns et al., 1979). Alcohol causes chronic irritation and inflammation to the oesophageal mucosa (Enzinger and Mayer, 2003). Alcohol consumption and tobacco smoking have been shown to have a synergistic effect on the risk of oesophageal cancer. It has been suggested that alcohol acts as a solvent for the carcinogens in tobacco smoke, enhancing the risk of developing the disease (Crew and Neugut, 2004).

1.1.3.3 Diet and Nutrients

As mentioned previously, oesophageal cancer is a disease associated with lower socio-economic groups and it has been suggested that nutritional factors may play a role in the pathogenesis (Blot and Mclaughlin, 1999). Deficiencies in vitamins and trace minerals such as vitamin A, B_{12}, C, E, niacin, riboflavin, folic acid and zinc may increase the risk of OSCC, while diets rich in fresh fruit, raw vegetables and antioxidants are thought to be protective (Blot and Mclaughlin, 1999). Also, evidence suggests that a chronic low intake of micronutrients, together with an inadequate protein intake, increases the predisposition of the oesophageal epithelium to malignant transformation (Blot and Mclaughlin, 1999; Ribeiro et al., 1996). Throughout the world, in areas endemic for OSCC, maize and/or wheat comprise the dietary staples (van Rensburg, 1981). These diets are deficient in riboflavin, niacin, vitamin C and other micronutrients. Riboflavin deficiency has been implicated in the early stages of oesophageal cell proliferation and dysplasia (Muñoz et al., 1987).

Other dietary factors that are known risk factors for oesophageal cancer are salt pickled and salt cured foods such as pickled vegetables, smoked fish, cured meat and dried red chillies, all of which contain high concentrations of nitrosamines (Ribeiro et al, 1996). High doses of nitrosamines are known to be carcinogenic and extensive research in China has implicated nitrosamines and their precursors as probable aetiological factors in high incidence areas (Lu et al., 1991).

1.1.3.4 Fungal Mycotoxins

Fungi such as *Fusarium verticillioides, Aspergillus, Penicillium, Cladosporium, Alternaria* and *Geotrichum Spp* have been implicated as risk factors for OSCC as they have been shown to promote the formation of nitrosamines (Chang et al., 1992). Additionally, a molybdenum deficiency in the soil has been associated with an increased susceptibility of maize to a variety of fungal species such as *Fusarium* and *Aspergillus* (Chang et al., 1992). Epidemiologic studies in the high incidence regions of South Africa and China, have identified a strong association between the consumption of maize contaminated with *Fusarium* and the incidence of OSCC (Marasas, 2001; Yoshizawa et al., 1994).

1.1.3.5 Human Papilloma Virus

The human papilloma virus (HPV) has long been implicated as a risk factor for oesophageal cancer. *In vitro* and *in vivo* studies have confirmed the oncogenic properties of HPV types 16 and 18. The proteins E6 and E7 produced by these viruses are oncoproteins that have the capacity to immortalise various human cell types, inactivate host proteins (such as p53 or pRb), and induce mutations in the host cell DNA (Caldeira et al., 2000; Mantovani and Banks, 1999; zur Hausen, 1999).

Studies from high risk areas for OSCC have suggested a role of HPV in the aetiology of OSCC, whereas other studies from low risk areas have failed to find any association (Chang et al., 2000; Syrjänen, 2002).

1.1.3.6 Associated diseases

Several diseases such as the Plummer-Vinson syndrome, coeliac disease, scleroderma, tylosis, oesophageal diverticula and achalasia are thought to be risk factors for oesophageal cancer. Patients presenting with these conditions reportedly have a significantly increased risk of developing OSCC (Ferguson and Kingstone, 1996; Larsson et al., 1975; Marger and Marger, 1993; Whitaker and Bishop, 1979).

1.1.3.7 Genetic predisposition

Tylosis is the only recognised familial syndrome that predisposes individuals to OSCC. It is a rare autosomal dominant disorder which confers up to a 95% risk of OSCC by the age of 70 years (Marger and Marger, 1993). A higher risk of OSCC has however been observed among relatives of oesophageal cancer patients. This familial aggregation has been reported in several countries, including the high incidence regions in China (Chang-Claude et al., 1997). Ethnic differences in the frequency of OSCC suggest a genetic contribution but no specific genetic factor has yet been identified (Lam, 2000). Polymorphisms in several genes such as *glutathione S-transferase* (*GST*) and *cytochrome P450 2E1* (*CYP2E1*) have been associated with an increased risk for OSCC. The CYP2E1 protein is involved in the metabolic activation of nitrosamines, and genetic variations may therefore contribute to early carcinogenic events of OSCC (Lin et al., 1998).

1.1.4 The Oesophagus: Structure and Function

The oesophagus extends from the lower end of the pharynx to the stomach and is divided into three distinct anatomic portions: cervical, thoracic and abdominal (Damjanov and Linder, 1996). It crosses the thorax through the posterior part of the mediastinum, behind the trachea and left main bronchus, through the left crus of the diaphragm and into the stomach (Damjanov and Linder, 1996). Structurally, the oesophagus is a hollow, tubular organ which is in a collapsed state most of the time although it distends to allow the passage of food and saliva, swallowing or regurgitation. The entrance of oesophagus is bordered by the crico-pharyngeus muscle which acts as an upper oesophageal sphincter. This has a dual function, firstly to prevent regurgitation of gastric contents into the oesophagus and secondly to relax during swallowing to allow the passage of food (McGee et al., 1992). The lower oesophageal sphincter aids in the role of swallowing and is located at the abdominal oesophagus. There are four distinct layers forming the walls of the oesophagus: the mucosa, submucosa, muscularis propria and a peri-oesophageal fibrous layer (Figure 1.1) (McGee et al., 1992,). The four principal layers are further subdivided into eight layers according to varying cell types (Figure 1.1).

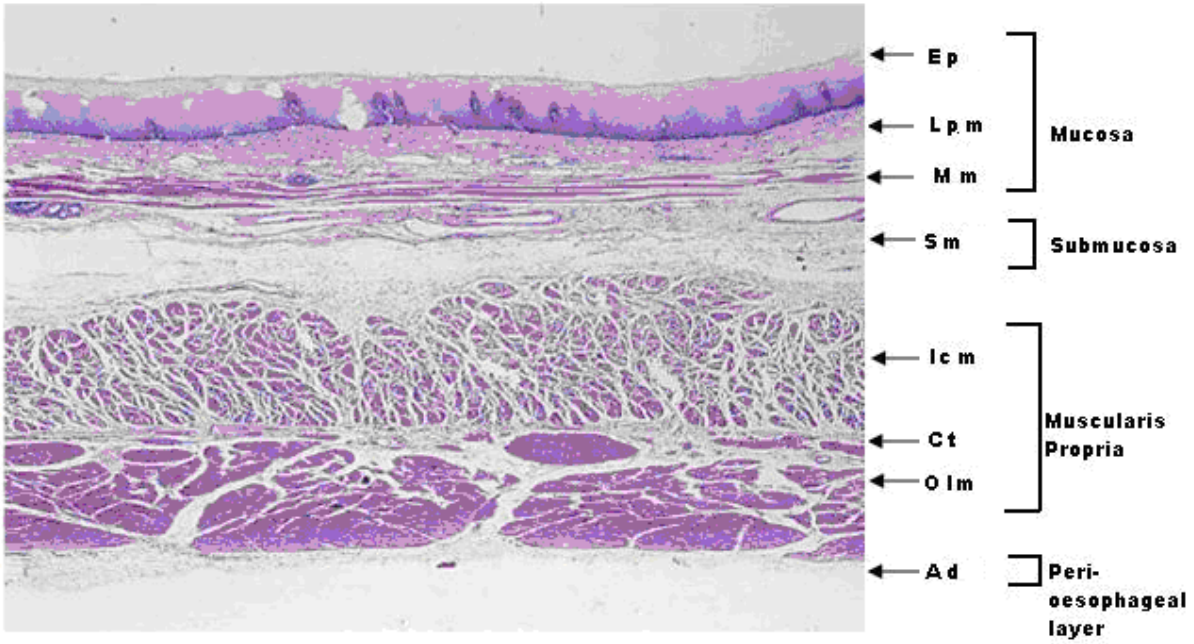

Figure 1.1 Histopathologic section of the normal oesophageal wall. Ep: epithelium, Lpm: lamina propria mucosae, Mm: muscularis mucosae, Sm: submucosa, MP: muscularis propria, Icm: inner circular muscle, Ct: intermuscular connective tissue, Olm: outer longitudinal muscle, Ad: adventitia layer. (Hematoxylin-Eosin (H&E) stain; original magnification, x 6.) Diagram modified from (Yamada et al., 2006).

The first layer of the oesophageal wall is the epithelium layer (mucosa) which consists of pale stratified non-keratinizing squamous epithelim. Below the epithelium is the lamina propria that comprises loose connective tissue and overlies the muscularis mucosae consisting of a thin bundle of smooth muscle fibres (Damjanov and Linder, 1996). The submucosa contains a network of lymphatics, lymphocytes and blood vessels as well as mucus producing glands that open into the lumen through excretory ducts (McGee et al., 1992).

The muscularis propria section consists of an inner circular and an outer longitudinal coat of smooth muscle, innervated by the vagus, glossopharyngeal nerve and sympathetic ganglia (McGee et al., 1992). The last layer of the oesophageal wall is the adventitia (serosa) that comprises loose connective tissue and blood vessels (Damjanov and Linder, 1996).

1.1.5 Pathophysiology

The majority of oesophageal tumours (>50%) arise in the middle third of the oesophagus, approximately a third occur in the lower oesophagus and the remainder appear in the upper oesophagus (Damjanov and Linder, 1996). Tumours are usually described as polyploid (60%), ulcerating (25%) or infiltrating (15%), although mixed patterns are common (Damjanov and Linder, 1996). Oesophageal tumours are categorised into four different types: superficial (type 0), protruding (type 1), ulcerative and localised (type 2), ulcerative and infiltrative (type 3) (Japanse Society for Esophageal Diseases, 1999) (Figure 1.2).

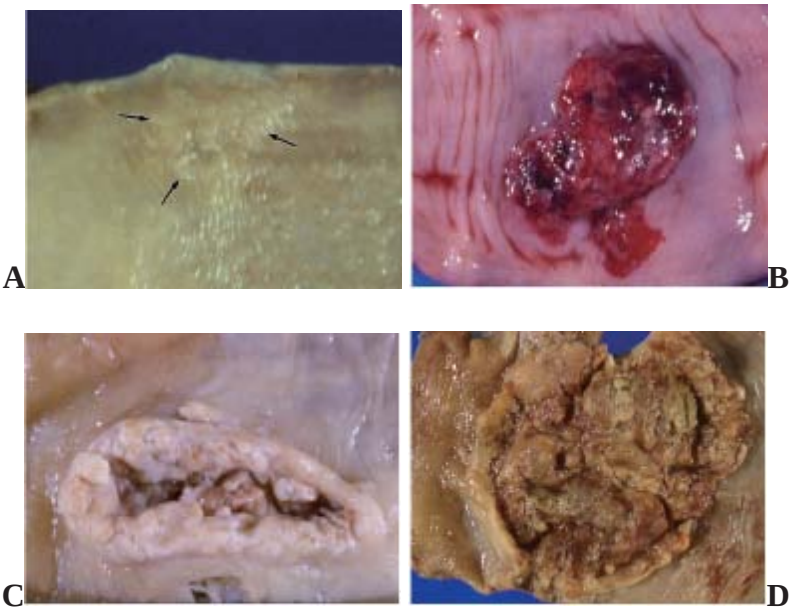

Figure 1.2. Macroscopic images in four different types of oesophageal carcinoma are shown (A-D). A: Superficial and flat type (type 0–IIa-IIc). Arrows show an irregular thickening. B: Protruding type (type 1). C: Ulcerative and localised type (type 2). D: Ulcerative and infiltrative type (type 3) (Yamada et al., 2006).

1.1.5.1 Differentiation of oesophageal tumours

Differentiation of oesophageal tumour cells refers to the extent of resemblance, both morphologically and functionally, to cells of the tissue of origin. In comparison to normal cells, tumour cells display marked irregularity in their nuclei. Some of these differences include: irregularity in shape or form (pleomorphism), larger nuclei, prominent irregular nucleoli and numerous mitoses and atypical mitoses (Kumar et al, 2003). Oesophageal tumours are also classified microscopically as well, moderately or poorly differentiated (Figure 1.3). Most tumours are moderately differentiated but some display advanced differentiation, forming whorls of tumour cells known as “keratin pearls” (Damjanov and Linder, 1996).

Well differentiated tumours contain abundant amounts of keratin, have easily observed intercellular bridges and cell layers undergoing differentiation, whereas poorly differentiated tumours have little or no keratin, intercellular bridges or differentiation of cell layers. Tumour cells also usually fail to develop recognisable patterns of orientation to each other, that is, they lose normal polarity and grow in sheets and loose normal structural patterns (Watanabe et al., 1990).

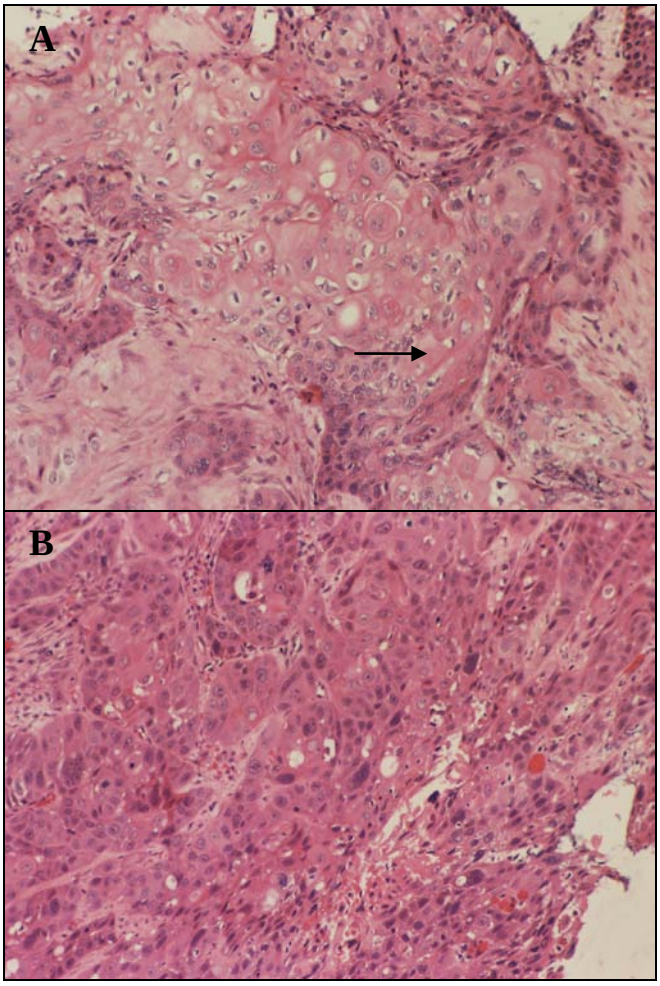

Figure 1.3. Photomicrographs of oesophageal tumours. **A.** Well differentiated squamous cell carcinoma of the oesophagus with large areas of pink staining keratin. Small epithelial pearls are visible (arrow) **B.** Poorly differentiated squamous cell carcinoma of the oesophagus comprising enlarged hyperchromatic nuclei and showing no visible keratin.

1.1.5.2 Early oesophageal squamous cell carcinoma

Oesophageal dysplasia is a precursor lesion of OSCC. It is typically encountered only in the epithelium and exhibits a loss of uniformity in individual cells, as well as a loss of architectural orientation. The presence of dysplasia in the squamous epithelium suggests potential for malignant transformation. Dysplastic cells may be seen in the mucosa adjacent to the tumour and display very similar characteristics to the cancerous cells with regards to pleiomorphism, hyperchromatic nuclei and frequent mitotic events. When dysplastic changes are marked and involve the entire thickness of the epithelium, the lesion is known as *'carcinoma in situ'*, a pre-invasive stage of cancer (Kumar et al, 2003). Dysplasia does not necessarily progress to cancer although mild, moderate and severe dysplasia may precede carcinoma or may be associated with growth at presentation (McGee et al., 1992). A follow up study of early asymptomatic patients with *in situ* carcinoma of the oesophagus revealed that 3-4 years elapsed before the development of OSCC (Guanrei et al., 1982).

1.1.5.3 Advanced oesophageal squamous cell carcinoma

Oesophageal cancers are characterised by widespread local growth and lymph node involvement before dissemination. Malignant neoplasms disseminate by one of three pathways: seeding within body cavities, lymphatic spread or haematogenous spread. The submucosal segment of the oesophageal wall is rich in lymphatics that extend longitudinally as well as laterally. Therefore submucosal spread of the tumour is common. The longitudinal network of lymphatics allows frequent spread to the nodes in the neck, thorax and abdomen despite tumour location. Once a tumour has invaded muscular layers of the oesophagus, the incidence of positive regional lymph nodes exceeds 75% (Greene et al., 2002).

Widespread distant metastases are almost always present at the time of death in patients with OSCC (Mandard et al., 1981). Studies have shown that the length of the oesophagus invaded by the carcinoma is directly correlated with the extent of involvement of adjacent structures and inversely related to prognosis (Merendino et al., 1952; Takagi and Karasawa, 1982).

1.1.6 Detection and Diagnosis

1.1.6.1 Clinical symptoms

Most oesophageal cancers do not cause symptoms until they have reached an advanced stage, resulting in late diagnosis of the disease and a poor prognosis. The principle symptom of oesophageal cancer is difficulty swallowing or dysphagia accompanied by weight loss (Enzinger and Mayer, 2003). Long-standing gastroesophageal reflux disease is often a nonspecific sign of OSCC (Nebel et al., 1976). Dyspnoea, cough, hoarseness and pain occur less frequently but may reflect the presence of extensive unresectable disease (Freitag et al., 1996). Lymphadenopathy, particularly in the left supraclavicular fossa (Virchows node), hepatomegaly and pleural effusion are all common signs of metastatic disease (Enzinger and Mayer, 2003).

1.1.6.2 Diagnostic investigations

Initial investigation comprises either an oesophagoscopy and incisional biopsy for confirmation of tumour and tumour subtype, or a barium swallow aimed at detecting either strictures or ulcerations of the oesophagus, or both (Enzinger and Mayer, 2003). Further pre-treatment evaluation is generally performed with a computer tomography (CT) scan, magnetic resonance tomography (MRT), or endoscopic ultrasound (EUS) to determine tumour extent.

The presence of distant metastases in the abdomen is determined by a CT scan or ultrasound or both (Stein et al., 2001). Positron-emission tomography (PET) has also been used to detect metastatic disease as it is less invasive than thoracoscopic or laparoscopic techniques (Enzinger and Mayer, 2003). Mass screening programs in high incidence areas, such as China, have helped in the early detection of OSCC. Early detection methods include abrasive brush cytology, occult blood bead detection and endoscopy in conjunction with Lugol iodine solution (Chen et al., 1999).

1.1.7 Staging

The union internationale contre le cancer (UICC) tumour-node-metastases (TNM) staging system is used to determine the extent of disease progression (Hermanek and Sobin, 1987). This system takes into account the characteristics of the primary tumour, regional node metastases and distant metastases (Table 1.1). Staging of the tumour is the key to diagnosis, appropriate treatment and determination of prognosis of OSCC.

Table 1.1 The TNM classification system for the staging of oesophageal cancer

Primary Tumour (T)	TX	Primary tumour cannot be assessed	
	T0	No evidence of primary tumour	
	Tis	Carcinoma in situ	
	T1	Tumour invasion of lamina propria or submucosa	
	T2	Tumour invasion of muscularis propria	
	T3	Tumour invasion of adventia	
	T4	Tumour invasion of adjacent structures	
Regional Lymph Node (N)	NX	Regional lymph nodes cannot be assessed	
	N0	No regional node metastasis	
	N1	Regional lymph node metastasis	
Distant Metastasis (M)	MX	Presence of distant metastasis cannot be assessed	
	M0	No distant metastasis	
	M1	Distant metastasis	
Stage Grouping			
Stage 0	Tis	N0	M0
Stage I	T1	N0	M0
Stage IIA	T2	N0	M0
	T3	N0	M0
Stage IIB	T1	N1	M0
	T2	N1	M0
Stage III	T3	N1	M0
	T4	Any N	M0
Stage IV	Any T	Any N	M1

1.1.8 Treatment and prognosis

Oesophageal carcinoma has one of the lowest rates of cure with overall 5-year survival rates of 10% (Holmes and Vaughan, 2006). Prognosis depends on the depth of tumour penetration of the oesophagus and the extent of lymph node metastases (Ellis et al., 1993). In the early stage disease (Stage I-II) surgical treatment with curative intent is offered to patients who are in good medical condition (Enzinger and Mayer, 2003). In patients with intra-epithelial cancer, the risk of lymph node metastasis is low and resection of the tumour by means of a complete or partial oesophagectomy carries a good prognosis (Sugimachi et al., 1993). The incidence of perioperative complications such as infections, anastomosis leakage, and pulmonary complications is however high (26-41%) (Enzinger and Mayer, 2003). In tumours that have invaded the submucosa, the incidence of lymph node metastasis is as high as 60%, indicating a poor prognosis (Kato et al., 1993).

At the time of diagnosis of oesophageal cancer, more than 50 percent of patients have either unresectable tumours or radiographically visible metastases, and an expected survival time of less than one year. Management methods for advanced disease include palliative resection, radiotherapy, brachytherapy, chemotherapeutic drugs, and dilatation techniques for maintaining the oesophageal lumen (Enzinger and Mayer, 2003). In an attempt to improve survival rates, combined treatment modalities including radiotherapy and chemotherapy together with surgery have been investigated in several randomised clinical trials. Although these studies of new combination chemotherapeutics have reported higher response rates, the survival rates for patients with advanced disease remain unchanged (Bleiberg et al., 1997).

1.2 Carcinogenesis

Knowledge of the molecular basis of cancer aetiology and progression may lead to a clearer understanding of oesophageal cancer. The transformation of a cell from a normal state to a malignant one is known as carcinogenesis. This process can be divided into three different phases: initiation, promotion and progression. Initiation involves an irreversible genetic change, usually a mutation in a single gene. Promotion is the increased proliferation of initiated cells while progression is the subsequent accumulation of a further sequential series of genetic mutations or alterations that produce the malignant phenotype (Martinez et al., 2003). Each of these genetic alterations is thought to provide the developing tumour cell with significant growth advantages that allow tumour cells to outnumber normal neighbouring cells (Nowell, 1976).

Three classes of normal regulatory genes are the principle targets of genetic damage. These are growth promoting proto-oncogenes, growth-inhibiting tumour suppressor genes (anti-oncogenes), and genes that regulate programmed cell death or apoptosis (Martinez et al., 2003). Proto-oncogenes that have undergone mutational damage are known as oncogenes. These genes are capable of transforming cells despite the presence of a normal chromosomal counterpart, that is, they are dominant in nature. In contrast, tumour suppressor genes are recessive in nature as both normal alleles must be affected for transformation to occur (Martinez et al., 2003). The DNA repair genes are another class of genes that are important in carcinogenesis. These genes affect cell survival and proliferation as they have the capability to repair non-lethal damage to DNA. Loss of function of DNA repair genes as a result of mutational changes, leads to widespread mutations in the genome and neoplastic transformation.

The complexity of the wide variety of different cancer types, together with the broad and diverse range of cancer associated genes, confounds the exact cause underlying the process of carcinogenesis. It has been suggested that the majority of cancer cell genotypes result in six essential alterations in cell physiology that lead to malignant growth, namely,

1. Self sufficiency in growth signals
2. Insensitivity to growth inhibitory signals
3. Evasion of apoptosis
4. Limitless replicative potential
5. Sustained angiogenesis
6. Tissue invasion and metastasis

Mutations or altered functions in the genes that regulate these cellular traits are seen in most cancers, although the precise genetic events that give rise to these properties may differ between cancers (Hanahan and Weinberg, 2000).

1.2.1 Mutations

The types of mutations or genetic alterations that can occur in carcinogenesis include point mutations, frame-shift mutations, chromosomal imbalance or instability, chromosomal translocations or rearrangements and epigenetic modifications to DNA (Bertram, 2001). Spontaneous mutations are a frequent event due to the inherent instability of DNA and arise either as a consequence of errors in replication or direct damage to DNA.

Most mutations are overcome by DNA repair genes (Bertram, 2001). The protein products of these genes survey the genome for damage and then restore the damaged sequence, protecting against immediate and long term effects of excessive mutational rates.

Defects in these repair processes result in an increase in the rate of mutation and consequently the rate of neoplastic progression. Both chemical and physical agents that cause damage to DNA are known as environmental carcinogens. These include chemical carcinogens such as polycyclic aromatic hydrocarbons, dimethylnitrosamine, N-nitrosamines, and chemotherapeutic agents and physical agents such as ionising and ultraviolet radiation. Chemical damage to DNA alone is not a mutagenic event. It is DNA replication and consequent cell division that converts chemical damage to a reproducible change in DNA. Abnormal cellular proliferation is a major factor in the development of tumours despite numerous checkpoints in normal cellular processes designed to restrict uncontrolled growth. Malignant cells must acquire several mutations in key genes to maintain autonomous replication and invasion (Bertram, 2001).

1.2.2 Epigenetic changes

The normal functioning of genes can also be disrupted through genetic alterations which modify the expression of the gene (Martinez et al., 2003). These epigenetic mechanisms, such as DNA methylation, can result in gene silencing, early loss of cell cycle control, altered regulation of gene transcription factors and multiple types of genetic instability all of which are characteristic of neoplasia. Hypermethylated genes implicated in human cancers include tumour suppressor genes that cause familial forms of cancer when mutated in the germline e.g *adenomatous polyposis coli gene (APC), breast cancer gene (BRCA-1)* and *epithelial cadherin gene (E-cadherin)* (Martinez et al., 2003).

1.2.3 Telomeres

Most normal human cells have a turnover capacity of 50 to 100 generations after which replicative senescence occurs. This is the result of progressive shortening of telomeres at the ends of chromosomes which leads to chromosome abnormalities and cell death. In contrast, most tumour cells are capable of unlimited replication by avoiding cellular senescence. Massive proliferation is required for the progression of carcinogenesis and 85-95% of cancers, including oesophageal tumours, have been shown to reactivate telomerase in order to retain telomere length (Bertram, 2001).

1.2.4 Cell cycle

The cell cycle directs cellular proliferation. It consists of a series of checks and balances that monitor nutritional status, cell size, the presence or absence of growth factors and the integrity of the genome. Cell division consists of four stages namely, gap phase 1 (G1), synthesis (S), gap phase 2 (G2) and mitosis (M). Resting cells are said to be in the gap phase 0 (G0). DNA is replicated during the S phase and chromosome segregation takes place during the M phase. Once cells enter the replicative stages they are committed to complete cell division. Exit from the G1 stage and entry into the S stage is stringently controlled in normal cells but often misregulated in tumour cells that exhibit uncontrolled proliferation. Amongst key genes orchestrating the cell cycle are *cyclins*, *cyclin-dependent kinases (CDKs)* and *cyclin-dependent kinase inhibitors (CDKIs)*. Mutations that dysregulate the activity of these genes appear to favour cell proliferation and are a frequent event in neoplastic transformation (Martinez et al., 2003).

1.2.5 Apoptosis

The ability of tumour cell populations to increase in number is determined by both the rate of cell proliferation and the rate of cell attrition. Programmed cell death, or apoptosis, is genetically controlled and essential for processes such as embryogenesis and maintenance of cellular homeostatic balance. The apoptotic pathway is regulated by sensors and effectors. Sensors monitor the intracellular and extracellular environment for conditions that influence the fate of the cell. Signals by sensors evoke effectors that are either survival or death factors (Hanahan and Weinberg, 2000). Factors such as DNA damage, signaling imbalance provoked by oncogene action, survival factor insufficiency or hypoxia cause sensors to evoke the death pathway (Evan and Littlewood, 1998). Acquired resistance towards apoptosis or the ability to evade apoptosis are characteristics of many types of cancer. Enabling strategies include overexpression of the *Bcl-2* oncogene, inhibition or mutations of the *Fas* receptor gene and mutations of the *p53* gene (Hanahan and Weinberg, 2000).

1.2.6 Oncogenes

As mentioned previously, oncogenes are normal host cellular regulatory genes (proto-oncogenes) that have become dysregulated as a consequence of mutations or genetic alterations. They contribute to the carcinogenic process by the acceleration of cell proliferation or the reduction of sensitivity to cell death. To achieve this, oncogenes produce aberrantly functioning proteins which are able to activate growth signaling circuits even in the absence of normal growth promoting signals. This drives cellular proliferation beyond the levels of normal cellular growth (Weinberg, 1994).

The different types of oncogenes include growth factors, growth factor receptors, cytoplasmic tyrosine kinases, serine-threonine tyrosine kinases, nuclear proteins, cytoplasmic proteins and membrane-associated guanine nucleotide-binding proteins that influence cell survival (Martinez et al., 2003). For example, *human epidermal growth factor receptors-1 and -2* (*HER1, HER2*) are oncogenes that are activated by amplification mutations and are frequently associated with many different types of carcinoma, including OSCC as will be discussed in section 1.3.1.

1.2.7 Tumour suppressor genes

Cellular proliferation can be inhibited by the action of tumour suppressor genes. Direct inhibition of cell growth by these gene products is rate limiting (Martinez et al., 2003). Both normal alleles of tumour suppressor genes need to be functionally affected for tumours to develop. Mutations that inactivate only one allele are frequently inherited through the germline, and in combination with a somatic mutation on the other allele, can cause cancer predisposition syndromes. For example, multiple mutations in the *p53* tumour suppressor gene result in the Li-Fraumani syndrome (Bertram, 2001). The *retinoblastoma (Rb)* and *p53* genes are well documented examples of tumour suppressor genes. The *Rb* gene regulates the entry of cells into the cell cycle. Loss of *Rb* function causes the deregulation of the cell cycle resulting in uncontrolled cell proliferation and ultimately tumour formation. Homozygous mutations in the *Rb* gene are frequently found in breast, lung and bladder cancers (Kumar et al., 2003). In oesophageal cancer, alterations in the *Rb* gene have been reported in some tumours (Jiang et al., 1993; Roncalli et al., 1998).

The *p53* tumour suppressor gene directs the cell towards an appropriate response, cell cycle arrest or apoptosis, in order to maintain genomic stability. When DNA damage occurs, the p53 protein detects and contributes to DNA repair by causing cell cycle arrest and inducing DNA repair genes. Cells with irreparable DNA are bound for apoptosis directed by the *p53* gene. When there is homozygous loss of *p53* function, DNA damage remains unrepaired, leading to malignant transformation (Bertram, 2001). Over 70% of human cancers have defects in the function of the *p53* gene (Levine, 1997). The prevalence of *p53* aberrations in oesophageal cancer ranges from 10 to 85% (Lam et al., 1995). Immunohistochemical studies carried out in South Africa indicated that *p53* is overexpressed in approximately 40-50% of oesophageal cancer tumours (Chetty and Simelane, 1999; van Heerden et al., 1998).

1.3 Oesophageal cancer-related genes

There are numerous genes implicated in carcinogenesis of the oesophagus. These include oncogenes, tumour suppressor genes, genes for apoptosis, growth factors, growth factor receptors, cell cycle regulators and signal transducers (Lam et al., 1995; Lam, 2000). The present study focuses on the expression of four genes that are implicated in oesophageal carcinogenesis. These include the genes for *human epidermal growth factor receptors-1 and -2* (*HER1* and *HER2*), *vascular endothelial growth factor* (*VEGF*) and *matrix metalloproteinase 2* (*MMP2*).

1.3.1 Human epidermal growth factor receptor-1 and -2

Human epidermal growth factor receptor-1 (HER1), also known as epidermal growth factor receptor (EGFR) or ErbB-1 and human epidermal growth factor receptor-2 *(HER2)* also known as ErbB-2 or Neu, belong to the HER family of receptor tyrosine kinases (RTK) (Yarden, 2001). Ancestral forms of the HER molecule that exhibit tyrosine kinase activity are found in invertebrates and in simple life forms such as the worm *Caenorhabditis elegans* and the fruit fly *Drosophila melanogaster* (Yarden, 2001). This family of receptor tyrosine kinases regulates a variety of signal transduction cascades that modulate growth, differentiation, cell motility and survival. The aberrant activity of members of this receptor family is a vital feature in the development and growth of tumour cells (Yarden, 2001).

1.3.1.1 Structure of the HER Family

The HER family consists of four closely related growth factor receptors: HER1, HER2, HER3, and HER4 (Yarden, 2001). Each of these receptors has an extracellular ligand-binding domain, a single hydrophobic transmembrane domain and a cytoplasmic tyrosine kinase containing domain (Olayioye et al., 2000). The intracellular tyrosine kinase domain of the HER receptors are highly conserved, with the exception of HER3 which contains substitutions of vital amino acids and hence lacks kinase activity (Guy et al., 1994). The extracellular domains of the four receptors are less conserved implying that they have different specificities in ligand binding (Olayioye et al., 2000). The HER2 receptor is encoded by the *HER2* gene, a proto-oncogene mapped to chromosome 17q21. It is a 1255 amino acid, 185kD transmembrane glycoprotein (Coussens et al., 1985). The *HER1* gene is located on chromosome 7p12 and encodes the HER1 receptor which is a 170kD cell surface glycoprotein consisting of 1186 amino acids (Arteaga, 2001).

1.3.1.2 Ligands of HER receptors

Human epidermal growth factor receptors are activated by binding to the ligands within epidermal growth factor (EGF) family. These ligands consist of a characteristic EGF-like domain that confers binding specificity and extra structural motifs such as immunoglobulin-like domains, heparin-binding sites and glycosylation sites (Normanno et al., 2005). Ligand binding to HERs results in the formation of receptor homo- or hetero-dimerisation, tyrosine kinase activation and initiation of signaling cascades. Receptor dimerisation is essential because it allows a signaling network to transmit a diverse array of biological messages (Olayioye et al, 2000).

The HER1 receptor binds to several ligands. These include EGF, transforming growth factor α (TGF-α), amphiregulin (AR), betacellulin (BTC), heparin-binding growth factor (HB-EGF) and epiregulin (EPR) (Carraway et al., 1997; Chang et al., 1997; Zhang et al., 1997). None of the EGF family of peptides binds HER2 (Normanno et al., 2005). HER2 has a greater capacity for heterodimerisation due to its structure and conformation and is the preferred dimerisation partner for all other HER receptors (Graus-Porta et al., 1997; Tzahar et al., 1996). The HER2 containing heterodimers are the most effective complexes, increasing biological responses such as cellular proliferation, migration and invasion. The combination of HER2/HER3 is the most potent signaling molecule and is often seen in carcinoma cells (Citri et al., 2003).

1.3.1.3 Biological function of the HER family

The HER family of growth factor receptors forms part of an intricate signal transduction network which is central to important cellular processes such as cell proliferation, migration, survival and adhesion. The type and duration of signal transduction pathways activated by HERs depend on the identity of the ligand, constitution of the receptor complex, and structural determinants of the ligands. For example, the ras/raf/MEK/mitogen-activated protein kinase (MAPK) which drives cellular proliferation, and the phosphoatidylinositol 3-kinase /Akt pathway which regulates cellular survival and anti-apoptotic signals, are both activated by all HER ligands (Citri et al., 2003). The HERs also interact with integrins which mediate cell-cell adhesion, cell-matrix association, intracellular signaling and cell migration, as well as activating many transcription factors, such as c-fos and c-myc (Olayioye et al., 2000; Sieg et al., 2000). All the intracellular signaling pathways activated through HERs occur in the nucleus where cell cycle regulators and transcription factors control the biological outcome of HER activation (Normanno et al., 2005). Several negative regulatory pathways exist which attenuate signaling through HERs in order to maintain suitable signal regulation for normal development. In humans, the main signal attenuation is through the downregulation of surface receptor levels by a procedure known as “ligand-induced endocytosis” (Carpenter, 2000). During signal termination, ligand-receptor complexes are internalised through the plasma membrane and then either degraded or recycled to the cell surface (Prenzel et al., 2001).

1.3.1.4 Role of HERs in carcinogenesis

The HER system is associated with many human cancers. The dysregulation of signaling pathways induced through these receptors stimulates characteristic processes typical of cancer cells such as, proliferation, migration, angiogenesis, stromal invasion and resistance to apoptosis (Klapper et al., 2000). Hyperactivation of the HER network occurs in an autocrine or paracrine manner. Tumour cells overproduce growth factors and their receptors by using autocrine secretory loops or depend on adjacent stromal cells to provide HER ligands (Salomon et al., 1995). Evidence suggests that overexpression of both HER1 and HER2 in a ligand-dependent manner, is a contributing factor in carcinogenesis (Frederick et al., 2000). Aberrant growth of cells can also occur through constitutive receptor activation, that is, the activation of a growth factor receptor in the absence of a ligand (Lonardo et al., 1990). EGFRvIII is a common HER1 mutant that stimulates cellular proliferation in the absence of ligands (Ekstrand et al., 1994). It is frequently found in malignant gliomas, breast carcinomas, non-small-cell lung carcinomas and ovarian carcinomas (Garcia de Palazzo et al., 1993; Moscatello et al., 1995; Moscatello et al., 1996; Wikstrand et al., 1995).

Gene amplification, overexpression, re-arrangements or mutations of *HER1* and *HER2* are found in many human malignancies. It has been reported that cancers with high expression of either *HER1* or *HER2* have a better prognosis than cancers that have a high expression of both receptors (Iwase et al., 1997; Xia et al, 1999). In a study by Brabender and colleagues (2001), co-expression of *HER1* and *HER2* was a better predictor for treatment failure and poor survival than *HER1* expression alone in patients with non-small cell lung carcinoma (NSCLC) (Brabender et al., 2001).

Several studies have investigated the use of *HER2* expression to predict clinical behaviour in breast cancer patients. It was reported that *HER2* gene amplification and/or protein overexpression in node positive breast cancer patients was predictive of a poor outcome, independently of other prognostic indicators. In contrast, HER2 expression in node negative patients was less informative (Gullick, 1990; Ravdin and Chamness, 1995). Due to the frequent overexpression and high signaling potential, *HER1* and *HER2* are promising therapeutic targets in human cancer. One of the most successful examples is the development of the monoclonal antibody, Herceptin (Trastuzumab), which recognises the extracellular domain of HER2 and was one of the first target-selective drugs raised against the oncogenic cell-surface receptor (Fendly et al., 1990). Clinical studies have shown Herceptin to be well tolerated in women with metastatic breast cancer overexpressing HER2 and to produce durable objective responses (Baselga et al., 1996; Cobleigh et al., 1999).

Overexpression of *HER1*, ranging from 2 to 100 fold, is a frequent genetic alteration in premalignant oesophageal dysplastic lesions and in the early stages of OSCC, and has been correlated with a poor prognosis (Hirai et al., 1998; Iihara et al., 1993; Inada et al., 1999; Lin et al., 1984). The overexpression of HER1 has also been associated with depth of invasion of the tumour, suggesting that it may play a role in the process of tumour infiltration (Hanawa et al., 2006). In a study by Andl and colleagues (2003), it was demonstrated that HER1 overexpression in OSCC was not sufficient to induce cancer but led to increased cell proliferation, migration and aggregation. Amplification of the *HER1* gene was also reported in this study and suggested to occur in the early stages of carcinogenesis (Andl et al., 2003).

With respect to *HER2*, overexpression has been reported in several studies on OSCC and has been associated with gene amplification and poor survival (Chiang et al., 1999; Dreilich et al., 2006; Kleef et al., 2002; Lam et al., 1998; Nakamura et al., 1994).

1.3.2 Vascular endothelial growth factor

Vascular endothelial growth factor (VEGF) is the most common growth factor observed at almost all sites of angiogenesis. In addition, levels of VEGF have been correlated with blood vessel growth (Robinson and Stringer, 2001). Angiogenesis is the process by which new blood vessels develop from pre-existing blood vessels and it impacts significantly on many disease states including cancer, ischaemic cardiovascular disease, wound healing and inflammation (Dvorak, 2002).

1.3.2.1 Identification of VEGF

VEGF was first identified as a vascular permeability-inducing factor secreted by tumour cells and was called vascular permeability factor (VPF) (Senger et al., 1983). It was thought to be a mediator of the high permeability of tumour blood vessels. Subsequently, a diffusible endothelial cell-specific mitogen known as vascular endothelial growth factor (VEGF) was discovered in bovine pituitary folliculo-stellate cells (Ferrara and Henzel, 1989; Plouët et al, 1989). Amino acid sequencing showed that this protein was distinct from any other known endothelial cell mitogen while cDNA cloning of VPF and VEGF demonstrated that VEGF and VPF were the same factor (Ferrara and Henzel 1989; Keck et al., 1989; Leung et al., 1989).

1.3.2.2 The *VEGF* gene and protein structure

The *VEGF* supergene family of growth factors include *VEGF*s A, B, C, D, E and placenta growth factor (PGF) (Dvorak, 2005). All have a structural homology to platelet-derived growth factor (PDGF) (Dvorak, 2002). The VEGF protein is a highly conserved disulphide-bonded homodimeric glycoprotein of 45 kD. The two chains that constitute VEGF form an anti-parallel homodimer covalently linked by two disulphide bridges (Muller et al., 1997). Each monomer is characterised by an intrachain disulphide bonded knot motif at one end of a four stranded β sheet. The principle element within the monomer is the cysteine knot motif (Muller et al., 1997). The VEGF-A protein is encoded by a single gene that is located on chromosome 6p21.3 (Vincenti et al., 1996). The coding region spans 14kb and contains eight exons. Alternative splicing of a single mRNA molecule can yield several different isoforms of VEGF-A that vary in length i.e. 121, 145, 165, 189 and 206 amino acids, and differ by the presence or absence of sequences located in exons 6 and 7 (Robinson and Stringer, 2001). Exon 8 is common to all isoforms (Tischer et al., 1991). The VEGF 165 is reported to be the predominant isoform. The information encoded by this alternative splicing determines whether VEGF is freely soluble or bound to the extracellular matrix or plasma membrane proteins, or has properties of both.

1.3.2.3 VEGF receptors

VEGF-A binds two related RTKs, namely VEGFR-1 (also called fms-like tyrosine kinase [Flt-1]) and VEGFR-2 (also referred to as kinase insert domain, [KDR] and murine homologue [Flk-1]). These two receptors share 44% homology and have a typical structure consisting of seven immunoglobulin-like domains, a single transmembrane domain, and a consensus tyrosine kinase domain interrupted by a kinase insert domain (Shibuya et al., 1990).

The VEGFR-1 is a high affinity receptor for VEGF-A, but also has the ability to bind to VEGF-B and PGF. Studies have reported that this receptor is essential for physiological and developmental angiogenesis, and is a potent positive regulator of angiogenesis during tumourigenesis (Peters et al., 1993; Fong et al., 1995; Hiratsuka et al., 2001). The VEGFR-2 is a high affinity receptor for VEGF-A as well as VEGF-C and D and also plays an important role in vasculogenesis (Robinson and Stringer, 2001). The VEGFR-3 (also called fms-like tyrosine kinase 4 [Flt-4]) binds to VEGF-C and VEGF-D but not VEGF-A, and has been mainly associated with lymphangiogenesis (Kaipainen et al., 1995).

1.3.2.4 Biological activities of VEGF-A

The VEGF-A together with the fibroblast growth factor (FGF) and activators of integrins, is one of the main stimulators of angiogenesis (Folkman, 2003). As mentioned previously, angiogenesis is essential for a wide range of fundamental physiological processes such as embryogenesis, somatic growth, wound healing, tissue and organ regeneration. Aberrant and uncontrolled proliferation of blood vessels is an important component of diseases such as cancer, rheumatoid arthritis, psoriasis, retrolental fibroplasias and retinopathies (Ferrara et al., 1992). The angiogenic cascade is a complex process that is mediated by the endothelial cells that line blood vessels. The VEGF-A mediates angiogenesis and other functions through the stimulation of specific receptors on endothelial cells to activate the expression of endothelial cell genes. This leads to the production of proteins such as procoagulant tissue factor, proteins associated with fibrinolytic pathway, matrix metalloproteases, nitric oxide synthase, integrins and various mitogens (Dvorak, 2002).

Activation of the VEGF-VEGF-receptor axis triggers many signaling networks that result in endothelial cell survival, mitogenesis, migration and differentiation, vascular permeability and mobilization of endothelial progenitor cells (Hicklin and Ellis, 2005). Endothelial cell migration and invasion following the degradation of the basement cell membrane is an important step in the initiation of angiogenesis (Rafii and Lyden, 2003).

1.3.2.5 VEGF-A and tumour angiogenesis

Tumour angiogenesis is the vascular proliferation of a network of blood vessels that penetrates into cancerous growths, supplying nutrients and oxygen and removing waste products. It allows the tumour to maintain its growth advantage and also facilitates metastatic spread by establishing connections to the existing vasculature (Folkman, 1971). The vessels formed by tumour angiogenesis are highly abnormal, non-uniformly distributed, irregularly branched, with arterio-venous shunts, hyperpermeable to plasma and plasma proteins and do not conform to a clear hierarchical pattern (Dvorak, 2003). The angiogenic cascade leading to tumour vascularisation is divided into the prevascular phase, also known as the “angiogenic switch” and the vascular phase (Pepper et al., 1996). When tumour cells undergo transformation to the angiogenic phenotype, phenotypic changes on endothelial cells as well as other cell types are induced. At this point avascular tumours can acquire their own blood supply and grow rapidly (Norrby, 1997). Tumours lacking adequate vasculature become necrotic or apoptotic, whereas tumours that have undergone neovascularisation enter a phase of exponential growth and have increased metastatic potential (Brem et al., 1976; Holmgren et al., 1995).

The VEGF-A is a key regulator of normal and pathological angiogenesis. Its expression in active cells is controlled by a variety of external factors. Some of these factors are briefly discussed below and include hypoxia, growth factors and cytokines, oncogenes and tumour suppressor genes.

As tumours expand, the cells within the expanding mass are deprived of oxygen as distance from the nearest blood vessels increases, resulting in hypoxic regions within tumours. Cells in hypoxic regions respond by stimulating VEGF-A production which in turn activates angiogenesis (Ferrara and Davis-Smyth, 1997). Hypoxic transcriptional regulation of VEGF-A is mediated by hypoxia-inducible factor 1 (HIF-1) (Dvorak, 2002).

Many studies have shown that certain growth factors and cytokines can also induce angiogenesis. The *HER1* and *HER2* genes have been shown to be involved in VEGF-A regulation and angiogenesis in tumours such as colon carcinoma, renal cell carcinoma and breast cancer (Ciardiello et al., 2000; Kedar et al., 2002; Yang et al., 2002). Prostaglandins have also been implicated in tumour angiogenesis by upregulation of VEGF-A expression (Gately, 2000). In addition, prostaglandin-endoperoxide synthase-2/ cyclo-oxygenase-2 (COX-2) overexpression has been shown to be associated with tumour progression and elevated angiogenesis in several solid malignancies including breast, colon and pancreatic cancers (Aoki et al., 2002; Costa et al., 2002; Tsujii et al., 1998). Platelet derived growth factors (PDGFs) also reportedly modulate angiogenesis by inducing VEGF-A (Cao et al., 2002).

Many oncogenes and tumour suppressor genes have been associated with the modulation of angiogenesis in solid tumours due to the ability to induce pro-angiogenic growth factors such as VEGF. The induction of VEGF by a mutant *Ras* oncogene has been reported in several types of cancer (Rak and Kerbel, 2001). The *p53* tumour suppressor gene impacts on the regulation of VEGF-A in malignant tumours by suppressing VEGF-A transcription.

1.3.2.6 *VEGF*-A in cancer

In many different types of carcinomas, including oesophageal, overexpression of *VEGF*-A has been reported to correlate with poor prognosis (Adams et al, 2000; Borre et al., 2000; Cascinu et al., 2000; Kaya et al., 2000; Loncaster et al., 2000; Mineta et al., 2000; Shen et al., 2000; Shih et al., 2000; Slaton et al., 2001; Tabone et al., 2001; Yudoh et al., 2001). In addition, *VEGF*-A expression correlated with one or more of the following prognostic measures: tumour size, metastasis, and overall survival, thereby providing evidence that the amount of *VEGF*-A expressed by tumours affects clinical outcome. The identification of VEGF-A as a central regulator of angiogenesis has led to efforts to exploit its therapeutic potential. Anti-angiogenesis treatment modalities currently in preclinical and clinical development focus on the inhibition of the VEGF-A pathway, using different approaches (Ellis et al., 2001). These include synthetic neutralising antibodies to VEGF-A or VEGF receptors, tyrosine kinase inhibitors to VEGF receptors, and soluble VEGR receptors/ VEGF receptor hybrids (Ellis et al., 2001).

1.3.3 Matrix metalloproteinase 2 (MMP 2)/ gelatinase A

Matrix metalloproteinases are involved in a variety of normal biological processes such as embryonic development, blastocyst implantation, organ morphogenesis, nerve growth, ovulation, cervical dilatation, bone remodeling, wound healing and angiogenesis. They are also implicated in pathological processes, such as arthritis, cancer, cardiovascular disease and neurological disease. The main function of MMPs is the removal of the extracellular matrix (ECM) during tissue resorption and the alteration of biological functions of extracellular matrix macromolecules by specific proteolysis (Nagase and Woessner, 1999).

1.3.3.1 Identification of matrix metalloproteinases

Matrix metalloproteinases belong to a family of zinc dependent endopeptidases of the superfamily metzincins. In humans, more than 21 MMPs have been identified. They all have the characteristic ability to cleave ECM proteins (Birkedal-Hansen et al., 1993). The MMPs were initially divided into collagenases, gelatinases, stromelysins and matrilysins on the basis of their specificity for ECM components. However, due to the identification of increasing numbers of substrates, a sequential numbering system was adopted. The MMPs are now grouped according to their structure (Stamenkovic, 2000).

1.3.3.2 Structure of matrix metalloproteinase 2

Matrix metalloproteinase 2 belongs to the group of gelatinases. These proteins preferentially degrade denatured collagens and gelatins. Structurally, MMP2 is a 72 kDa type IV collagenase and is coded for by the gene located on chromosome 16q13 (Visse and Nagasse, 2003).

All MMPs are produced as zymogens containing a secretory signal sequence and a propeptide whose proteolytic cleavage is needed for MMP activation (Visse and Nagasse, 2003). In general, MMPs contain a signal peptide, a propeptide, a catalytic domain with the highly conserved zinc binding site and a hemopexin-like domain linked to the catalytic domain by a hinge region as seen below in Figure 1.4 (Egeblad and Werb, 2002).

Figure 1.4. Protein structure of MMP2, a gelatin binding matrix metalloproteinase, containing a prepeptide (Pre) with an amino-terminal signal sequence, a propeptide (Pro) with a zinc interacting thiol group (SH), and a catalytic domain with a zinc binding site and inserts of fibronectin (Fi) hinged (H) to hemopexin domains that are linked by a disulphide bond (S-S) (Egeblad and Werb, 2002)

The propeptide domain has a conserved amino acid sequence. A Cysteine within this region, known as the "cysteine switch", ligates the catalytic zinc binding motif to maintain the latency of pro-MMPs (Becker et al., 1995; Bode et al., 1993). Additionally, MMP2 contains fibronectin type II inserts within the catalytic domain (Nagase and Woessner, 1999).

1.3.3.3 MMP2 activation

Matrix metalloproteinases are expressed in tissues at various stages of development. They are rapidly induced by external stimuli such as growth factors and cytokines, as well as by changes in cell-cell and cell-ECM interactions. The activity of MMPs is controlled at three levels: transcription, proteolytic activation of the zymogen and inhibition of the active enzyme (Stamenkovic, 2003).

Most MMPs, including MMP2, are secreted in latent precursor form and are activated in the extracellular space. The propeptide latency is established by the cysteine switch (Stamenkovic, 2003). When this switch is disrupted, the propeptide is removed resulting in the activation of the MMPs. Secreted pro-peptides are activated *in vitro* by proteinases and by non-proteolytic agents such as SH reactive agents, mercurial compounds, reactive oxygen and denaturants (Nagase and Woessner 1999).

In vitro, MMPs are able to mutually activate each other as well as autoactivate, for example, MMP1 and MMP12 can activate latent MMP2 (Stamenkovic, 2000). Matrix metalloproteinase 2 is activated mainly by cell surface activation as pro-MMP2s are not easily activated by proteinases. Pro-MMP-2 forms a tight complex with tissue inhibitors of MMP2 (TIMP-2) in its process of activation (Strongin et al., 1995). Tissue inhibitors of MMPs (TIMPs) are major endogenous regulators of MMP activity. Four types are known, TIMP-1 to TIMP-4, as well as the serum proteinase inhibitor, α-2 macroglobulin (Baker et al., 2002). Tissue inhibitors bind to conserved regions of active MMPs and inhibit their proteolytic activity.

1.3.3.4 Biological function of MMPs

As mentioned previously, matrix metalloproteinases, including MMP2, are responsible for proteolytic degradation of the extracellular matrix (ECM) and the basement membrane during tissue remodelling. The ECM and basement membrane play a crucial part in both tissue architecture and homeostasis, the exact nature of which depends on the tissue type. Thus each tissue has different types of ECM. The basement membrane is a specialised form of ECM. It is a thin flexible mat that separates epithelial cells from the underlying stroma.

Matrix metalloproteinases are important in embryonic development as ECM remodelling is a key component of tissue growth and morphogenesis (Visse and Nagase, 2003). Matrix metalloproteinases also influence many developmental and physiological cellular functions by degradation and alteration of the ECM micro-environment leading to cell migration, proliferation, apoptosis or morphogenesis. Metalloproteinases modulate the activity of growth factors, growth factor receptors and proteases by cleavage from the ECM or by cleavage of enzymes or their inhibitors (Vu and Werb, 2000).

1.3.3.5 Matrix metalloproteinase 2 and tumour progression

Tumour cell invasion and metastasis is a multi step process involving the proteolytic degradation of basement membranes, altered cell adhesion and physical movement of tumour cells. Matrix metalloproteinases are believed to create an environment that supports the initiation and growth of primary tumours, enhances tumour angiogenesis and neovascularisation, and enables the disruption of local tissue architecture and penetration of connective tissue barriers. This facilitates dissemination of cancer cells and metastatic spread (Ohtani, 1998).

The process of tumour cell invasion and metastasis involves extensive remodeling of the ECM and basement membranes. For the change from *in situ* to invasive malignancy, tumour cells must penetrate their delimiting basement membranes and move through surrounding stroma. A metastatically competent cell must have access to the vascular or lymphatic systems and extravasate at a distant site to establish new proliferating colonies (Egeblad and Werb, 2002). Cleavage of ECM components by MMPs generates proteolytic fragments that enhance tumour cell migration.

Cleavage of laminin-5 and -14 by MMP2, results in laminin fragments that trigger migration signals in cells (Gianneli et al, 1997; Koshikawa et al., 2000). Several studies have provided evidence for involvement of MMPs in the metastatic process. Overexpression of MMP2 protein has been shown to promote cellular invasion in tumour cell lines and animal models, strongly implicating the *MMP2* gene in metastasis (Deryugina et al., 1997; Itoh et al., 1998). *In vitro* and *in vivo* studies have also implicated a role for MMPs in angiogenesis. The *MMP2* gene has been demonstrated to be necessary for the switch to an angiogenic phenotype while the inhibition of the gene resulted in suppression of tumour growth (Fang et al., 1999). In addition, MMPs have been shown to act anti-angiogenically through the cleavage of plasminogen resulting in the generation or release of an angiogenesis inhibitor, angiostatin, from the ECM (Cornelius et al., 1998). More recent studies in animal models showed that synthetic and endogenous MMP inhibitors reduced tumour angiogenesis (Li et al., 2001; Oh et al., 2001; Xu et al., 2001).

1.3.3.6 Matrix metalloproteinase 2 expression in cancer

Matrix metalloproteinase 2 expression has been investigated in several studies. In oesophageal cancer, MMP2 activation has been associated with lymph node metastasis and vascular invasion (Koyama et al., 2000; Shima et al., 1992). Polymorphisms in the *MMP2* promoter regions are reported to be a genetic susceptibility factor for the occurrence and metastasis of oesophageal carcinoma (Yu et al., 2004). The overexpression of *MMP2* has been associated with a shorter survival in breast cancer, metastatic invasion in ovarian, prostratic and lung cancer, as well as an aggressive phenotype of pancreatic cancer (Bramhall et al., 1996; Fishman et al., 1996; Stearns and Stearns, 1996; Talvensaari-Mattila et al., 1998; Tokuraku et al., 1995).

Inactivation of MMPs by either overexpression of TIMPs or administration of synthetic MMP inhibitors may prevent initiation of MMP activation cascades, and regulate ECM degradation (Brown, 1999). Currently several synthetic inhibitors of MMPs are being tested in clinical trials for several types of cancer (Baker et al., 2002; Brown, 1999; Hoekstra et al., 2001). Unpleasant side effects have been a problem due to the broad substrate specificity.

1.3.4 Gene expression studies in OSCC

The current knowledge of genes and pathways involved in the process of OSCC tumourigenesis is limited. Previous studies on OSCC have investigated the molecular alterations present in aberrant cell cycle control, DNA repair, cellular enzymes, growth factor receptors, and nuclear receptors (Lam et al., 2000). Differential gene expression is one of the important mechanisms of pathogenesis in human diseases. Variations in expression include altered levels of normal gene products as well as modified proteins resulting from mutations. Detection of differential expression during early pathogenesis may help elucidate the underlying mechanisms of carcinogenesis and suggest therapeutic approaches. Real time PCR technology can now be used to detect variant gene expression.

1.4 Study Objectives

The aim of this study therefore, was firstly, to validate a novel real time PCR probe gene expression system by comparison with existing fluorescent technology, and secondly, to determine levels of expression of particular genes known to be associated with OSCC using real time PCR technology.

The specific aims of the study were:

1. To validate a novel real time PCR probe system by comparison with existing fluorescent dye technology.

2. To evaluate gene expression quantification strategies by the comparison of two different relative quantification methods, namely a standard curve method and the Pfaffl model.

3. To determine the gene expression of *HER1*, *HER2*, *VEGF*-A and *MMP2* in surgically classified normal and tumour tissue of the oesophagus.

4. To correlate gene expession data with patient survival, and clinical and histological information (where available).

5. To evaluate the tissue sampling method used in this study for gene expression analysis.

Chapter 2: Methods and Materials

2.1 Introduction to Methods

Real time PCR methods using a universal probe library system (UPL) and SYBR Green I technology were used in this study to determine the gene expression of four genes known to be associated with oesophageal cancer. These genes were *HER1*, *HER2*, *VEGF-A* and *MMP2*. *VEGF-A* in this study will be referred to as *VEGF*. The gene for gylceraldehyde-3-phosphate dehydrogenase (GAPDH) was used as the reference gene. A brief overview on the sequence of methodologies utilised in this study is shown in Table 2.1, followed by a review on the principles of real time PCR technology.

Table 2.1 Summary of procedures used in this study to quantitate expression of genes associated with oesophageal cancer.

---

1) Extraction and quantification of RNA from oesophageal tissue.

2) Reverse transcription of RNA (cDNA synthesis).

3) Real time PCR to determine the relative expression of the *VEGF* gene using a standard curve method and SYBR Green I technology in order to compare real time PCR detection systems.

4) Real time PCR to determine the relative expression of the *VEGF*, *HER1*, *HER2* and *MMP2* genes using a standard curve method and novel universal probe library (UPL) technology.

5) Real time PCR using the Pfaffl model to determine the relative expression of firstly, the *VEGF* gene using the SYBR Green I system, and secondly, all 4 genes using UPL technology, in order to compare relative gene expression quantification methods.

2.1.1 Polymerase Chain Reaction

The amplification of RNA and DNA has conventionally been performed by the polymerase chain reaction developed by Kary Mullis in the 1980s. This technology allows more than a billion fold amplification of DNA (Mullis and Faloona, 1987; Mullis, 1990). Each cycle of the PCR theoretically doubles the amount of DNA targeted by the primers in the reaction. A typical amplification reaction includes the target DNA, a thermostable DNA polymerase, two oligonucleotide primers which flank the sequence of interest, deoxynucleotide triphosphates (dNTPs), reaction buffer and magnesium chloride ($MgCl_2$). The initial step of the amplification reaction denatures the target DNA by heating to 94°C or higher for 15 seconds to 2 minutes. The helical DNA strands separate from each other to yield single stranded DNA template for replication by thermostable DNA polymerase (Figure 2.1). In the second step of the cycle, the temperature is reduced to approximately 40-60˚C so that the oligonucleotide primers can form stable associations (anneal) with the denatured target DNA and serve as primers for DNA polymerase. This step lasts approximately 15 to 60 seconds. In the final step, the addition of dNTPs by DNA polymerase initiates the synthesis of new DNA strands. The reaction temperature is raised to 70 to 74°C for the DNA polymerase to work optimally. The extension step lasts approximately 1 to 2 minutes and the next cycle begins with a return to 94˚C for denaturation. Figure 2.1 below is an illustrative summary of the steps involved in a PCR reaction (www.ncbi.nlm.nih.gov/.../probe/doc/TechPCR.shtml).

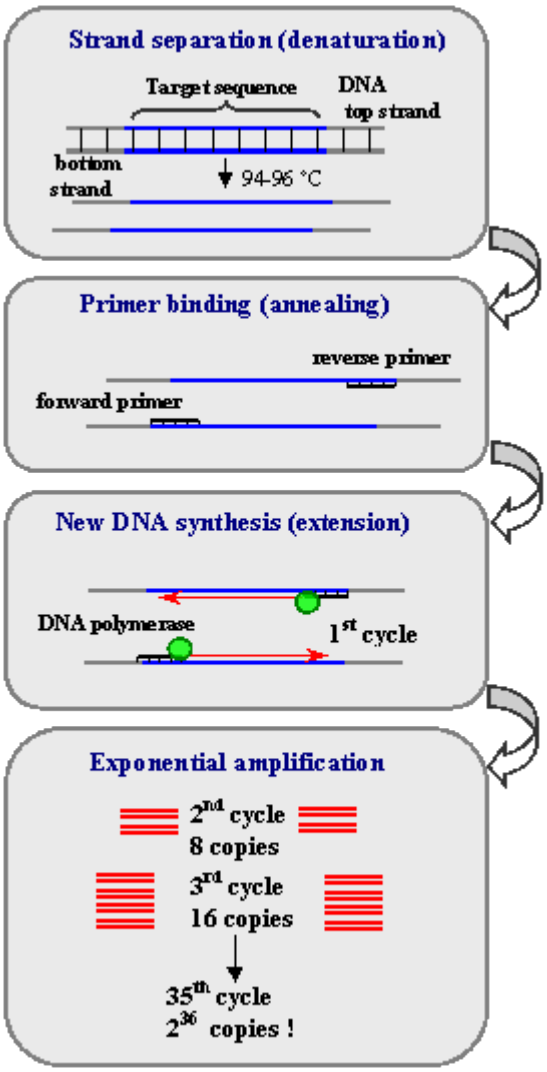

Figure 2.1 Schematic representation of the Polymerase Chain Reaction.

2.1.2 Real Time PCR

The analysis of PCR products during the amplification procedure is known as 'real time PCR' (Meuer et al., 2001). The amount of double stranded PCR product is monitored at each cycle by means of fluorescence and is plotted against cycle number, to allow the visualisation of the accumulation of PCR products, as shown in Figure 2.2 (Meuer et al., 2001).

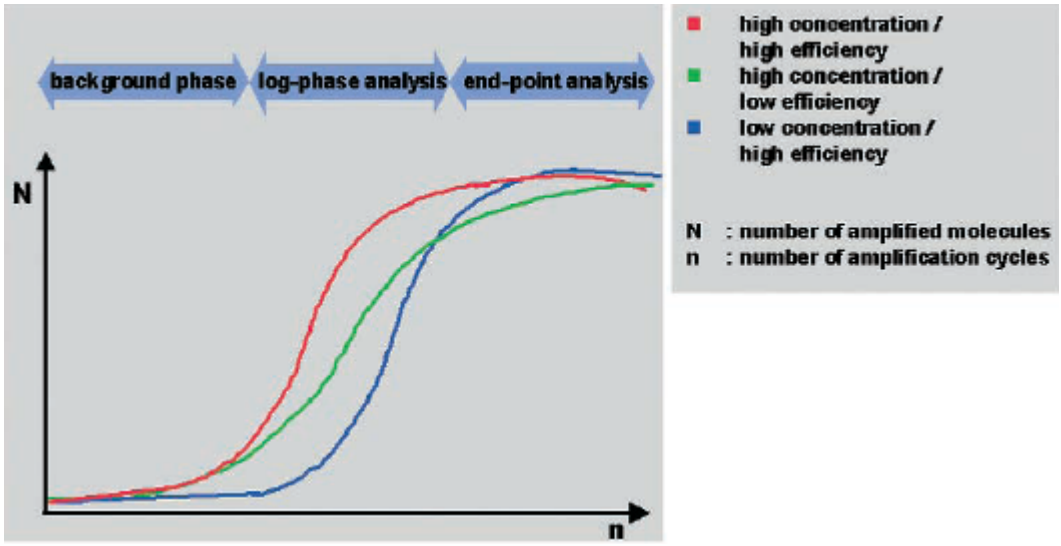

Figure 2.2. A typical PCR amplification curve (Roche Applied Science, 2003).

The first phase of a real time PCR amplification reaction is the assessment of background fluorescence. The second phase is an exponential linear amplification of the product which is reflected as a sharp increase in fluorescence that can be detected above background. Lastly there is a plateau phase which is defined as the attenuation in the rate of exponential product accumulation (Kainz, 2000). The point at which the fluorescent signal significantly rises above background is known as the threshold cycle (Ct) and always occurs during the exponential phase of amplification (Bustin, 2000).

Theoretically the PCR is described by the formula,

$$N_n = N_0 \times 2^n$$

where N represents the number of amplified molecules and n, the number of amplification cycles (Roche Applied Science, 2003).). Efficiency is assumed to be optimal and constant in this reaction, in which every PCR product is replicated once every cycle.

This, however, may not be the case in reality since many factors influence the PCR and the efficiency may not always be optimal. A more accurate representation of the PCR amplification is expressed by the following equation,

$$N_n = N_0 \times (E_{const.})^n$$

whereby E represents PCR efficiency. In the final phases of the PCR, the exponential curve bends towards a plateau and the efficiency becomes variable making it difficult to obtain accurate measurements during these last stages. This occurs with conventional PCR, where DNA is amplified and detected at the 'end point' of an amplification curve and there is no direct relation of DNA input to amplified target (Kainz, 2000). Additionally, measurements taken at the end-point of a PCR cannot easily distinguish variations in the amount of starting material or amplification efficiency. Reactions with low initial copy number can reach the same plateau as reactions with higher initial template concentrations and/or different PCR efficiencies, as seen in Figure 2.2. (Roche Applied Science, 2003). Real time PCR allows for more accurate measurements as quantification is extracted in the log-linear phase of the amplification curve where the amplification efficiency of each reaction is constant (Roche Applied Science, 2003).

2.1.3 Real time PCR instrumentation

The real time instrument used in this study was the Lightcycler (Roche Diagnostics, Mannheim, Germany) which consists of three parts: a sample carousel, thermal chamber and fluorimeter component. The sample carousel is centrally positioned within the cylindrical thermal chamber and holds 32 glass capillaries, which serve as cuvettes for flourimetric analysis. The glass capillaries contain a reaction volume of 10-20µl with a surface-volume ratio to allow rapid thermal transfer within the reaction solution, thus ensuring efficient temperature transitions during PCR cycles (Roche Molecular Biochemicals, 2000). The thermal chamber contains a temperature sensor near the glass capillaries to measure and control the temperature within the chamber. Optimal homogenous air temperature is moderated by a blower that consists of separate heating coils located at the base of the thermal chamber and a high velocity fan, which evenly distributes incoming air throughout the chamber. A vent at the side of the chamber releases surplus air. The fluorimeter is directly connected to the thermal chamber by the optical system. The optical component consists of a blue light emitting diode (LED) for fluorophore excitation energy, a stepper motor for the rotation of glass capillaries to a specific position for excitation and measurement, as well as dichroic mirrors that divert light from the capillaries into detection channels. The detection channels are composed of combination filters to detect fluorophores at various emission wavelengths, allowing for multiple colour detection and application flexibility (Roche Molecular Biochemicals, 2000). Data are displayed on a computer screen for real time monitoring of the PCR reaction.

2.1.4 Real time PCR chemistries

At present there are four well established methods to detect amplicons with similar sensitivity (Wittwer et al., 1977). The simplest method utilises fluorescent dyes, such as SYBR Green I, that bind specifically to double stranded DNA (Morrisson et al., 1998). Other methods such as molecular beacons, hybridisation probes and hydrolysis probes, rely on the hybridisation of fluorescence-labelled probes to a specific amplicon (Bustin, 2000). Each system has unique features but all employ a change in the intensity of fluorescence to determine DNA amplification. The two methods discussed here are fluorescent dyes and hydrolysis probes.

2.1.4.1 SYBR Green I

SYBR Green I dye emits little fluorescence in solution but when bound to the minor groove of double stranded DNA, it releases a one thousand fold greater fluorescence. An increase in fluorescence reflects an increase of double stranded DNA (Bustin, 2000). Prior to amplification, the reaction mixture contains the denatured DNA, primers, and dye. The unbound dye molecules fluoresce weakly, producing a minimal background fluorescence signal which is subtracted during analysis. After the primers have annealed, some dye molecules bind to the short double strand DNA sequence, resulting in increase in the flourescence of SYBR Green I molecules. During the elongation step of the PCR additional SYBR Green I molecules bind to the newly synthesised DNA and an increase in fluorescence is seen in real time. On denaturation of the DNA in the next heating cycle, the dye molecules are released and the fluorescence signal falls (Wittwer et al., 1977). As DNA binding dyes do not bind specifically, this type of analysis is more likely to detect non specific fluorescence.

The dissociation curve (melt curve) of the amplified product is analysed in order to determine the melting point (Tm) of that product. The presence of two or more peaks implies that amplification was not specific for a single DNA target (Valasek and Repa, 2005).

2.1.4.2 Universal probe library

The universal probe library (UPL) system was developed by a Danish company, Exiqon, in 2004. Sets of probes have been made available for genomes of various species, including human (Mauritz et al., 2005). The UPL consists of 90 short pre-validated probes that provide genome wide coverage. The probe library design is based on particular 8- to 9-mer sequence motifs that appear with very high frequency throughout the whole genome (Mauritzen et al., 2005). Ninety percent of all transcripts in the Ensemble human gene database which are based on exon-exon splice junctions, are targeted by the library probes, as are 99% of all transcripts recorded in the human gene RefSeq database at the National Center for Biotechnology Information (NCBI) (Mauritz et al., 2005).

In comparison to conventional DNA probes which are normally 20 to 25 nucleotides in length and target specific sequences, UPL probes are limited to only 8 or 9 nucleotides which can target many different transcripts (Mauritzen et al., 2005). Adequate duplex stability and compatibility in standard real time PCR assays is ensured by the substitution with the high affinity DNA analogue, locked nucleic acid (LNA) (Mauritz et al., 2005). This novel nucleic acid analogue enhances hybridisation and stability, and also increases base-pairing specificity of the probes relative to DNA (Hertoghs et al., 2003. Thus the combination of the gene specific PCR primers and the UPL probe, results in a highly specific assay (Mauritzen et al., 2005).

2.1.4.2.1 UPL primer and probe design

The Assay Design Center software (www.probelibrary.com) is incorporated into the probe library package to allow for the selection of sequence specific probes and primers from the Probe Library for a given target (Mauritzen et al., 2005). The probe finder software identifies exon-exon boundaries from the given sequence and designs intron-spanning amplicons for the real time assay (Mauritzen et al., 2005). Intron recognition by the software is based on either an intron prediction algorithm following a Basic Local Alignment Search Tool (BLAST) search of target transcript against relevant genome sequence, or reference to the Ensemble database of target sequence (Mauritzen et al., 2005). After intron site detection, the software searches the target sequence for sites complementary to UPL probes and generates possible probes for use in the assay. Potential primers are moderated by an *in silico* PCR algorithm that explores the genome and transcriptome sequences to guarantee a high measure of specificity (Mauritzen et al, 2005).

2.1.4.2.2 UPL performance

Functional assays performed for 96% of 175 RefSeq transcripts without any optimisation strategies have demonstrated a PCR efficiency of 100% using LinRegPCR software (Mauritzen et al., 2004; Ramakers et al., 2003). Time and cost spent on assay optimisation can be avoided by replacing an inadequately performing assay with another assay from the probefinder software list (Mauritzen et al., 2005). Experiments comparing Hyb-Probes, SYBR Green I and UPL probes were also undertaken and showed that crossing point values for SYBR Green I were lower than those of the UPL and Hyb-probe assays due to the higher specificity of the probe based assays (Mauritzen et al., 2005).

2.1.4.2.3 UPL Assay

Hydrolysis probes are also called 5'-nuclease probes and consist of two types of fluorophores: reporters and quenchers. The reporter dye is usually a long-wavelength coloured dye, and is attached to the 5´ end of the probe, whereas the quencher dye is normally a short-wavelength coloured dye attached to the 3´ end (Mauritz et al., 2005). When the probe is either attached or unattached to the template DNA, or attached but prior to the action of the Taq polymerase, the quencher fluorophore absorbs the fluorescence from the reporter fluorophore through fluorescence resonance energy transfer, also called Főrster transfer (Mauritz et al., 2005). After the addition of nucleotides, cleavage of the reporter dye by Taq polymerase occurs resulting in an increase in fluorescence, which is quantified by the analysis software. The total fluorescence detected is proportional to the amount of specific DNA present.

2.1.5 Real time PCR relative quantification strategies

Relative quantification associates the PCR signal to an input copy number by using a standard curve (calibration curve). Serial dilutions of an external standard with a predefined known concentration are used to create a standard curve which then allows for the determination of unknown sample concentration on the basis of the cycle threshold (Ct) value (Wong and Medrano, 2005). The amplification efficiency is assumed to be equal for both standards and samples. With this kind of relative quantification, the quantity of the unknown sample is determined using a standard curve and then expressed relative to the reference gene (Livak and Schmittgen, 2001). Commonly used reference genes are so-called housekeeping genes that are vital for normal cell function and believed to have stable expression. These include the genes for glyceraldehyde-3-phosphate dehydrogenase (GAPDH), ß-actin and ribosomal RNA

(rRNA) (Wong and Medrano, 2005). The optimal reference gene should not be regulated under experimental conditions, as a stable and constant reference is vital for normalisation.

It has been shown that the expression level of some housekeeping genes varies according to biological material type or conditions (Bustin, 2000). Care should therefore be taken when selecting a housekeeping gene for relative quantification.

Relative quantification can also be calculated without a standard curve, in which case, concentrations of the target and reference gene are a function of amplification efficiency (Wong and Medrano, 2005). The efficiency of the PCR is an important factor in quantification strategies as the assumption is that of an ideal efficiency, in which the PCR product doubles during the exponential phase of every cycle of the reaction (Liu and Saint, 2002). However in reality, PCRs do not have ideal efficiencies so that calculations without correction for efficiency result in less accurate quantification values (Liu and Saint, 2002). In addition, the efficiency of a reaction calculated from the data of a standard curve does not take into account the change in the efficiency during the reaction. Each reaction is relatively stable in the early exponential phase but slowly deteriorates to zero as the reaction progresses, due to a number of factors such as, depletion of PCR elements, degradation of polymerase enzyme activity and competition of PCR products (Liu and Saint, 2002).

There are several mathematical models based on PCR kinetics that endeavour to accurately quantify relative gene expression with efficiency correction. One such model is that of Pfaffl et al., (2002) which incorporates gene quantification and normalisation into a single equation:

$$\textbf{Ratio} = (E_{\textbf{target}})^{\Delta CP\ \textbf{target (control-sample)}} / (E_{\textbf{ref}})^{\Delta CP\ \textbf{ref (control-sample)}}$$

This equation quantifies the relative expression of a target gene (target) in comparison to a reference (ref) gene by using crossing points (CP), PCR efficiencies (E) and the difference (Δ) between an unknown sample versus a control ($\Delta CP_{\text{control-sample}}$). The relative expression software tool (REST©) which runs on Microsoft® Excel and employs the Pairwise Fixed Reallocation Randomization Test©, was used to calculate significance of the results (Pfaffl et al, 2002). In this study, relative gene expression was calculated using the Pfaffl model (Pfaffl et al, 2002), as well as the standard curve method in order to compare the two quantification strategies.

2.2 Patients and specimens

A randomly selected cohort of 30 patients who had undergone oesophagectomies at the Department of Cardio-Thoracic Surgery, Inkosi Albert Luthuli Central Hospital (IALCH), Durban, KwaZulu-Natal (KZN), were enrolled into the study. Tumour and normal tissue classified into cancerous and non-cancerous regions during surgery, were frozen at -70˚C after collection. Additional clinical data were supplied by the Department of Cardio-Thoracic Surgery, IALCH, KZN. Histological assessment of samples was performed by the Department of Anatomical Pathology, IALCH, KZN.

The patient cohort was divided into two groups designated **A** and **B**. Group **A** comprised the original 30 patient cohort and group **B** comprised a 22 patient sub-cohort of group **A,** which consisted of the original 30 patient cohort less 8 patients who were removed following a retrospective assessment of samples. This is discussed in detail in sections 2.9 and 3.6. Gene expression analyses and histological assessment were performed on both groups in order to evaluate the effect of the sample classification method.

The histological assessment was carried out on groups A and B, but 3 patients had unavailable clinical data and thus complete assessment was carried out on 27 and 19 patients, respectively. In group A there were 17 females and 10 males who had a mean age of 57.2 years and range of 33–78 years. A more detailed demographic profile is shown in Figure 3.6 in Chapter 3.

2.3 Ethics

Ethical approval was granted for this study on the 08/10/2004 by the Biomedical Research Ethics Committee, UKZN, reference no: H147/04.

2.4 RNA preparation

High quality RNA is essential for successful real time PCR. To achieve this, the RNA must be free of contaminants such as DNA, chloroform and phenol as these can interfere with amplification.

2.4.1 Isolation

Paired samples of tumour and normal oesophageal tissue from each patient were collected at resection from the Department of Cardio-Thoracic surgery, IALCH and frozen at -70˚C until

use. The tissue was allowed to thaw on ice and RNA was extracted using the TRIZOL method with minor modifications to improve the yield of RNA (Perou et al., 1999). The method is described in Appendix C.

2.4.2 Purification

The isolated RNA was purified and treated for possible DNA contamination using the Aurum Total RNA mini kit (Biorad, catalog number 7326820) according to the manufacturer's instructions with minor modifications as described in Appendix D. Any DNA contamination can result in inaccurate RNA quantification and erroneous levels of PCR products.

2.4.3 Electrophoresis

The quality of RNA samples was assessed on a denaturing MOPS gel (Appendix F). The 18S and 28S subunits of RNA were visualized under ultraviolet radiation at a wavelength of 300nm using the Chemidoc UV transilluminator. This procedure was carried out to confirm that the RNA was not degraded and was of sufficiently good quality for use in real time PCR. The gel image was scanned electronically and the Quantity One V.4.4.1 software was used to adjust the light and contrast of the image before printing.

2.4.4 Quantification

Quantification of RNA was performed in triplicate using a Nanodrop ND-1000 UV/Vis Spectrophotometer at 260 nm, according to manufacturer's instructions (Nanodrop Technologies Inc., Washington, USA). The purity and concentration of the sample was calculated by on-board software. The RNA was required to have a 260/280 nm ratio reading ranging from 1.8- 2 to ensure the purity of the sample.

2.4.5 Storage of RNA

The isolated RNA samples were aliquoted into 20µl volumes and stored at -70˚C until use.

2.4.6 Reverse transcription

One microgram of total RNA was subjected to reverse transcription using the iScript cDNA synthesis kit (Biorad), according to the manufacturer's instructions. The GeneAmp 9700 PCR system (Applied Biosystems, California, USA) was used to carry out the reverse transcription reaction. The products were verified by performing a *GAPDH* PCR as described below. The remaining cDNA was stored at -20˚C until use.

2.5 *GAPDH* PCR

The *GAPDH* PCR was performed to confirm successful reverse transcription. In addition, since primers were designed to include an intronic region, the presence of any contaminating genomic DNA would be easily detected since contaminated cDNA would yield a larger product size than the expected 250 bp cDNA product. The *GAPDH* primers were synthesised by Roche Diagnostics (Mannheim, Germany):

5´AAG GTC GGA GTC AAC GGA TT 3´ (forward)

5´ CTC CTG GAA GAT GGT GAT GG 3´ (reverse)

A PCR core kit (Roche Diagnostics) comprising of 10x PCR reaction buffer that consisted of 100mmol/l Tris-HCl, 15mmol/l $MgCl_2$ and 500mmol/l KCl, dNTP mix and Taq DNA polymerase was used. The final reaction volume was 25µl and the reaction mix comprised 2.5µl of 10x PCR reaction buffer, 0.5µl dNTP mix (10mmol/l), 0.15µl Taq DNA polymerase (5U/µl), 1µl of each primer (200nmol/l), 16.85µl sterile water and 3µl cDNA template. The GeneAmp 9700 PCR system was used to carry out the PCR reaction.

The initial denaturation was at 95ºC for 5 minutes followed by 35 cycles at 1 minute. Primers annealed at 64˚C for 30 seconds and extension occured at 72˚C for 30 seconds followed by a final extension at 72˚C for 10 minutes. Genomic DNA used as a positive control and sterile water was substitituted for cDNA as a negative control. The products were verified on agarose gel electrophoresis as described in Appendix E.

2.6 Real Time PCR using SYBR Green I

SYBR Green I technology was used in the generation of amplicons for the construction of standard curves.

2.6.1 Optimisation of PCR conditions

Factors such as annealing temperatures, primer and $MgCl_2$ concentrations and cycling conditions were optimised for each gene examined. All optimisations were carried out using the Faststart DNA Master SYBR Green I kit (Roche Diagnostics) on the Roche Lightcycler.

Primer titrations to determine the most favourable primer concentration for each gene (*HER1*, *HER2*, *VEGF*, *MMP2* and *GAPDH*) were performed using primer concentrations decreasing from 1000nmol/l to 10nmol/l. A primer concentration of 20nmol/l was found to be optimal for all genes with the SYBR Green I system. Magnesium titrations were also carried out for all genes (*HER1*, *HER2*, *VEGF*, *MMP2* and *GAPDH*), using a $MgCl_2$ gradient of 1.5, 3, 4.5 and 6mmol/l to determine the optimal $MgCl_2$ concentration for each gene. The optimal $MgCl_2$ concentration for all genes was found to be 3mmol/l.

The optimised PCR conditions for the *GAPDH* gene were: denaturation at 95˚C for 1 minute followed by 45 cycles comprising denaturation at 95˚C for 5 seconds, annealing at 65˚C for 6 seconds, elongation at 72˚C for 6 seconds, and a further extension at 83˚C for 10 seconds. The melt curve segment comprised of 1 cycle of 95˚C for 30 seconds, 70˚C for 10 seconds and 95˚C for 0 seconds. Finally the PCR was cooled for 1 cycle at 40˚C for 30 seconds. Cycling conditions similar to those used for *GAPDH* were used for all the genes, with some modifications. The primer annealing temperature for *VEGF*, *HER1*, *HER2* and *MMP2* was 58˚C. The further extension step for *HER1* and *HER2* was carried out at 80˚C for 6 seconds. The increased temperature for the further extension step melts the non specific PCR products and eliminates the non specific fluorescence signal resulting in an enhanced accurate quantification of the desired real time PCR products.

2.6.2 Templates for standard curves

After optimising the magnesium and primer concentrations for each gene, cDNA amplicons were generated for each gene using the optimised PCR conditions. The concentration of amplified cDNA was calculated on triple readings, using the Nanodrop spectrophotometer on a cDNA setting. The mean concentration and mean absorbance at 260nm were used to calculate number of molecules using the following series of calculations (Roche Diagnostics):

Number of molecules of amplified DNA = number of moles of DNA (n) x Avogadros number (6.022 x 10^{23}), where **n** = concentration of double stranded DNA (**GM**)/ Molecular weight of ds DNA (**MW**)

*[**MW** of ds DNA = number of base pairs of DNA x average mass of base pair (660DA) and **GM** = absorbance at 260nm x concentration (ng/µl)/1000 = µg]*

These PCR products were then stored at -20˚C until used as templates to create standard curves with both the UPL and SYBR Green I systems.

2.6.3 Relative gene expression of *VEGF* and *GAPDH* using SYBR Green I

Standard curves were created for the *VEGF* and *GAPDH* genes by carrying out real time PCR on ten fold serial dilutions of the respective PCR products. The Lightcycler Faststart DNA Master SYBR Green I kit (Roche Diagnostics) was used for these reactions. The normal and tumour samples from each patient were then analysed under the optimised SYBR Green I conditions (section 2.6.1) with any two standards/calibrators from the corresponding previously constructed standard curves.

The Lightcycler Faststart DNA Master SYBR Green I kit (Roche Diagnostics) was used for all of these reactions. The second derivative maximum setting was used to calculate the absolute gene expression of the samples by comparison with the standard curves that were created. The absolute *VEGF* gene expression in each sample was normalised by dividing by the housekeeping gene (*GAPDH*) expression value, in order to obtain a relative gene expression of *VEGF* for each sample.

2.7 Relative gene expression using UPL technology

Various nucleic acid sequences, particularly reference sequences, of each gene were selected from the NCBI using BLAST. The sequences were then compared and aligned using Bioedit which identifies conserved regions of target genes (Appendix G).

Probes and primers for these sequences were manufactured by Roche Diagnostics using the Assay design software (www.probelibrary.com) and the Probefinder software V2.04 which identifies and designs appropriate primer and probes for the target gene sequence. Primers were stored at a concentration of 1000nmol/l and probes at a concentration 500nmol/l, at -20°C (Appendix G).

Standard curves for *HER1*, *HER2*, *VEGF*, *MMP2* and the housekeeping gene *GAPDH* were created using ten fold serial dilutions of their PCR products (section 2.6.2). At least 7 dilutions were used from the dilution series to ensure that samples with low gene expression fell into the range of the standard curve. The Lightcycler Taqman Master kit (Roche Diagnostics) was used to carry out the real time PCR. The total reaction volume was 20µl, comprising 4µl Taqman master, 0.2µl of each primer (200nmol/l), 0.2µl of the respective probe (100nmol/l), 10.4µl sterile water and 5µl of template.

The PCR mixture was incubated at 95˚C for 10 minutes, followed by 30 cycles of denaturation at 95˚C for 10 seconds, annealing at 60˚C for 30 seconds, extension at 72˚C for 1 second and 1 cooling cycle at 40˚C for 30 seconds (Roche Diagnostics). The on-board lightcycler software (V.3.5) performed all analytic calculations using a software algorithm that identifies the first turning point of the fluorescence curve which serves as the crossing point (CP). In this study the second derivative maximum setting was used for CP determination in all real time PCR reactions.

The normal and tumour samples from each patient were analysed with two standards/calibrators from the corresponding previously constructed standard curves for each of the 5 genes. The absolute gene expression of all 5 genes in each sample was obtained by comparison to the external standard curves that were created. The absolute gene expression values of all genes (*VEGF*, *HER1*, *HER2*, *MMP2*) in each sample were normalised by dividing these values by the housekeeping gene (*GAPDH*) expression values, in order to obtain the relative gene expression of each gene in each sample.

2.8 Relative gene expression using the Pfaffl model

As previously described, according to the Pfaffl model (Pfaffl et al., 2001), the relative expression ratio of a target gene is based on real time PCR efficiency and the crossing point deviation of an unknown sample compared with a control. This method does not require a standard curve. Efficiency curves for each gene (*HER1*, *HER2*, *VEGF*, *MMP2* and *GAPDH*) were created with the UPL system and appropriate cycling conditions (section 2.7).

The efficiency curve template was composed of 1µl of cDNA made up of a pooled mixture of all normal and tumour samples serially diluted (1300, 260, 130, 26, 13, 2.6, 1.3 ng), based on the method described by Pfaffl et al. (2002). Each PCR was carried out in duplicate. Efficiency curves were also created for *VEGF* and *GAPDH* using the SYBR Green I system under optimised cycling conditions (section 2.6.1). Each PCR was carried out in duplicate.

2.8.1 Calculation of relative gene expression using REST©

Real time PCR efficiencies for each efficiency curve were calculated from the slope generated by the Lightcycler software. The corresponding real time PCR efficiency (E) of one cycle in the exponential phase was calculated according to the established equation $E = 10^{[-1/slope]}$ (Rasmussen, 2001). The value of E ranges from 1 (minimum value) to 2 (theoretical maximum and optimum). Crossing points of normal and tumour samples for all genes using both the UPL and SYBR Green I systems were entered into the REST© Software database, as well as the calculated concentrations of pooled cDNA template and the corresponding CP for each gene on both UPL and SYBR Green I systems.

Calculated efficiencies for all efficiency curves were also entered into the REST© database. This database is a Microsoft Excel ® macro (Microsoft Corporation) attached to a purpose-built spreadsheet running in the background of REST©. The relative expression ratio for all genes was quantified using the REST© software (section 2.1.5) on the basis of group means for target genes (*HER1*, *HER2*, *VEGF*, *MMP2*) versus reference gene (*GAPDH*).

The group ratio results were tested for significance by using the pair wise fixed reallocation randomization test to analyse the differences in expression between reference and target genes. Randomisation tests made no distributional assumptions about the data. The p-values were calculated by obtaining the proportion of random allocations of the mean observed data to the reference and target genes.

2.9 Histopathological assessment of oesophageal samples

Clinicopathologic parameters of each tumour such as tumour type, size, histological grade, dysplasia, carcinoma in situ (CIS), necrosis, myenteric plexus and perineurial invasion, lymphatic vessel invasion, characteristics of tumour morphology (squamous keratin, anaplasia, atypical mitoses), mitotic rate, extent of tumour invasion, lymphatic node involvement and lymphocyte host response were assessed from Hematoxylin and Eosin (H&E) slides of the gross oesophagectomy specimen from each patient. The slides were viewed by both the pathologist and the investigator under a double headed Leitz Orthoplan microscope (Leica, Wetzlar, Germany). The relevant information was entered on to a histopathological proforma for correlation with gene expression data.

All parameters were classified according to the American Joint Committee on Cancer (AJCC) staging manual (Greene et al., 2002), with a few exceptions. The mitotic rate was classified as ≤ 50 or > 50. Mitotic figures were counted in 10 viewing fields with 400x magnification using a light microscope. The mitotic rate was taken as the fraction of cells that are in mitosis at any given time (Sadava, 1993). Regions with necrosis, inflammation and fibrosis were avoided as far as possible. Necrosis was stratified as mild (0-33%), moderate (34-66%) and extensive (>66%). Perineurial invasion was seen as the infiltration by cancer cells into the perineurium.

The tissue sampling method used in this study was retrospectively assessed from the available samples after experimental work was completed in order to evaluate its accuracy. Histological verification was carried out on nineteen matched pairs of frozen normal and tumour oesophageal tissue at the Department of Anatomical Pathology, IALCH. Each frozen oesophageal tissue specimen was thawed and processed for H&E staining using standard methods (Bancroft and Cook, 2002).

This process was carried out by pathology technicians and observed by the investigator. After H&E staining, each sample was viewed under a double headed light microscope and assessed by the pathologist as to whether there was agreement or discordance between surgical and microscopic classification of 'normal' or 'tumour' tissue. Photographs of some specimens were taken using a digital camera.

2.10 Statistical data analyses

Due to the discrepancies found between the microscopic and surgical classification of normal and tumour tissue to be discussed in section 3.6, statistical data analyses were performed on two groups: **A** and **B**. As mentioned earlier and discussed in section 3.6, Group A comprised of the original 30 patient cohort and group B comprised a 22 patient sub-cohort following exclusion of 8 patients who had discordant clinical and histopathological data. All statistical data analyses methods were performed by a biostatistician using current methods in the literature. These will be described in more detail in the relevant sections.

2.10.1 Analysis of relative gene expression

Absolute gene expression values for the tumour and normal samples from each patient were generated by the Lightcycler software for each of the target genes: *HER1*, *HER2*, *VEGF* and *MMP2*. These values were normalised by dividing by the values obtained for the housekeeping gene (*GAPDH*) in order to obtain the relative gene expression values. Descriptive statistical analyses of the comparison between tumour and normal tissue for each patient and each gene were carried out using the Statistical Package for the Social Sciences 15.0 (SPSS Inc. Chicago, IL). The tests used are described below. Unless otherwise stated, statistical significance for all tests was defined as $p < 0.05$.

The Wilcoxon signed ranks test and a two-tailed p-test were used to compare the difference between the median values of matched tumour and normal tissue for each gene (Chiu et al., 2005; Duraker et al., 2003; Hashimoto et al., 2005; Shih et al, 2000; Yu et al., 2005).

For each patient, a gene was defined as upregulated if the tumour/normal gene expression ratio was >1. If this value was <1, the gene was defined as downregulated. For each gene, a median fold change for the cohort was calculated (Chiu et al., 2005; Duraker et al., 2003; Hashimoto et al., 2005; Shih et al, 2000; Yu et al., 2005). Comparison of the UPL system and SYBR Green I system was also carried out by using the Wilcoxon signed ranks test and two-tailed p-test. The Chi-squared and McNemar tests (using binomial distribution) were used to calculate the level of discordance between the systems. All graphs were drawn using Graphpad Prism V.4 (Graphpad software Inc., CA, 2003)

2.10.2 Correlation between clinicopathologic factors and gene expression

The upregulation or downregulation of each gene (*VEGF*, *HER1*, *HER2* and *GAPDH*), in each patient, was correlated statistically with important clinicopathologic factors (section 2.9) using the Chi-squared or Fishers exact test with SPSS (Chiu et al., 2005; Duraker et al., 2003; Hashimoto et al., 2005; Shih et al, 2000; Yu et al., 2005).

2.10.3 Correlation of gene expression between genes

The mRNA expression levels of each gene were analysed in relation with the levels obtained for every other gene, using correlation and linear regression analyses to determine if there was any relationship in gene expression between the target genes, *VEGF*, *HER1*, *HER2* and *MMP2* (Chiu et al., 2005; Duraker et al., 2003; Hashimoto et al., 2005; Shih et al, 2000; Yu et al., 2005).

Chapter 3: Results

3.1 RNA preparation

3.1.1 Isolation

A representative gel illustrating isolated total RNA is shown in Figure 3.1. The integrity and quality of RNA was confirmed by the presence of the 28S and 18S subunits of RNA.

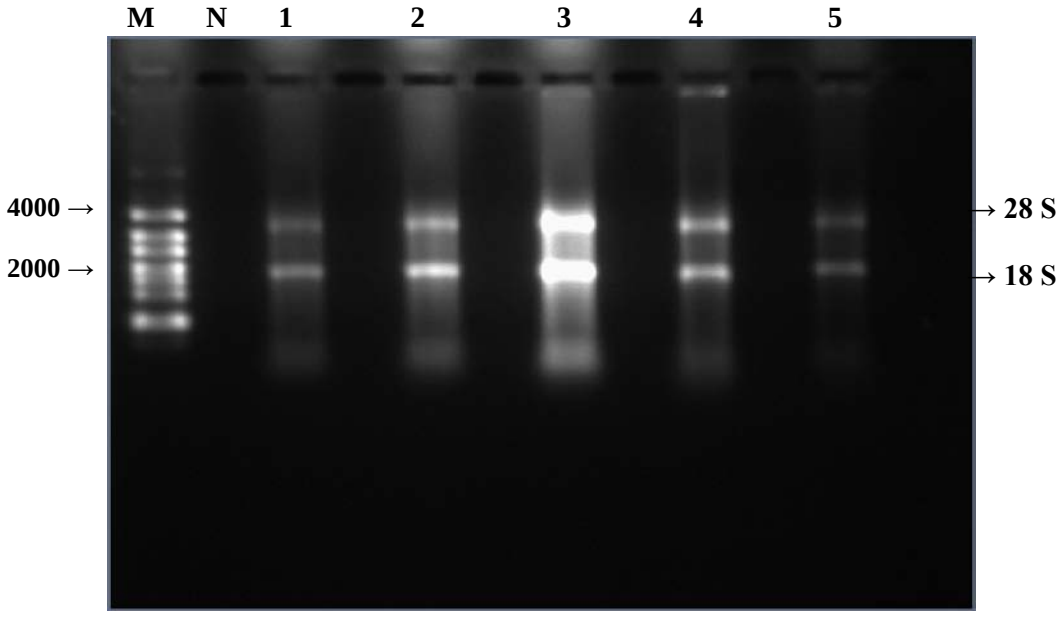

Figure 3.1. Denaturing MOPS gel showing isolated total RNA. Lane M represents a RNA marker (Riboruler^{TM} RNA ladder, #SM1823, Fermentas Life Sciences, Lithuania), lane N is a negative control (water), lanes 1-5 are RNA bands corresponding to 4000 and 2000 bases. The quality of RNA is confirmed by the presence of 28S and 18S subunits of RNA.

3.1.2 Reverse transcription

A PCR of a segment of the *GAPDH* gene sequence was carried out to verify the efficacy and integrity of the reverse transcriptase reaction. A representative agarose gel showing the 225 bp *GAPDH* PCR product obtained from cDNA samples is shown in Figure 3.2.

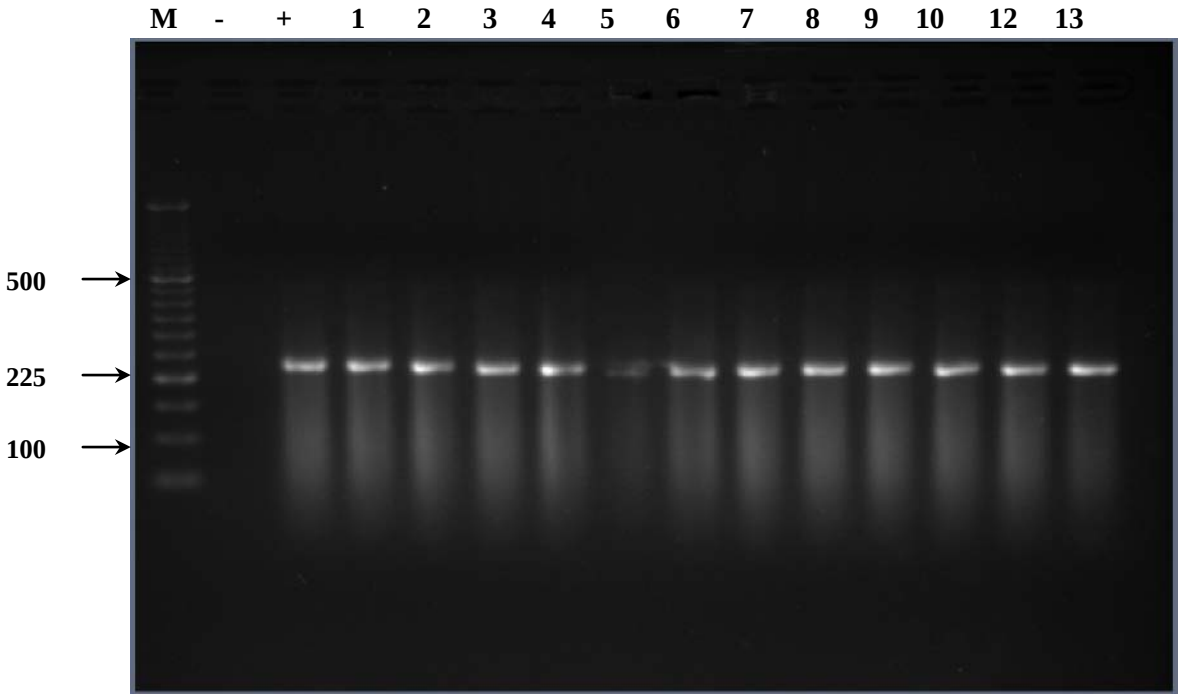

Figure 3.2. Agarose gel showing the 225 base pair *GAPDH* PCR product obtained from cDNA samples in lanes 1-13. Lane (+): positive control, lane (-): negative 'no DNA' control and lane (M) shows the Marker (O'Range Ruler ™ 50 bp DNA ladder, #SM0618, Fermentas Life Sciences).

3.2 Real time PCR optimisation using SYBR Green I

3.2.1 Primer titration

A representative real time PCR melting curve profile for the *HER2* and *MMP2* genes is shown in Figures 3.3 and 3.4. The graphs depict primer titrations using SYBR Green I dye. The primer concentrations tested ranged from 10 to 1000nmol/l. A primer concentration of 20nmol/l was selected for all genes (*HER1*, *HER2*, *VEGF*, *MMP2*, *GAPDH*) because of the absence of non specific amplification products, such as primer dimers, at this primer concentration, and to allow standardisation of the reaction conditions for all genes.

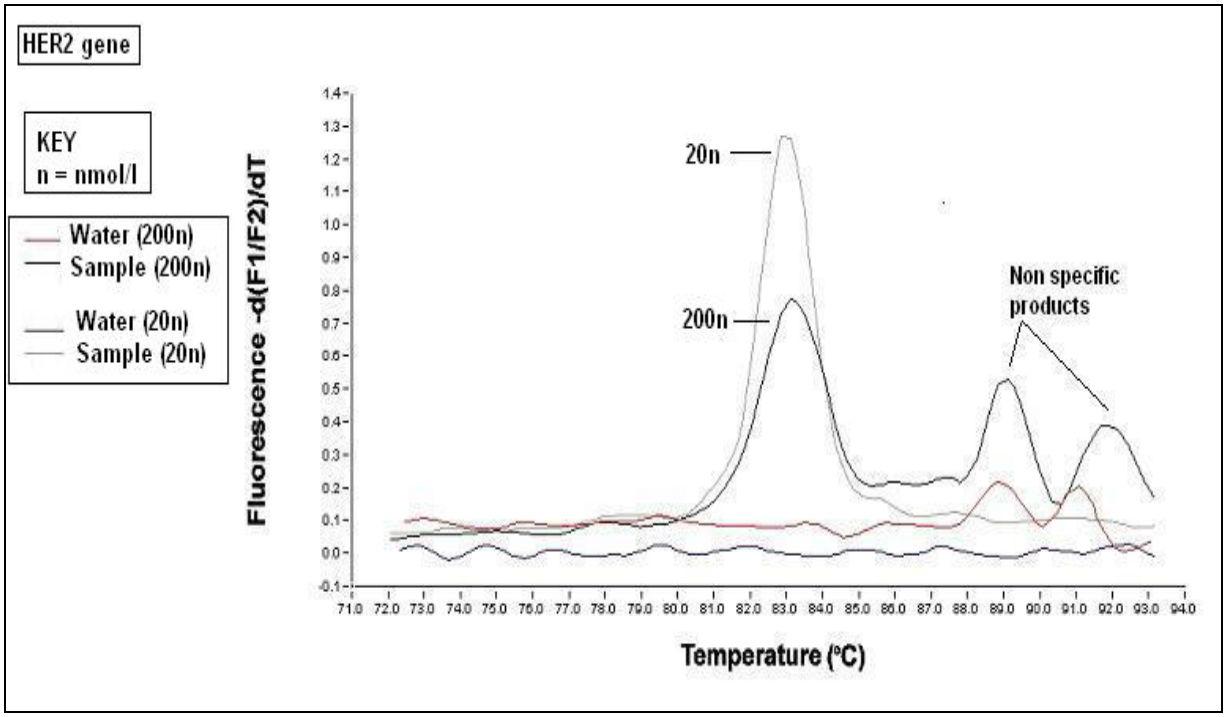

Figure 3.3. Primer titration melting curve analysis for *HER2* amplification products with SYBR Green I dye. The graph shows the negative derivative of fluorescence plotted against temperature. Non specific amplification products were present with primer concentrations of 200nmol/l but not with 20nmol/l.

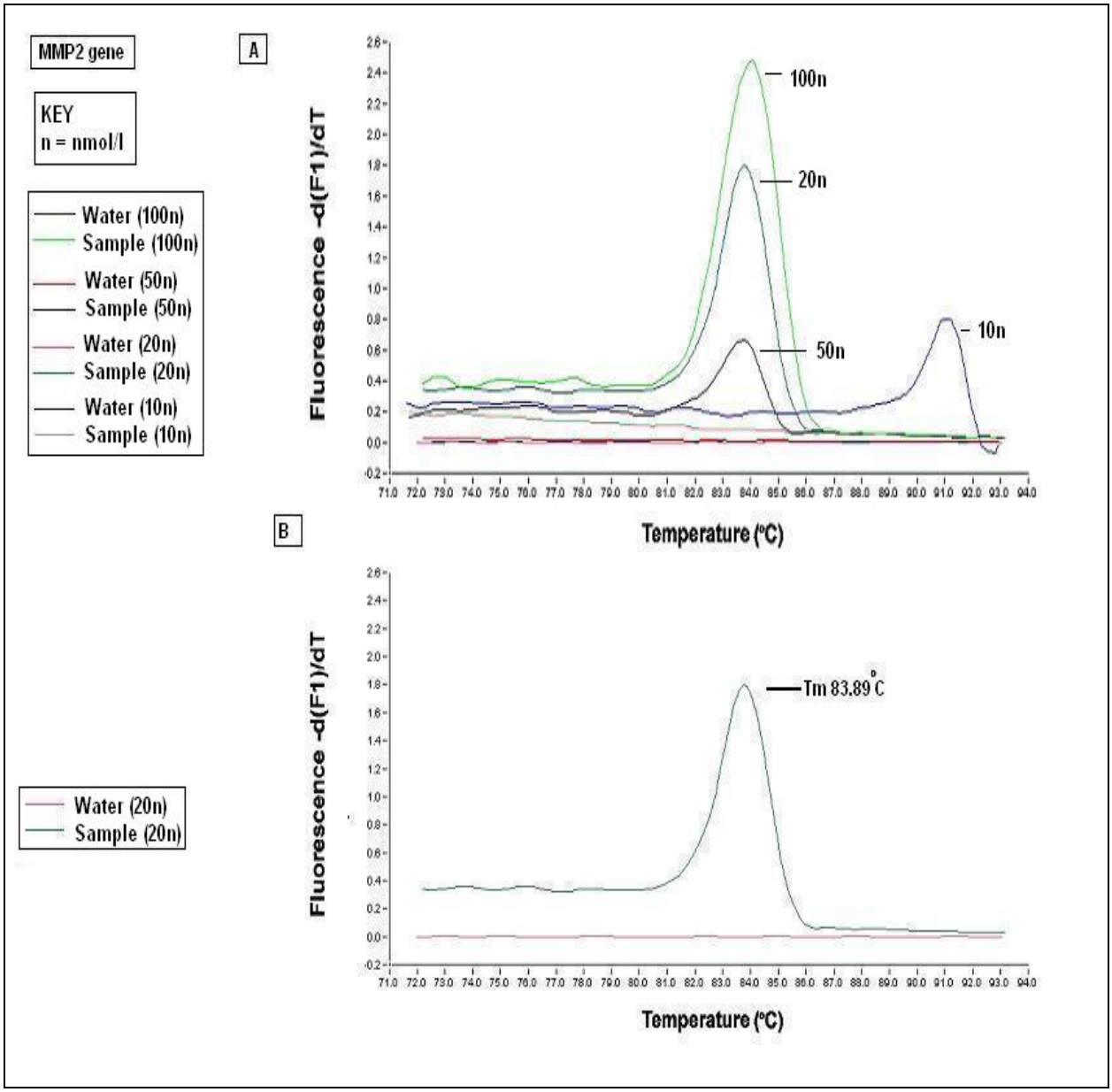

Figure 3.4. Primer titration melting curve analysis for *MMP2* amplification products with SYBR Green I dye. The graphs show the negative derivative of fluorescence plotted against temperature. Graph **A** demonstrates the different primer concentrations tested with 20nmol/l and 100nmol/l being the most efficient concentrations. Graph **B** indicates the specificity of the amplification reaction at the chosen optimal primer concentration (20nmol/l) as represented by a single peak with a melting temperature (Tm) of 83.9˚C.

3.2.2 Magnesium chloride titration

Figure 3.5 shows a representative real time PCR melting curve profile for the *MMP2* PCR products obtained with different $MgCl_2$ concentrations using the SYBR Green I detection system. The $MgCl_2$ concentrations ranged from 1.5mmol/l to 6mmol/l. The most efficient standardised $MgCl_2$ concentration was shown to be 3mmol/l for all genes (*HER1*, *HER2*, *VEGF*, *MMP2*, *GAPDH*) based on the efficiency of the amplification reaction and the absence of non specific amplification products.

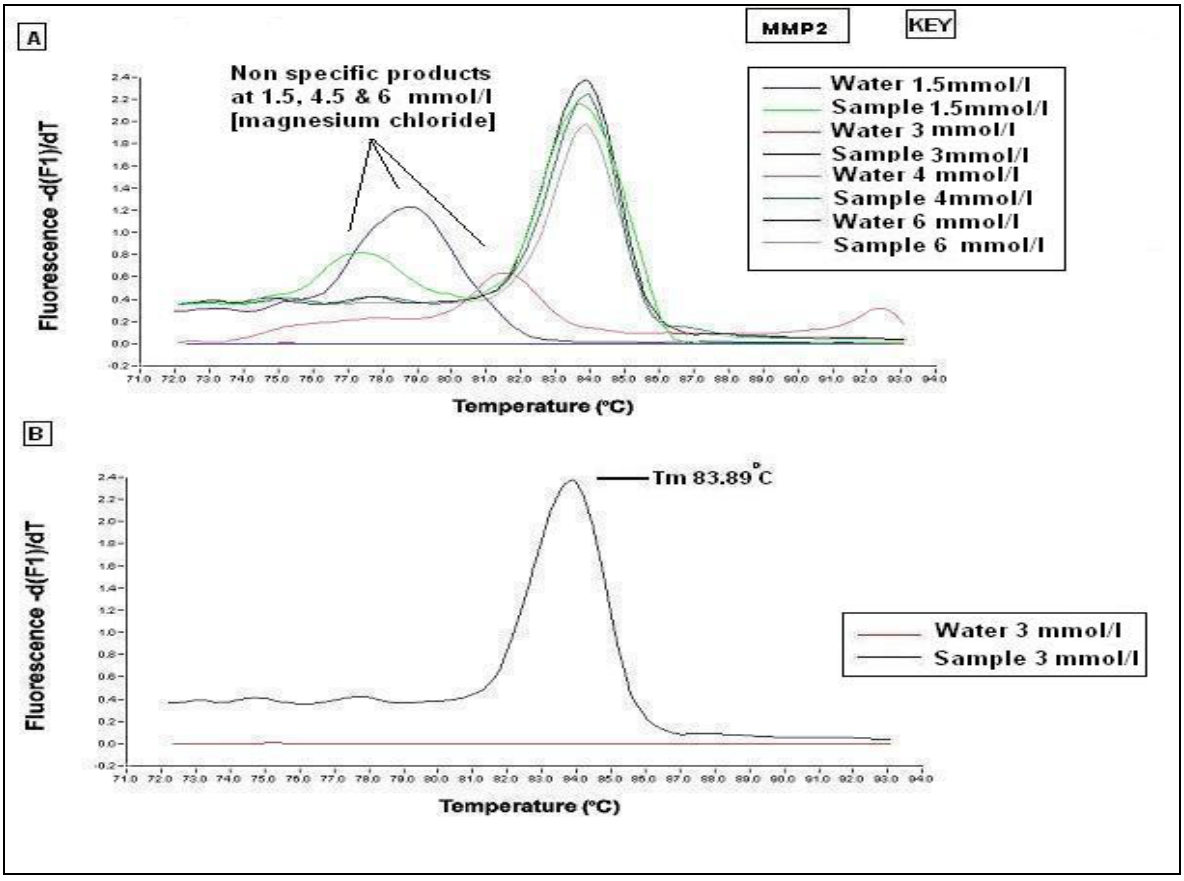

Figure 3.5. $MgCl_2$ titration melting curve analysis for *MMP2* amplification products with SYBR Green I dye. The graphs show the negative derivative of fluorescence plotted against temperature. Graph **A** shows non specific amplification products at the various $MgCl_2$ concentrations and graph **B** shows 3mmol/l $MgCl_2$ concentration to be the most efficient.

3.3 Relative gene expression of *VEGF* and *GAPDH* using SYBR Green I

Real time PCR with the SYBR Green I system was used to create standard curves for the *GAPDH* and *VEGF* genes. As mentioned previously in section 2.6.2, standard curves comprised serial dilutions of amplified PCR products as a standard template. The number of molecules of amplified product was calculated and dilutions of the amplicon, in duplicate, were performed on order to construct the standard curve for each gene (*GAPDH* and *VEGF*). Standard curves were generated by plotting the logarithmic concentration of the number of molecules against the cycle number at which the PCR product was initially detected (crossing point) as seen in Figure 3.6, A and B.

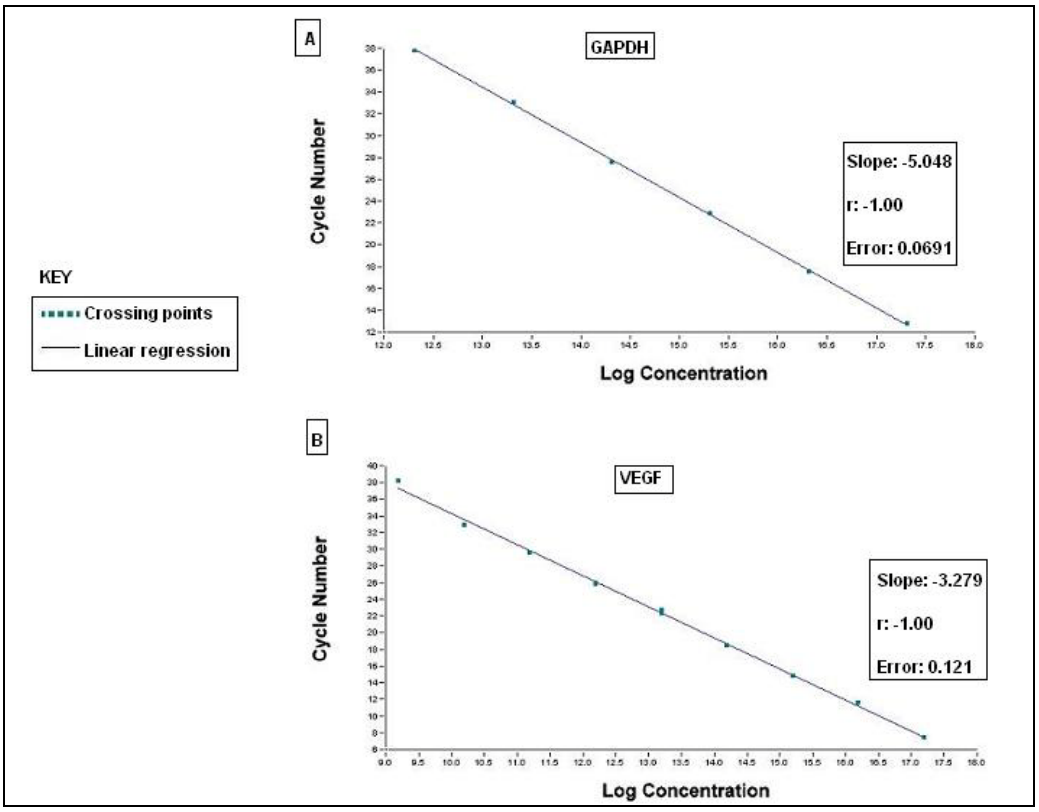

Figure 3.6. Standard curves for *GAPDH* (A) and *VEGF* (B) using the SYBR Green I system. The standard curve was generated by plotting the crossing points (cycle number) of each standard against the logarithmic concentration.

The error value reflects tube to tube variations and should be lower than 10^{-1}. The slope of the graph represents the overall reaction efficiency. For an optimal efficiency, the slope should be between -5.7 and -2.9 (Roche Molecular Biochemicals, 2000). The average efficiency of a PCR reaction was calculated as $10^{-1/slope}$. A theoretical efficiency of 2 suggests that 100% of the template is converted to product (Rasmussen, 2001). The efficiencies for each standard curve were calculated to be **1.58** for *GAPDH* and **2.02** for *VEGF*.

The melting temperature (Tm) of the gene products are seen in Figure 3.7 and were found to be 86˚C and 83˚C for the *GAPDH* and *VEGF* products, respectively. The Lightcycler melting curve analysis for *GAPDH* and *VEGF* with the SYBR Green I system showed pure homogenous PCR products for each gene, as reflected by the single tight melting peak in Figure 3.7. Melting curves were converted to melting peaks by plotting the first negative derivative (-d(F1/F2)dT)) against temperature.

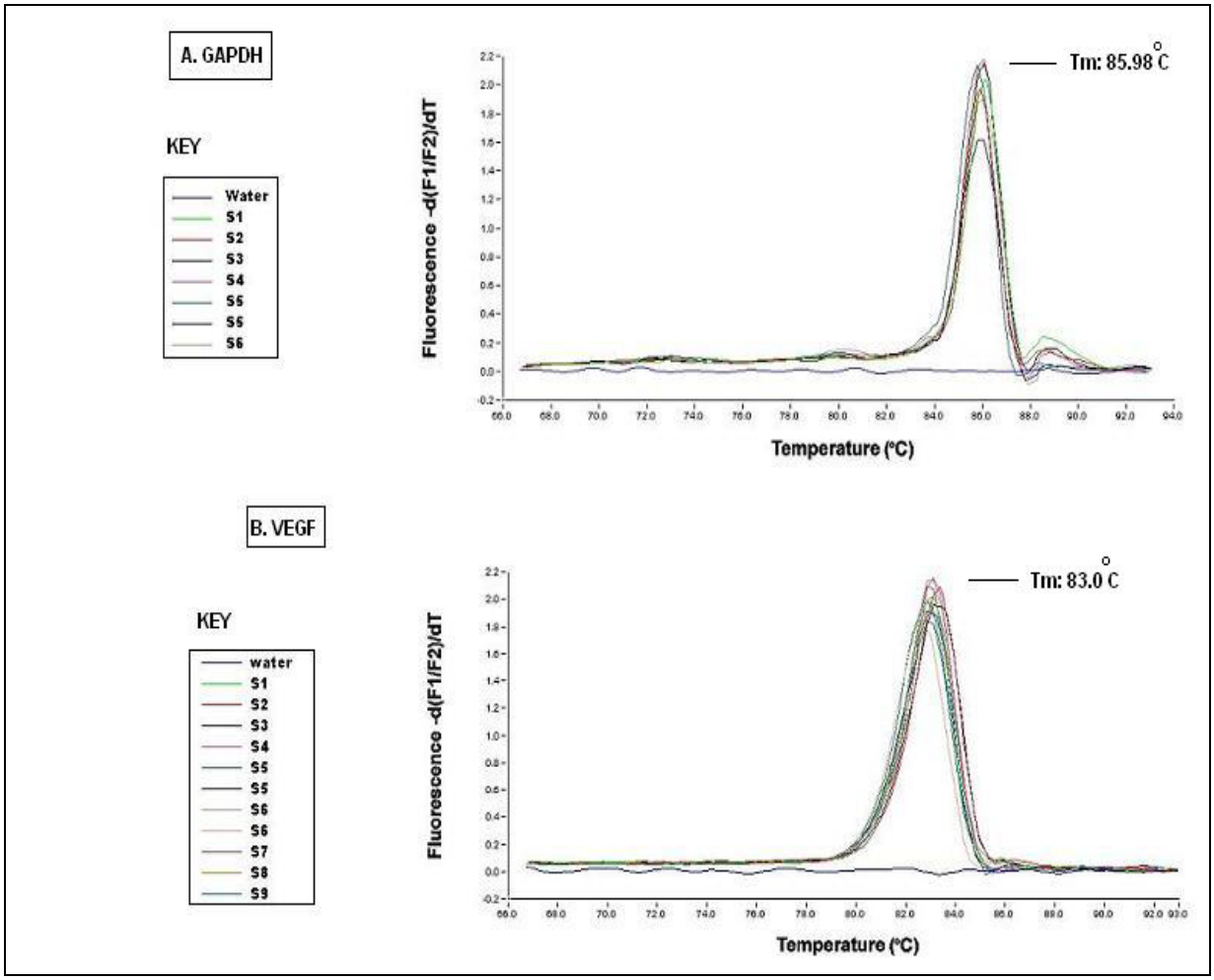

Figure 3.7. Melting peaks for PCR products of *GAPDH* (A) and *VEGF* (B). The melting temperature (Tm) of gene product which corresponds to the peak of the Gauss curve was 86˚C for *GAPDH* and 83˚C for *VEGF*.

The *VEGF* and *GAPDH* gene expression in tumour and normal tissue were quantified as illustrated in Figure 3.8. Standards from previously generated standard curves, as discussed above, were included in the real time PCR to quantify the respective gene expression in oesophageal tissue. Additionally, previously created standard curves were imported after the real time PCR was completed to allow the onboard Lightcycler software to calculate the respective gene expression in each sample. The data were then used for the statistical data analyses which are described in detail in section 3.7.

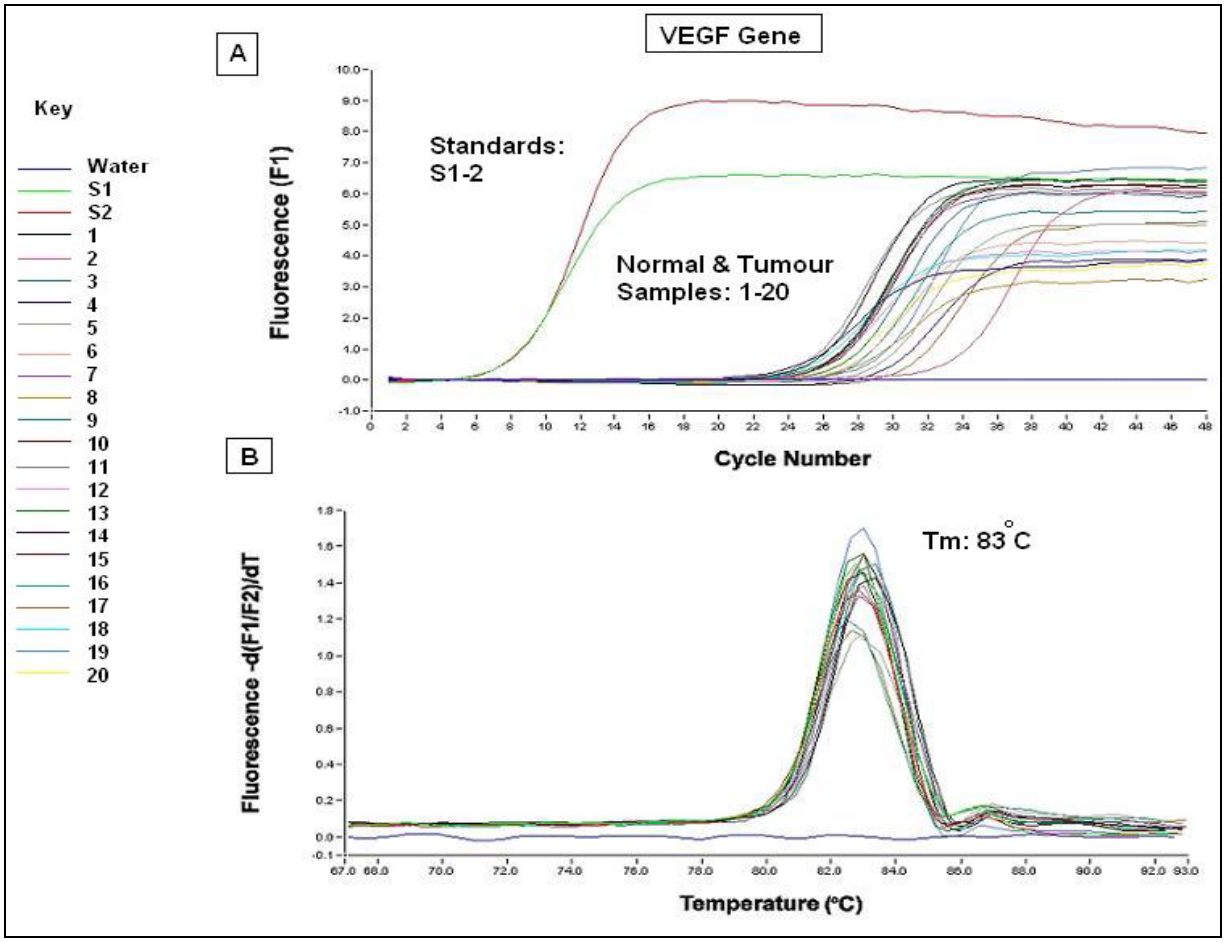

Figure 3.8. Real time PCR quantification of *VEGF* gene expression in normal and tumour oesophageal tissue samples using the standard curve method and SYBR Green I technology. Standards from previously constructed standard curves were used to quantify the *VEGF* gene expression in oesophageal tissue.

3.4 Relative gene expression using UPL technology

Standard curves for the *GAPDH*, *VEGF*, *HER1*, *MMP2* and *HER2* genes were generated using the UPL system. As mentioned previously in section 2.6.2, standard curves were produced by using serial dilutions of individual amplified PCR products as standard templates.

A significant increase in fluorescence above the baseline value indicated the detection of accumulated PCR product as illustrated in Figure 3.9 (A) for different dilutions of the gene product. Standard curves were generated by plotting the logarithmic concentration of the number of molecules against the cycle number at which the PCR product was initially detected (crossing point) as shown in Figures 3.9 (B), and 3.10 (A-D). The average efficiency of the PCR reaction was calculated as described in section 3.3 and found to be **1.94** for *GAPDH*, **2.04** for *VEGF*, **1.96** for *HER1*, **1.97** for *HER2* and **1.65** for *MMP2*.

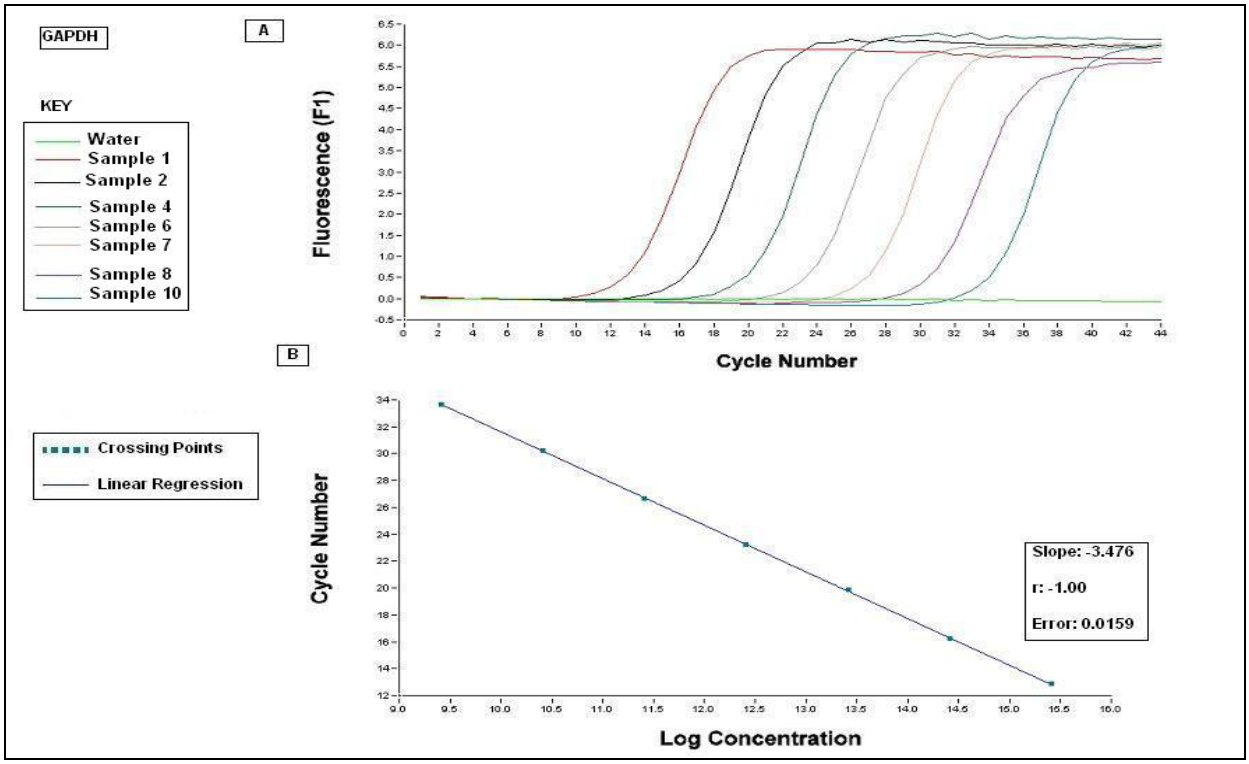

Figure 3.9. Representative standard curves for the *GAPDH* gene using the UPL system. **A.** PCR of a dilution series of *GAPDH* amplicon was used as a standard template to construct an amplification curve. The exponential phase of the PCR is represented by the log linear segment of the curve. **B**. The standard curve was produced by plotting the crossing points (cycle number) of each standard against the logarithmic concentration.

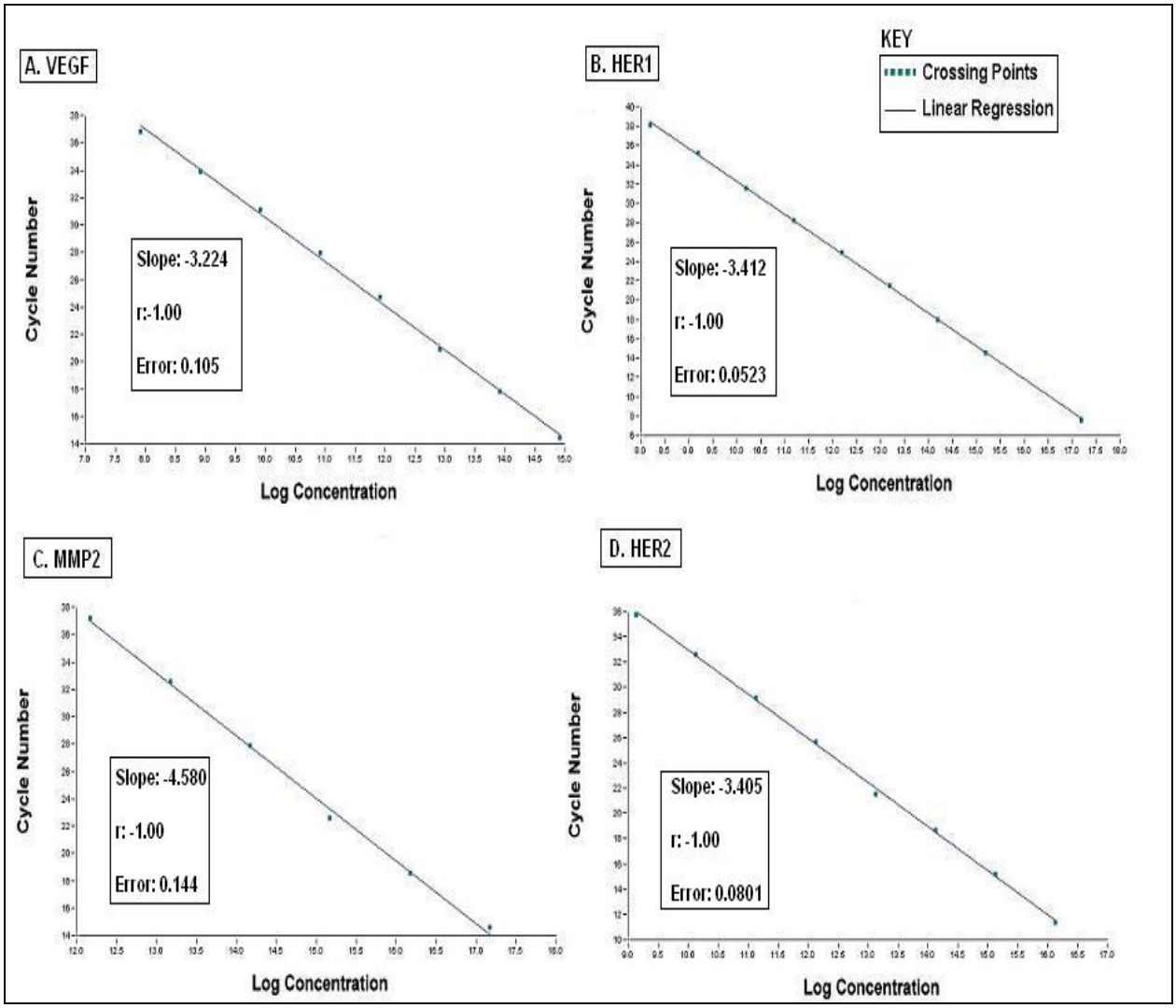

Figure 3.10. Standard curves for the genes *VEGF* (A), *HER1* (B), *MMP2* (C) and *HER2* (D) using the UPL system.

Gene expression of the different genes in tumour and normal oesophageal tissue was quantified using standards from previous standard curves in the real time PCR, as illustrated in Figure 3.11 for the *VEGF* gene. Additionally, previously generated standard curves, as discussed above, were imported after the real time PCR was completed to allow the onboard Lightcycler software to calculate the respective gene expression in each sample.

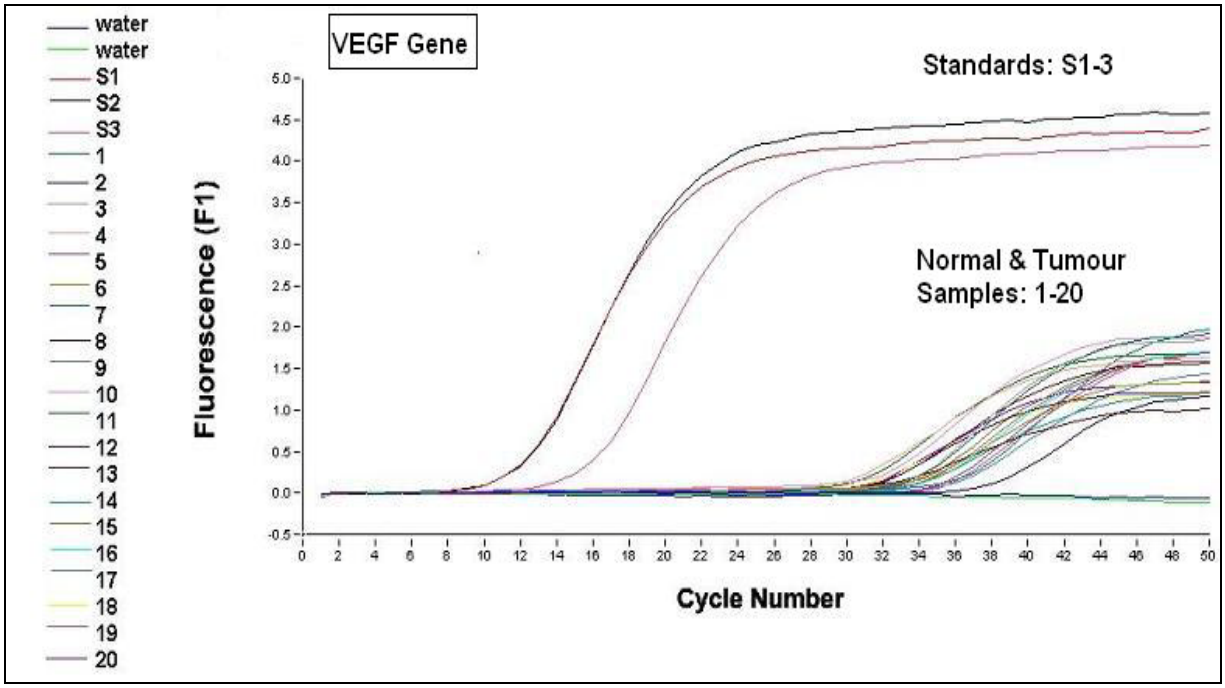

Figure 3.11. A representative real time PCR quantification of *VEGF* gene expression in normal and tumour oesophageal tissue using UPL technology. Standards from previously constructed standard curves were included in the experiment in order to quantify the *VEGF* gene expression in oesophageal tissue.

3.5 Relative gene expression using the Pfaffl model

The Pfaffl model of relative expression of target genes is based on real time PCR efficiencies. Efficiency curves were constructed for *GAPDH*, *VEGF*, *HER1*, *HER2* and *MMP2* using the UPL system as illustrated in Figure 3.12, and for *GAPDH* and *VEGF* using the SYBR Green I system as shown in Figure 3.13.

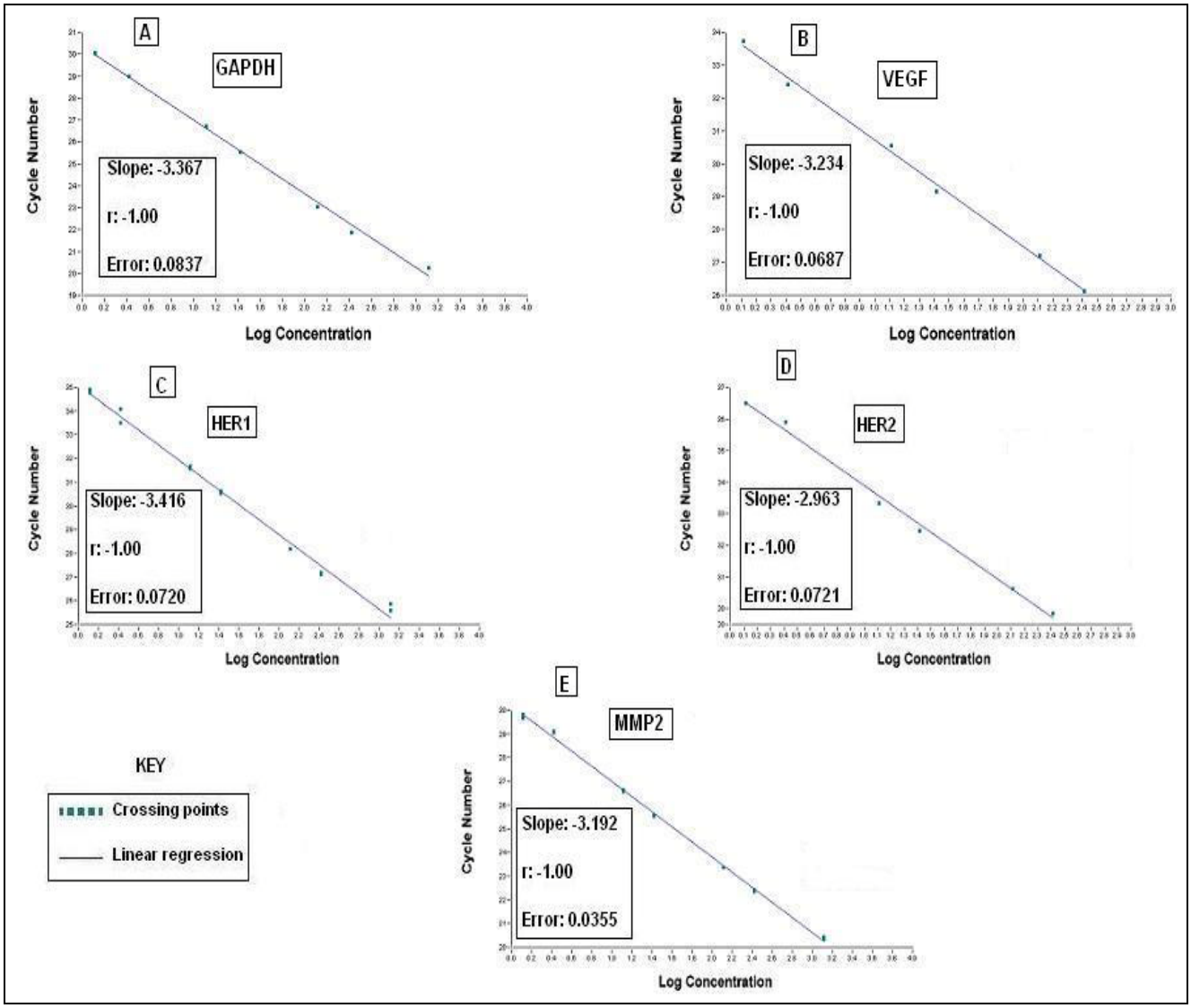

Figure 3.12. Real time PCR efficiency curves for *GAPDH* (A), *VEGF* (B), *HER1* (C), *HER2* (D) and *MMP2* (E) using the UPL system. The cycle number of crossing points was plotted against the log concentrations of cDNA (reverse transcribed total RNA) to calculate the slope. The corresponding real time PCR efficiency was calculated using the equation: $E = 10^{[-1/slope]}$.

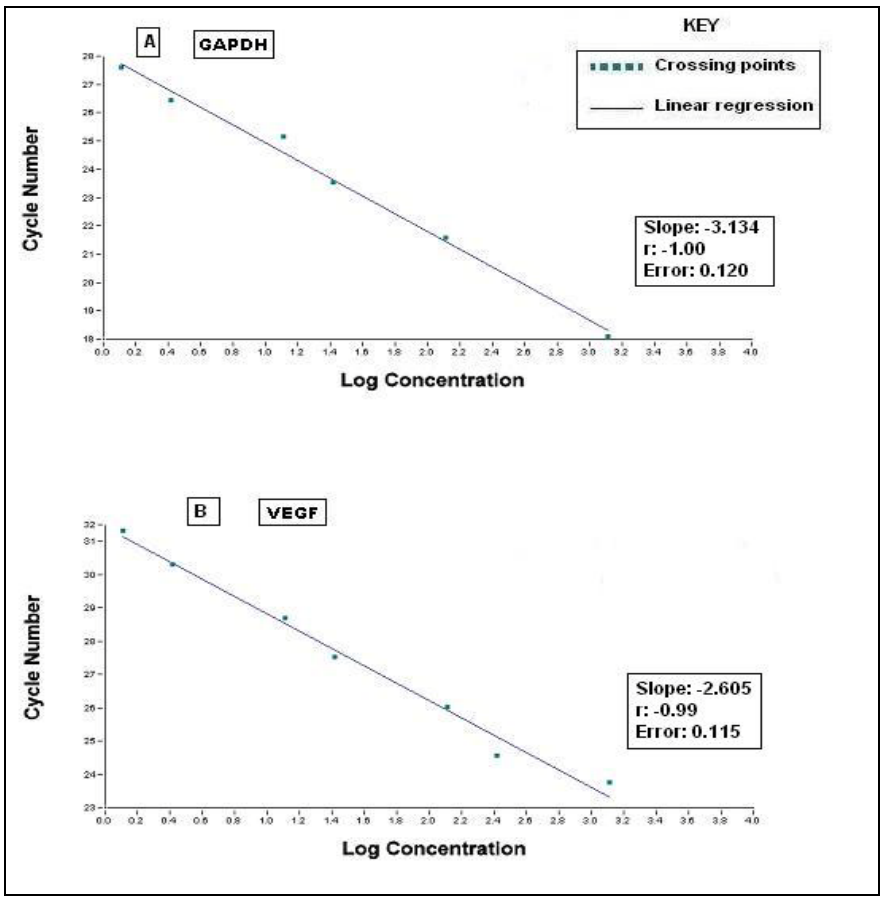

Figure 3.13. Real time PCR efficiency curves for *GAPDH* (A) and *VEGF* (B) using the SYBR Green I system. The cycle number of crossing points was plotted against the log concentrations of cDNA (reverse transcribed total RNA) to calculate the slope. The corresponding real time PCR efficiency was calculated using the equation: $E = 10^{[-1/slope]}$.

A pooled mixture of serial dilutions of cDNA of all normal and tumour oesophageal samples was used to create the efficiency curves, based on the method described by Pfaffl (2001) as described previously in Section 2.8. The efficiencies of the curves calculated by the REST software after the input of CP values, were **1.85** for *GAPDH* using UPL, **2.11** for *GAPDH* using SYBR Green I, **2** for *VEGF* using UPL, **2.38** for *VEGF* using SYBR Green I, **1.89** for *HER1* using UPL, **2.11** for *HER2* using UPL and **1.88** for *MMP2* using UPL.

The REST software used the incorporated pair-wise fixed reallocation randomization test and Pearson's correlation coefficient to generate relative expression ratios and p values, respectively, for the genes concerned as illustrated in Figure 3.14.

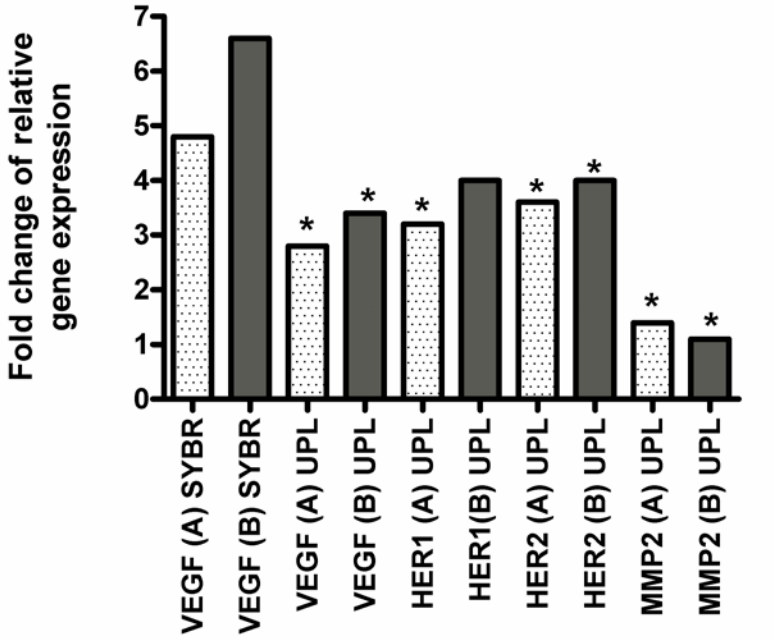

Figure 3.14. Fold change of the relative gene expressions of *VEGF*, *HER1*, *HER2* and *MMP2* in oesophageal tumours for both groups **A** and **B** calculated using the Relative Expression Software Tool (REST) © and the UPL system, and of *VEGF* using the SYBR Green I (SYBR) system. * indicates statistical significance of the differential gene expression of normal and tumour oesophageal tissue.

The relative expression ratios were described as being up or down regulated and were calculated by the comparison of gene expression values in normal and tumour oesophageal tissue, on the basis of their group mean values and normalised by the *GAPDH* gene expression values (Pfaffl et al, 2002).

Upregulation in groups A and B was found to be **2.8** and **3.4** fold respectively, for *VEGF* using the UPL system, and **4.8** and **6.6** using the SYBR Green I system, **3.2** and **4** for *HER1* using the UPL system, **3.6** and **4** for *HER2* using the UPL system and **1.4** and **1.1** for *MMP2* using the UPL system.

The statistical significance of gene expression differences between normal and tumour oesophageal tissue for each gene were tested by the REST software using the Pearson's correlation coefficient. The p values were calculated by obtaining the proportion of random allocations of the mean observed data to the normal and tumour samples (Pfaffl et al., 2002). Relative gene expression using the UPL system showed that the differential gene expression of normal and tumour oesophageal tissue was significantly upregulated in all genes, in group A and B ($p = 0.001$), except for *HER1* in group B. Differences in the *VEGF* gene expression of normal and tumour tissue was found to be insignificant in all samples with the UPL and SYBR Green I systems.

3.6 Histopathological assessment of oesophageal samples

Nineteen pairs of matched tumour and normal tissue from the 30 pair cohort were assessed by a pathologist and the investigator using a double-headed microscope (Appendix I). It was found that in 28 (**73.7%)** of the 38 specimens, there was agreement between the surgical and microscopic classification. Of these specimens:

- 7 'normal' specimens comprised deep oesophageal tissue (muscle) and fat. Surface epithelium was not represented
- 2 'tumour' specimens contained very little tumour tissue (<10 cells)

In 10 (**26.3%)** of the 38 specimens, there was disagreement between the surgical and microscopic assessment. Of these specimens:

- 5 ‘normal’ samples contained carcinoma (Figure 3.15)
- 2 ‘normal’ samples were equivocal for carcinoma due to poor quality (Figure 3.16)
- 2 ‘tumour’ samples did not contain tumour
- 1 ‘tumour’ sample was too degenerate for assessment (Figure 3.16)

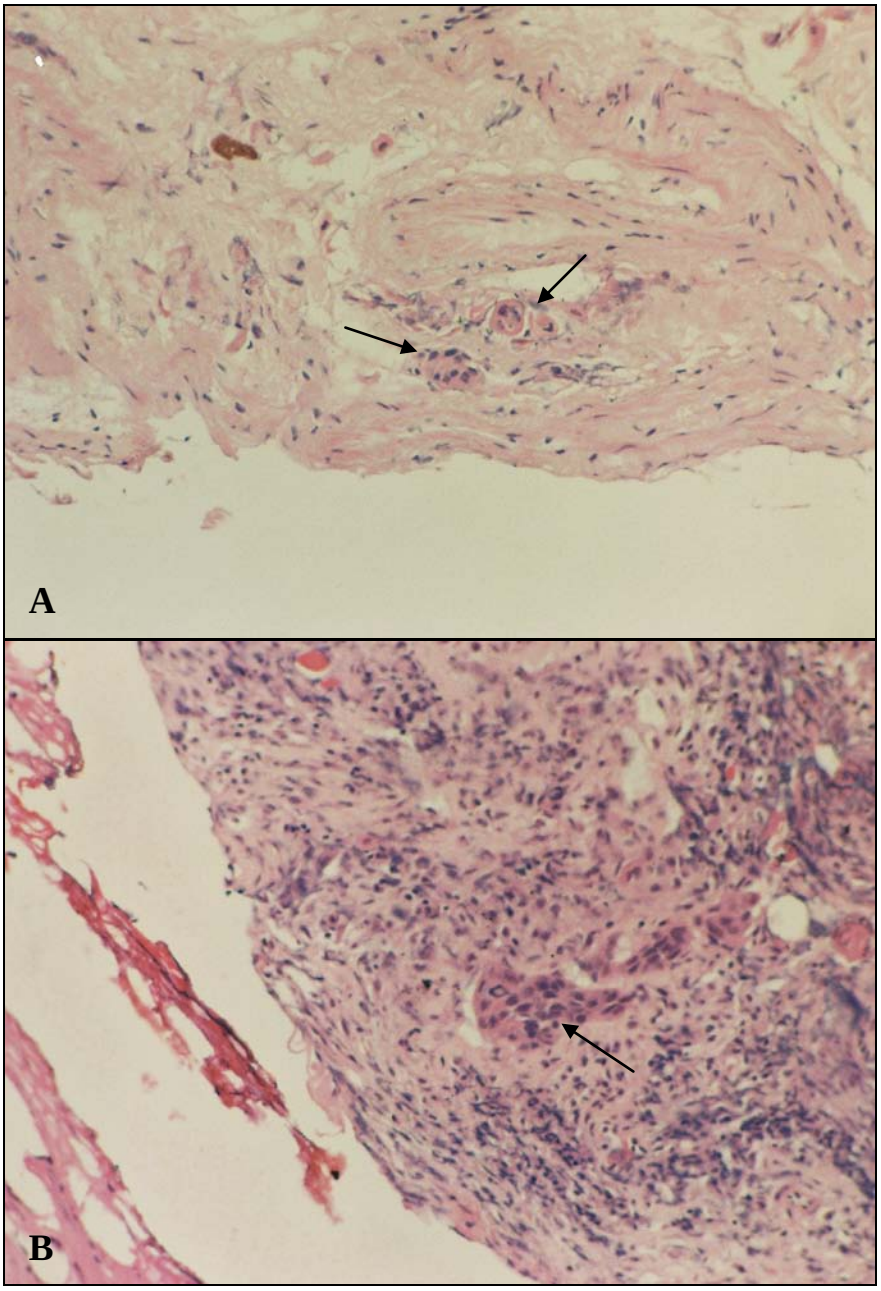

Figure 3.15. A and **B**, Histological section of visually classified ‘normal’ oesophageal tissue containing infiltrating tumour cells (arrow) (Sample 1 and 45) (H&E stain: original magnification, x 120).

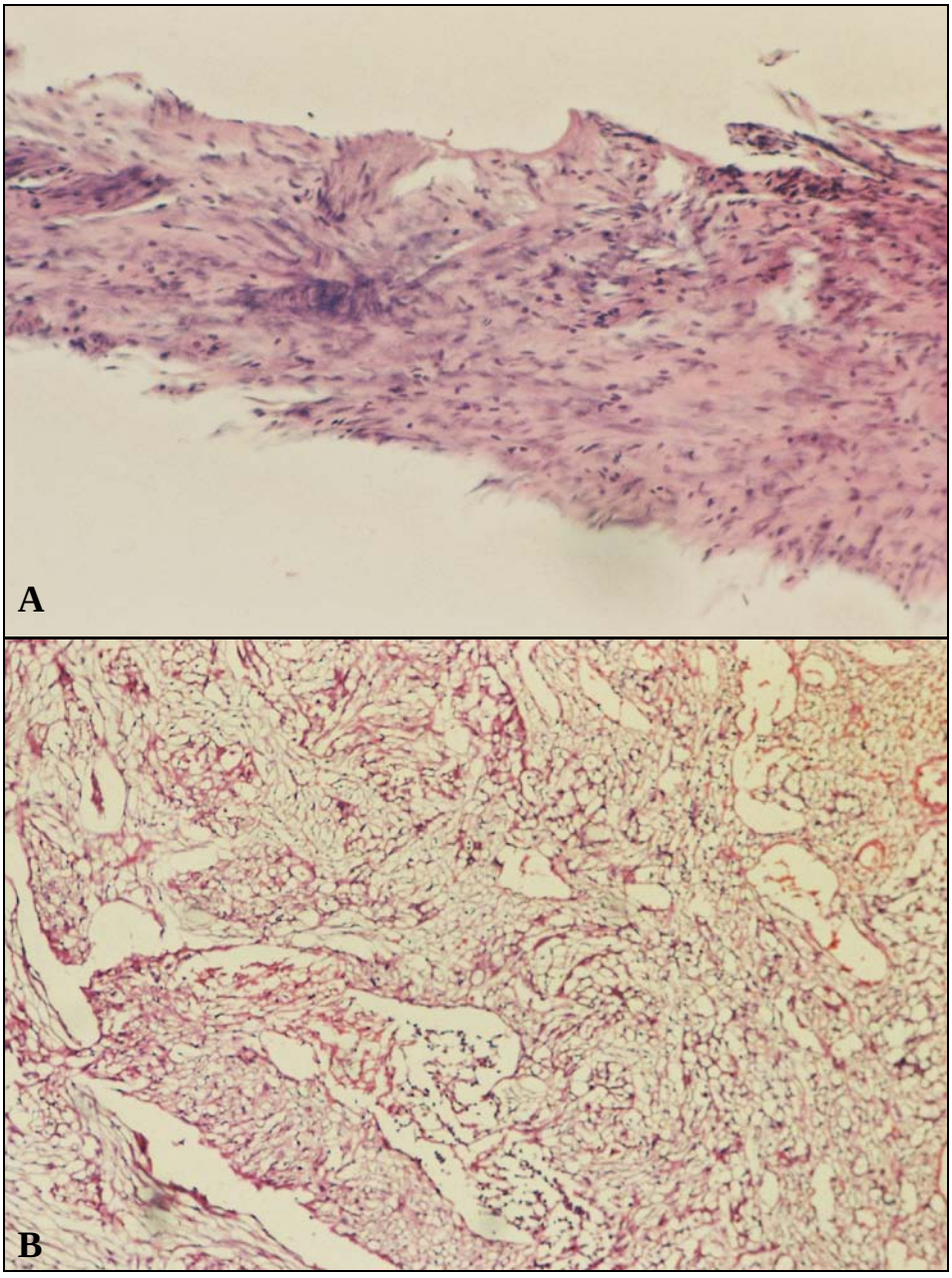

Figure 3.16. A. Degenerate oesophageal tissue (Sample 9, H&E stain: original magnification, x 120), **B.** Degeneration of oesophageal tissue due to freeze-thawing of sample (Sample 44, H&E stain: original magnification, x 240).

The 10 specimens that were discordant with the original classification affected 8 matched pairs, leaving 22 matched pairs for further analyses.

3.7 Statistical evaluation of relative gene expression using the standard curve method

As discussed previously in section 2.10.1, the relative gene expression values for each normal and tumour oesophageal sample was normalised by dividing by the respective housekeeping gene (*GAPDH*) values. The resulting values were the relative gene expression values for each gene in each sample. As discussed previously, two sets of data analyses were performed for the calculation of relative gene expression with the standard curve method. The first group designated **A**, included all 30 patients originally enrolled in the study. The second data set designated **B**, consisted of the 22 patients after the removal of 8 patients with discordant histology (refer to sections 2.10 and 3.6).

3.7.1 Relative gene expression of oesophageal tumours

The median relative expression data for all genes are presented in Table 3.1. The individual data were calculated by the Lightcycler software based on standard curves and CP values.

Table 3.1. The median relative gene expression values for normal and tumour oesphageal tissue obtained using the UPL and SYBR Green I systems.

	Group A	**Group B**
Gene/*GAPDH* (UPL)	**Median values**	**Median values**
VEGF Normal	0.01	0.18
VEGF Tumour	0.27	0.34
MMP2 Normal	350.09	247.38
MMP2 Tumour	443.42	361.94
HER1 Normal	0.47	0.04
HER1 Tumour	0.10	0.12
HER2 Normal	0.60	0.043
HER2 Tumour	0.99	0.064
Gene/*GAPDH* (SYBR)		
VEGF Normal	0.0021	0.0024
VEGF Tumour	0.0078	0.009

The median relative gene expression values for tumours were generally higher than those in normal tissue for all target genes, except for *HER1*, as calculated with both the UPL and SYBR Green I systems. The relative gene expression values for *MMP2* demonstrated a much higher range of values in comparison to the other genes.

Box-whisker plots shown below represent a comparison between the relative gene expression median values for tumour and normal oesophageal tissue. The Wilcoxon signed ranks test for matched pairs (non parametric) was used to compare the relative gene expression between normal and tumour oesophageal tissue for each patient. The Pearson's correlation coefficient was used to test if differences in results between the two groups were statistically significant. Statistical significance was taken at the level of $p < 0.05$.

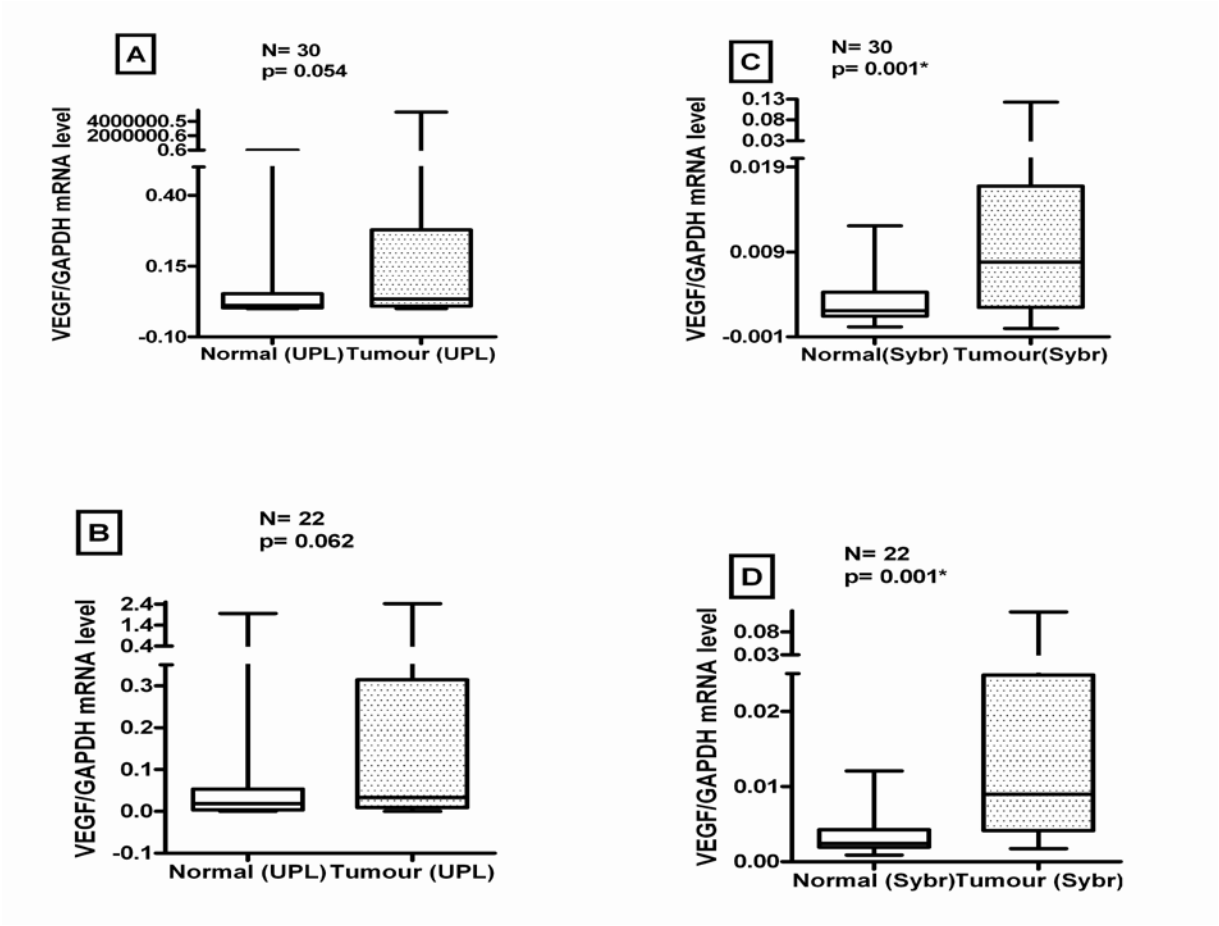

Figure 3.17. Box-whisker plots of the relative expression and variability in mRNA levels for the *VEGF* gene in normal and tumour oesophageal tissue in group A using UPL (A), group B using UPL (B), group A using SYBR Green I (C) and group B using SYBR Green I (D).
* indicates statistical significance.

The *VEGF* gene expression calculated using the UPL system was higher in tumour tissue compared with normal tissue for both data sets, but the differences were only of borderline significance. The *VEGF* gene expression in group B showed a smaller range of mRNA values in comparison with group A. The removal of discordant samples from group A removed those gene expression values that represented outliers. The relative *VEGF* gene expression as detected by the SYBR Green I system was significantly different in normal and tumour tissue for both groups A and B.

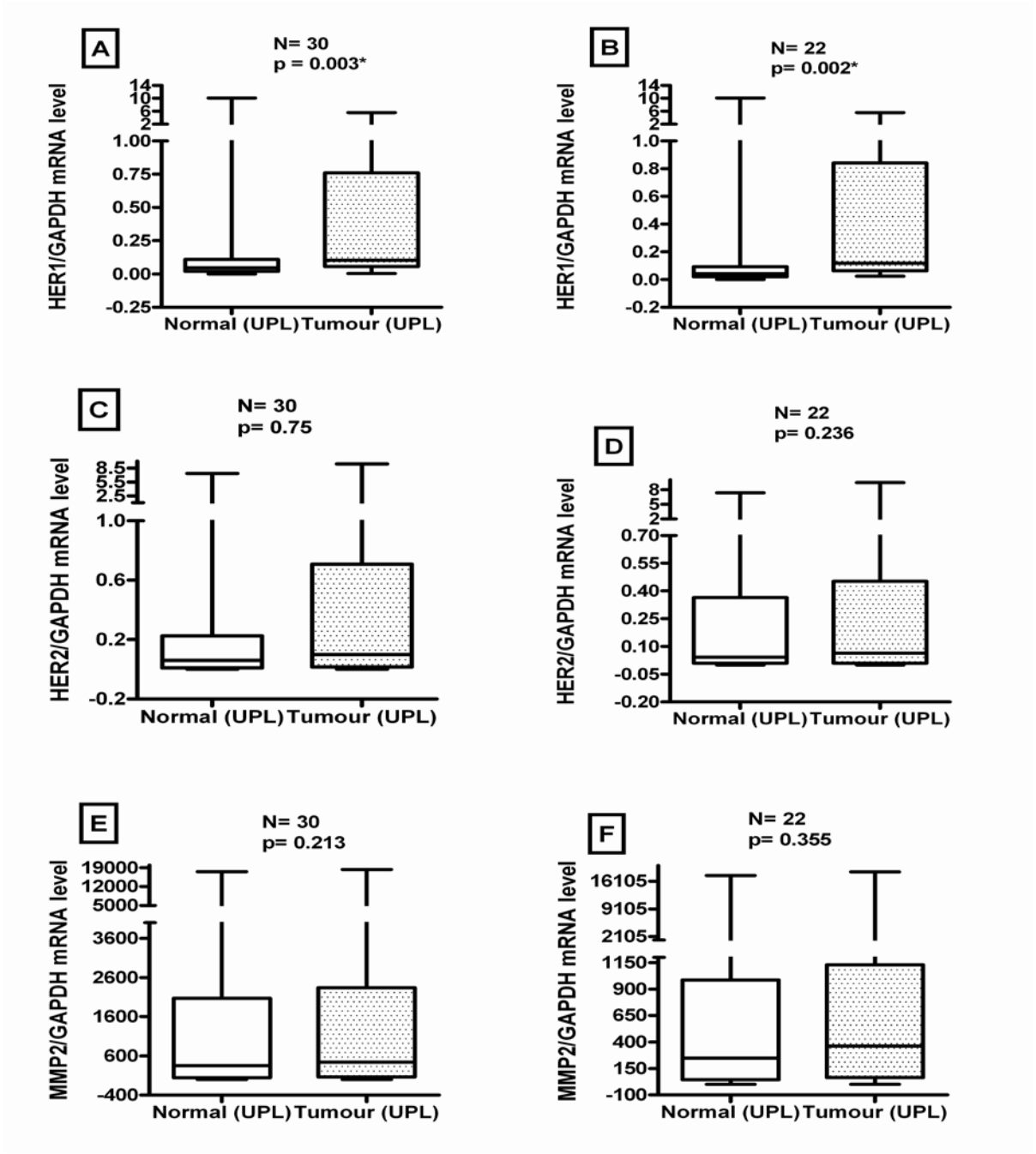

Figure 3.18. Box-whisker plots of the relative gene expression and variability in mRNA levels for: *HER1* in group A (A), *HER1* in group B (B), *HER2* in group A (C), *HER2* in group B (D), *MMP2* in group A (E) and *MMP2* in group B (F), in normal and tumour oesophageal tissue using the UPL system. * indicates statistical significance.

As seen Figure 3.18 above, the *HER1* gene expression calculated using the UPL system was significantly higher in oesophageal tumours compared with normal tissue for both groups A and B. The *HER2* and *MMP2* gene expressions calculated with the UPL system were however, not significantly different between tumour and normal samples.

3.7.2 Fold change of gene expression

As discussed previously in section 2.10.1, the tumour/normal ratio (T/N) is an average fold change (increase or decrease) in the expression of a gene in the sample population. The T/N ratio of sample mRNA expression values was considered to be upregulated when T/N **>1.0** (tumour higher than normal) or downregulated when T/N **< 1.0** (tumour lower than normal). The fold change values are illustrated in Figure 3.19 for each group studied and are represented by the median T/N values of normal and tumour oesophageal samples that are normalised by *GAPDH*.

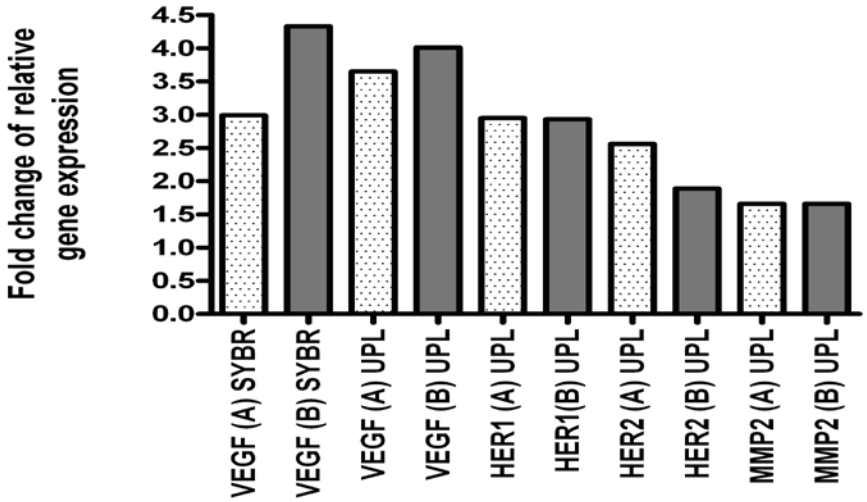

Figure 3.19. Fold change of the relative gene expression of *VEGF* in oesophageal tumours for both groups A and B using the SYBR Green I system (SYBR) and *VEGF*, *HER1*, *HER2* and *MMP2* using the UPL system and calculated using REST.

The fold change values in groups A and B were **3.6** and **4** for *VEGF* using UPL, **3** and **4** for *VEGF* using SYBR Green I, **2.9** in both groups for *HER1* using UPL, **2.6** and **1.9** for *HER2* using UPL and **1.7** in both groups for *MMP2*. The *VEGF* gene displayed the highest fold change in comparison to the other genes analysed with this system, while *MMP2* showed the least degree of upregulation in this cohort of patients.

The percentages of individuals within each group whose tumours showed an increase or decrease in the frequency of gene expression relative to normal tissue are shown in Table 3.2. The majority of individuals showed upregulation of all four genes examined.

Table 3.2. Frequency of fold change (Tumour/Normal) for all target genes in groups A and B.

Genes T/N (UPL)	**Upregulated (%)**	**Downregulated (%)**
A. *VEGF*	70	30
B. *VEGF*	72.7	27.3
A. *MMP2*	63.3	36.7
B. *MMP2*	63.6	36.4
A. *HER1*	83.3	16.7
B. *HER1*	90.9	9.1
A. *HER2*	63.3	36.7
B. *HER2*	59.1	40.9
Genes T/N (SYBR)		
A. *VEGF*	76.7	23.3
B. *VEGF*	86.4	13.6

3.7.3 Comparison between UPL and SYBR Green I systems

Table 3.3 shows the comparison of the expression of *VEGF* in groups A and B as detected by the UPL and SYBR Green I systems. The chi squared and McNemar tests were used to examine the level of discordance between both systems.

Table 3.3. Comparison of the *VEGF* relative gene expression frequency between the UPL and SYBR Green I systems.

	VEGF upregulation (%)		*VEGF* downregulation (%)		McNemar test (P)
	Group A	Group B	Group A	Group B	
VEGF UPL	**70**	**72.7**	**30**	**27.3**	
VEGF SYBR	**76.7**	**86.4**	**23.3**	**13.6**	
					0.688-Group A **0.250**- Group B

The percentage of *VEGF* upregulation was slightly higher using the SYBR Green I system than the UPL system, in both groups A and B but the differences were not statistically significant. Pearson's correlation coefficient was used to compare the normal, tumour and fold change values between the UPL and SYBR Green I systems. The normal, tumour and fold change values were significantly different from each other when comparing the UPL and SYBR Green I systems in group A (Table 3.4). In group B, the normal and tumour were significantly different from each other but not the fold change values. However, the chi squared and McNemar tests calculated that the UPL and SYBR Green I systems were similar, overall, in their detection of gene expression.

Table 3.4. Comparison of the *VEGF* relative gene expression in normal and tumour tissue and fold change value between the UPL and the SYBR Green I systems.

***VEGF* expression**	**P value (Group A)**	**P value (Group B)**
Normal tissue (UPL) vs Normal tissue (SYBR)	S (0.0)	S(0.0)
Tumour tissue (UPL) vs Tumour tissue (UPL)	S(0.001)	S (0.006)
T/N (UPL) vs T/N (SYBR)	S (0.015)	NS

3.8 Histopathological and clinical assessment of patients with OSCC

As mentioned previously (section 2.2 and 3.6), data evaluation was carried out on two groups: Group **A** comprised 30 patients and group **B** the remaining 22 patients after removal of discordant samples. For the histopathological analysis, 3 patients had no available clinical data. Therefore group A comprised 27 patients and group B, 19 patients.

Photomicrographs of the histopathological features of OSCC that were analysed in the study cohorts are illustrated in Appendix J. The clinicopathological profile of patients and tumours is presented in Table 3.5. The mean age was 57.2 years for group A and 59.0 years for group B. The majority of patients had a tumour size of less than 5 cm and tumours were mostly moderately differentiated. Most patients had tumours that involved the adventitia and were positive for myenteric plexus invasion as well as perineurial invasion, and did not show lymph node involvement. Several patients however did not have lymph node tissue available for analysis. Dysplasia, carcinoma *in situ* and atypical mitoses were evident in the majority of patients. Mild necrosis (as well as anaplasia and a mitotic rate of less than 50 were seen in most patients. The majority of patients in group A showed lymphatic vessel invasion whereas most patients in group B did not exhibit lymphatic vessel invasion.

Table 3.5. Patient and tumour characteristics of squamous cell carcinomas of the oesophagus.

Factors	Group A	Group B
Mean age (yrs)	57.2	59
≤50 yrs	6 (22.2%)	3 (15.8%)
>50 yrs	21 (77.8%)	16 (84.2%)
Gender ratio		
Male	10 (17%)	7 (36.85)
Female	17 (63%)	12 (63.2%)
Race ratio		
Black	21 (77.8%)	14 (73.7%)
Indian	6 (22.2%)	5 (26.3%)
Size of tumour		
< 5 cm	15 (55.6%)	11 (57.9%)
≥5 cm	11 (40.7%)	7 (36.8%)
unavailable	1 (3.7%)	1 (5.3%)
Histological type		
Moderately differentiated	25 (92.6%)	18 (94.7%)
Poorly differentiated	2 (7.4%)	1 (5.3%)
Depth of Invasion (pT)		
Muscularis propria (pT_2)	1(3.7%)	1 (5.3%)
Adventitia (pT_3)	25 (92.6%)	17 (89.5%)
Adjacent structures (pT_4)	1 (3.7%)	1 (5.3%)
Lymphatic node involvement		
(-)	12 (44.4%)	9 (47.4%)
(+)	9 (33.3%)	6 (31.6%)
Unavailable	6 (22.2%)	4 (21.1%)
Myenteric plexus invasion		
(-)	1 (3.7%)	1 (5.3%)
(+)	26 (96.3%)	18 (94.7%)
Perineurial invasion		
(-)	3 (11.1%)	2 (10.5%)
(+)	24 (88.9%)	17 (89.5%)
Lymphatic vessel invasion		
(-)	6 (22.2%)	14 (73.7%)
(+)	21 (77.8%)	5 (26.3%)
Dysplasia		
(-)	1 (3.7%)	0
(+)	26 (96.3%)	19 (100%)
Carcinoma in situ		
(-)	10 (37%)	4 (21.1%)
(+)	17 (63%)	15 (78.9%)
Atypical mitoses		
(-)	12 (44.4%)	8 (42.1%)
(+)	15 (55.6%)	11 (57.9%)
Necrosis		
Mild (0-33%)	23 (85.2%)	16 (84.2%)
Moderate (34-66%)	4 (14.8%)	3 (15.8%)
Mitotic rate (no/10 HPF)		
≤ 50	23 (85.2%)	15 (78.9%)
>50	4 (14.8%)	4 (21.1%)
Anaplasia		
(-)	3 (11.1%)	1 (5.3%)
(+)	24 (88.9%)	18 (94.74%)

3.8.1 Correlation between *VEGF* expression using UPL and clinicopathological factors

The percentages of up and down regulation of *VEGF* expression determined using the UPL system, in relationship to clinical and pathological features, are represented in Table 3.6. In group A, *VEGF* upregulation was significantly associated with gender ($p = 0.012$) and race ($p = 0.044$): all black male patients displayed *VEGF* upregulation (raw data not shown). In group B (percentages not shown), *VEGF* expression was significantly associated with gender ($p = 0.044$): all male patients displayed *VEGF* upregulation and most black patients displayed *VEGF* upregulation. Upregulation of *VEGF* was not significantly associated with age although most patients older than 50 years of age showed upregulation of this gene. The majority of patients with lymphatic node involvement, lymphatic vessel invasion, myenteric plexus invasion and perineurial invasion showed *VEGF* upregulation. In all pathological categories, the majority of tumours showed *VEGF* upregulation.

Table 3.6. Correlation between clinicopathologic variables and expression status of the *VEGF* gene.

	Group A (n = 27)			**Group B (n = 19)**
Factors	***VEGF*↑**	***VEGF*↓**	**P**	**P**
Age			N.S.	N.S.
≤50	4 (66.7%)	2 (33.3%)		
>50	15 (71.4%)	6 (28.6%)		
Gender			**S (0.012)[a]**	**S. (0.044)[a]**
Male	10 (100%)	0		
Female	9 (52.9%)	8 (47.1%)		
Race			**S (0.044)[a]**	N.S.
Black	17 (81%)	4 (19%)		
Indian	2 (33.3%)	4 (66.7%)		
Size of Tumour			N.S.	N.S.
< 5 cm	11 (73.3%)	4 (26.7%)		
≥5 cm	8 (72.7%)	3 (27.3%)		
unavailable	1			
Histological type			N.S.	N.S.
Moderately differentiated	17 (68%)	8 (32%)		
Poorly differentiated	2 (100%)	0		
Depth of Invasion (pT)			N.S.	N.S.
Muscularis propria (pT_2)	1 (100%)	0		
Adventitia (pT_3)	18 (72%)	7 (28%)		
Adjacent structures (pT_4)	0	1 (100%)		
Lymphatic node involvement			N.S.	N.S
(-)	8 (66.7%)	4 (33.3%)		
(+)	7 (77.8%)	2 (22.2%)		
Unavailable	4 (66.7%)	2 (33.3%)		
Myenteric plexus invasion			N.S.	N.S
(-)	1 (100%)	0		
(+)	18 (69.2%)	8 (30.8%)		
Perineurial invasion			N.S.	
(-)	3 (100%)	0		
(+)	16 (66.7%)	8 (33.3%)		
Lymphatic vessel invasion			N.S.	N.S.
(-)	3 (50%)	3 (50%)		
(+)	16 (76.2%)	5 (23.8%)		
Mitotic rate (no/10 HPF)			N.S.	N.S.
≤ 50	17 (73.9%)	6 (26.1%)		
>50	2 (50%)	2 (50%)		
Necrosis			N.S.	N.S.
Mild (0-33%)	17 (73.9%)	6 (26.1%)		
Moderate (34-66%)	2 (50%)	2 (50%)		
Anaplasia			N.S.	N.S.
(-)	3 (100%)	0		
(+)	16 (66.7%)	8 (33.3%)		

[a] Fisher's exact test (2-sided), [b] Pearson chi-square test (2-sided)

3.8.2 Correlation between *VEGF* expression using SYBR Green I and clinicopathological factors

The trends in *VEGF* expression as determined using the SYBR Green I system, in relation to clinicopathological features, are represented in Table 3.7. In group A, *VEGF* expression values showed a significant correlation with depth of invasion of tumour ($p = 0.046$). Most of the moderately invasive tumours showed upregulation of *VEGF*. In group B (percentages not shown), *VEGF* gene expression was not associated with any clinicopathological factors. Patients who were older than 50 years of age, or Black and male predominantly expressed *VEGF* upregulation. Tumours that had invaded the adventitia mostly expressed *VEGF* upregulation. Most patients with moderately differentiated tumours showed *VEGF* upregulation. Tumours less than 5 cm in size, positive for myenteric plexus invasion, perineurial invasion and lymphatic vessel invasion all showed *VEGF* upregulation. Tumours that displayed anaplasia, a mitotic rate of 50 or less than 50 as well as mild and moderate necrosis expressed *VEGF* upregulation. None of the differences in up and down regulation of the *VEGF* gene within individual clinicopathological categories were however statistically significant (Table 3.7).

Table 3.7. Correlation between clinicopathologic variables and expression status of the *VEGF* gene (SYBR Green I system).

	Group A (n = 27)			**Group B (n = 19)**
Factors	***VEGF*↑**	***VEGF*↓**	**P**	**P**
Age			N.S.	N.S.
≤50	3 (50%)	3 (50%)		
>50	17 (81%)	4 (19%)		
Gender			N.S.	N.S.
Male	8 (80%)	2 (20%)		
Female	12 (70.6%)	5 (29.4%)		
Race			N.S.	N.S.
Black	16 (76.2%)	5 (23.8%)		
Indian	4 (66.7%)	2 (33.3%)		
Size of Tumour			N.S.	N.S.
< 5 cm	13 (86.7%)	2 (13.3%)		
≥5 cm	7 (63.6%)	4 (36.4%)		
unavailable	1			
Histological type			N.S.	N.S.
Moderately differentiated	18 (72%)	7 (28%)		
Poorly differentiated	2 (100%)	0		
Depth of Invasion (pT)			**S (0.046)[b]**	N.S.
Muscularis propria (pT_2)	0	1 (100%)		
Adventitia (pT_3)	20 (80%)	5 (20%)		
Adjacent structures (pT_4)	0	1 (100%)		
Lymphatic node involvement			N.S.	N.S.
(-)	11 (91.7%)	1 (8.3%)		
(+)	5 (55.6%)	4 (44.4%)		
Unavailable	4 (66.7%)	2 (33.3%)		
Myenteric plexus invasion			N.S.	N.S.
(-)	1 (100%)	0		
(+)	19 (73.1%)	7 (26.9%)		
Perineurial invasion			N.S.	N.S.
(-)	2 (66.7%)	1 (33.3%)		
(+)	18 (75%)	6 (25%)		
Lymphatic Vessel invasion			N.S.	N.S.
(-)	4 (66.7%)	2 (33.3%)		
(+)	16 (76.2%)	5 (23.8%)		
Mitotic rate (no/10 HPF)			N.S.	N.S.
≤ 50	18 (78.3%)	5 (21.7%)		
>50	2 (50%)	2 (50%)		
Necrosis			N.S.	N.S.
Mild (0-33%)	16 (69.6%)	7 (30.4%)		
Moderate (34-66%)	4 (100%)	0		
Anaplasia			N.S.	N.S.
(-)	2 (66.7%)	1 (33.3%)		
(+)	18 (75%)	6 (25%)		

[a] Fishers exact test (2-sided), [b] Pearson chi-square test (2-sided)

3.8.3 Correlation between *HER1* expression using UPL and clinicopathological factors

Table 3.8 below shows the trends of *HER1* expression in relation to clinicopathologic factors. Upregulation of the *HER1* gene was not significantly associated with any clinicopathological factors. In all pathological categories, the majority of tumours showed *HER1* upregulation.

Table 3.8. Correlation between clinicopathologic variables and expression status of the *HER1* gene.

	Group A (n = 27)			**Group B (n = 19)**
Factors	***HER1*↑**	***HER1*↓**	**P**	**P**
Age			N.S.	N.S.
≤50	5 (83.3%)	1 (16.7%)		
>50	17 (81%)	4 (19%)		
Gender			N.S.	N.S.
Male	9 (90%)	1 (10%)		
Female	13 (76.5%)	4 (23.5%)		
Race			N.S.	N.S.
Black	17 (81%)	4 (19%)		
Indian	5 (83.3%)	1 (16.7%)		
Size of Tumour			N.S.	N.S.
< 5 cm	13 (86.7%)	2 (13.3%)		
≥5 cm	9 (81.8%)	2 (18.2%)		
unavailable	1			
Histological type			N.S.	N.S.
Moderately differentiated	20 (80%)	5 (20%)		
Poorly differentiated	2 (100%)	0		
Depth of Invasion (pT)			N.S.	N.S.
Muscularis propria (pT_2)	1 (100%)	0		
Adventitia (pT_3)	20 (80%)	5 (20%)		
Adjacent structures (pT_4)	1 (100%)	0		
Lymphatic node involvement			N.S.	N.S.
(-)	10 (83.3%)	2 (16.7%)		
(+)	7 (77.8%)	2 (22.2%)		
Unavailable	5 (83.3%)	1 (16.7%)		
Myenteric plexus invasion			N.S.	N.S.
(-)	1 (100%)	0		
(+)	21 (80.8%)	5 (19.2%)		
Perineurial invasion			N.S.	N.S.
(-)	3 (100%)	0		
(+)	19 (79.2%)	5 (20.8%)		
Lymphatic Vessel invasion			N.S.	N.S.
(-)	5 (83.3%)	1 (16.7%)		
(+)	17 (81%)	4 (19%)		
Mitotic rate (no/10 HPF)			N.S.	N.S.
≤ 50	19 (82.6%)	4 (17.4%)		
>50	3 (75%)	1 (25%)		
Necrosis			N.S.	N.S.
Mild (0-33%)	19 (82.6%)	4 (17.4%)		
Moderate (34-66%)	3 (75%)	1 (25%)		
Anaplasia			N.S.	N.S.
(-)	3	0		
(+)	19 (79.2%)	5 (20.8%)		

[a] Fisher's exact test (2-sided), [b] Pearson chi-square test (2-sided)

3.8.4 Correlation between *HER2* expression using UPL and clinicopathological factors

Table 3.9 below shows the trends in *HER2* expression in terms of clinical and pathological features. In group A, *HER2* upregulation was significantly associated with Black individuals whereas significantly more Indian patients displayed *HER2* down regulation ($p = 0.015$). This trend was seen in group B (percentages not shown), but was not statistically significant. Upregulation of *HER2* was predominant in most categories and especially in patients who were less than 50 years of age, in males more than females and in tumours that were less than or equal to 5cm. In group B, most tumours with mild necrosis and a mitotic rate of≤ 50 displayed *HER2* upregulation whereas tumours with moderate necrosis and a mitotic rate of above 50 showed *HER2* downregulation.

Table 3.9. Correlation between clinicopathologic variables and expression status of the *HER2* gene.

	Group A (n = 27)			**Group B (n = 19)**
Factors	***HER2*↑**	***HER2*↓**	**P**	**P**
Age			N.S.	N.S.
≤50	5 (83.3%)	1 (16.7%)		
>50	12 (57.1%)	9 (42.9%)		
Gender			N.S.	N.S.
Male	8 (80%)	2 (20%)		
Female	9 (52.9%)	8 (47.1%)		
Race			**S (0.015)[a]**	N.S.
Black	16 (76.2%)	5 (23.8%)		
Indian	1 (16.7%)	5 (83.3%)		
Size of Tumour			N.S.	N.S.
< 5 cm	11 (73.3%)	4 (26.7%)		
≥5 cm	6 (54.5%)	5 (45.5%)		
unavailable	1			
Histological type			N.S.	N.S.
Moderately differentiated	15 (60%)	10 (40%)		
Poorly differentiated	2 (100%)	0		
Depth of Invasion (pT)			N.S.	N.S.
Muscularis propria (pT_2)	1 (100%)	0		
Adventitia (pT_3)	16 (64%)	9 (36%)		
Adjacent structures (pT_4)	0	1 (100%)		
Lymphatic node involvement			N.S.	N.S.
(-)	8 (66.7%)	4 (33.3%)		
(+)	5 (55.6%)	4 (44.4%)		
Unavailable	4 (66.7%)	2 (33.3%)		
Myenteric plexus invasion			N.S.	N.S.
(-)	1 (100%)	0		
(+)	16 (61.5%)	10 (38.5%)		
Perineurial invasion			N.S.	N.S.
(-)	2 (66.7%)	1 (33.3%)		
(+)	15 (62.5%)	9 (37.5%)		
Lymphatic vessel invasion			N.S.	N.S
(-)	4 (66.7%)	2 (33.3%)		
(+)	13 (61.9%)	8 (38.1%)		
Mitotic rate (no/10 HPF)			N.S.	N.S.
≤ 50	16 (69.6%)	7 (30.4%)		
>50	1 (25%)	3 (75%)		
Necrosis			N.S.	N.S.
Mild (0-33%)	15 (65.2%)	8 (34.8%)		
Moderate (34-66%)	2 (50%)	3 (50%)		
Anaplasia			N.S.	N.S.
(-)	3 (100%)	0		
(+)	14 (58.3%)	10 (41.7%)		

[a] Fisher's exact test (2-sided), [b] Pearson chi-square test (2-sided)

3.8.5 Correlation between *MMP2* expression using UPL and clinicopathological factors

The trends of *MMP2* gene expression in terms of clinicopathological features are shown in Table 3.10. The only characteristic to show any significant relationship with *MMP2* expression was lymphatic node metastasis ($p = 0.030$) in group A. Patients with lymphatic node metastasis mainly showed *MMP2* downregulation and patients without lymphatic node metastasis showed *MMP2* upregulation. The *MMP2* gene expression in group B (percentages not shown) was not associated with any clinicopathologic factors but showed similar trends except with respect to ethnicity. In group A, most Indian male individuals presented *MMP2* upregulation whereas in group B most Black male individuals showed *MMP2* upregulation. In most pathologic categories the majority of tumours showed *MMP2* upregulation.

Table 3.10. Correlation between clinicopathologic variables and expression status of the *MMP2* gene.

	Group A (n = 27)			**Group B (n = 19)**
Factors	***MMP2*↑**	***MMP2*↓**	**P**	**P**
Age			N.S.	N.S.
≤50	2 (33.3%)	4 (66.7%)		
>50	15 (71.4%)	6 (28.6%)		
Gender			N.S.	N.S.
Male	7 (70%)	3 (30%)		
Female	10 (58.8%)	7 (41.2%)		
Race			N.S.	N.S.
Black	13 (61.9%)	8 (38.1%)		
Indian	4 (66.7%)	2 (33.3%)		
Size of Tumour			N.S.	N.S.
< 5 cm	11 (73.3%)	4 (26.7%)		
≥5 cm	6 (54.5%)	5 (45.5%)		
unavailable	1			
Histological type			N.S.	N.S.
Moderately differentiated	15 (60%)	10 (40%)		
Poorly differentiated	2 (100%)	0		
Depth of Invasion (pT)			N.S.	N.S.
Muscularis propria (pT_2)	1 (100%)	0		
Adventitia (pT_3)	15 (60%)	10 (40%)		
Adjacent structures (pT_4)	1 (100%)	0		
Lymphatic node involvement			**S (0.030)[b]**	N.S.
(-)	8 (66.7%)	4 (33.3%)		
(+)	3 (33.3%)	6 (66.7%)		
Unavailable	6	0		
Myenteric plexus invasion			N.S.	N.S.
(-)	1 (100%)	0		
(+)	16 (61.5%)	10 (38.5%)		
Perineurial invasion			N.S.	N.S.
(-)	1 (33.3%)	2 (66.7%)		
(+)	16 (66.7%)	8 (33.3%)		
Lymphatic Vessel invasion			N.S.	N.S.
(-)	4 (66.7%)	2 (33.3%)		
(+)	13 (61.9%)	8 (38.1%)		
Mitotic rate (no/10 HPF)			N.S.	N.S.
≤ 50	16 (69.6%)	7 (30.4%)		
>50	1 (25%)	3 (75%)		
Necrosis			N.S.	N.S.
Mild (0-33%)	15 (65.2%)	8 (34.85%)		
Moderate (34-66%)	2 (50%)	2 (50%)		
Anaplasia			N.S.	N.S.
(-)	3 (100%)	0		
(+)	14 (58.3%)	10 (41.7%)		

[a] Fisher's exact test (2-sided), [b] Pearson chi-square test (2-sided)

3.9 Comparison of the correlation of *VEGF* expression with clinicopathological factors using the UPL and SYBR Green I systems

The McNemar Chi–squared test showed that the correlation of clinicopathologic factors with *VEGF* gene expression was the same irrespective of which system (UPL or SYBR Green I) was used to detect gene expression ($p = 1.00$).

3.10 Evaluation of correlations between all clinicopathological factors

As shown in Table 3.11, lymphatic node metastasis was associated with tumour mitotic rate in both groups A and B, but was statistically significant only in group B. The depth of tumour invasion was the only clinicopathological feature shown to be significantly associated with anaplasia in group A. Large tumours were significantly associated with mitotic rate and necrosis in group B. Gender was significantly associated with race and perineurial invasion in group A.

Table 3.11. Correlation between clinicopathologic factors.

	P value (Group A)	**P value (Group B)**
Lymphatic node metastasis vs Mitotic rate	N.S. (0.063)	S (0.044)[a]
Depth of invasion vs Anaplasia	N.S.	S (0.043)[a]
Tumour size vs Necrosis	S. (0.015)[b]	N.S.
Tumour size vs Mitotic rate	N.S.	S (0.043) [a]
Gender vs Perineurial invasion	S (0.041)[a]	N.S.
Gender vs Race	S (0.057) [a]	N.S.

[a] Fishers exact test (2-sided), [b] Pearson chi-square test (2-sided)

3.11 Gene expression inter-relationships

The relationship between the expressions of each of the 4 genes studied was examined by carrying out correlation and linear regression analyses using the mRNA (Tumour/Normal) transcript levels of each gene relative to the other genes, as shown in Table 3.12. A Pearson's correlation (2-tailed) was calculated using the statistical package program SPSS. The linear correlation coefficient values shown in Table 3.12, is the measure of the strength and the direction of a linear relationship between the genes.

Table 3.12. Gene expression correlation coefficients between the four genes in Groups A and B.

	VEGF	*HER1*	*HER2*	*MMP2*
VEGF	___	**0.929* (A, B)**	0.046 (A)	**0.465* (A)**
			0.021 (B)	**0.893* (B)**
HER1	**0.929* (A, B)**	___	-0.043 (A)	**0.499* (A)**
			-0.062 (B)	**0.942* (B)**
HER2	0.046 (A)	-0.043 (A)	___	-0.026 (A)
	0.021 (B)	-0.062 (B)		-0.042 (B)
MMP2	**0.465* (A)**	**0.499* (A)**	-0.026 (A)	___
	0.893* (B)	**0.942* (B)**	-0.042 (B)	

Note: * Correlation is significant at p = 0.01

Positive slope: expression of the two genes tends to increase or decrease together

Negative slope: expression of one gene increases while the other decreases

Expression of the *VEGF* expression was significantly associated with expression of both the *HER1* and *MMP2* genes in a positive manner, while *HER1* expression was similarly associated with *MMP2* expression. Expression of the *HER2* gene was not associated with expression of any of the other genes studied. These relationships were observed in both groups A and B. The correlation coefficients were however all higher in group B than in group A suggesting that the removal of discordant samples from group A strengthened the correlation between gene expression.

The coefficient of determination (R squared linear) values were calculated for the correlation analysis between gene expressions, as seen in the figures below. These values represent the proportion of the variation of one gene that is predictable from the other gene. The fit of the regression line to the gene expression data shows how well the amount of variation between the genes can be explained by the linear relationship.

VEGF expression was associated with *MMP2* expression by a factor of 21.6% ($R^2 = 0.216$) in group A and 79.8% ($R^2 = 0.798$) in group B (Figure 3.20). The increase in the correlation observed between the expression of these two genes in group B was most likely due to the removal of discordant samples from group A. The discordant samples in group A presented outliers and did not fall into the normal trends of distribution of the gene expression values, as seen in Figure 3.20.

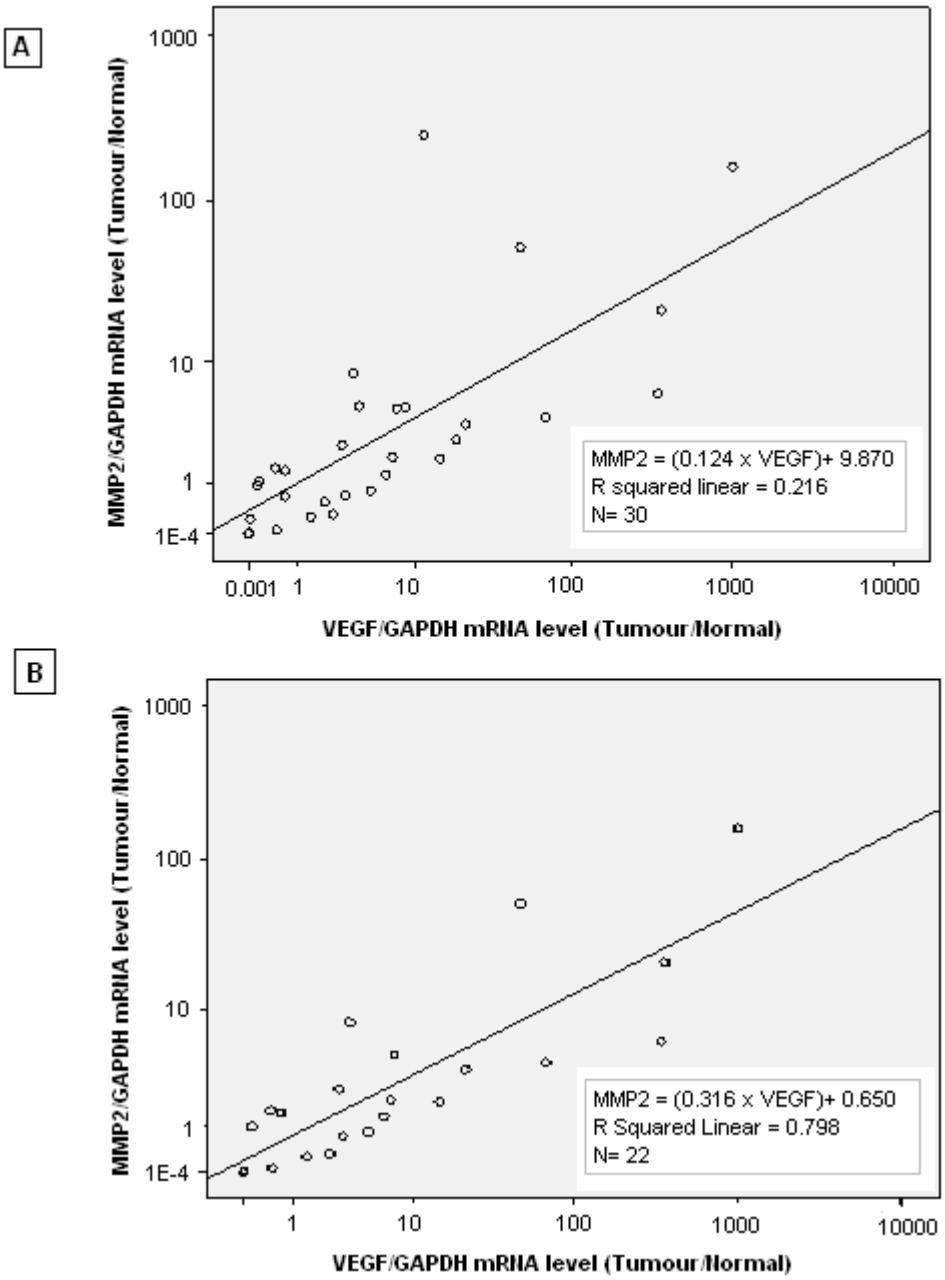

Figure 3.20. Correlation between the mRNA levels of *VEGF*/*GAPDH* and *MMP2*/*GAPDH* in Groups A and B.

HER1 expression was associated with *VEGF* expression by a factor of 86.3% ($R^2 = 0.863$) in group A and 86.4% in group B ($R^2 = 0.863$) as shown in Figure 3.21.

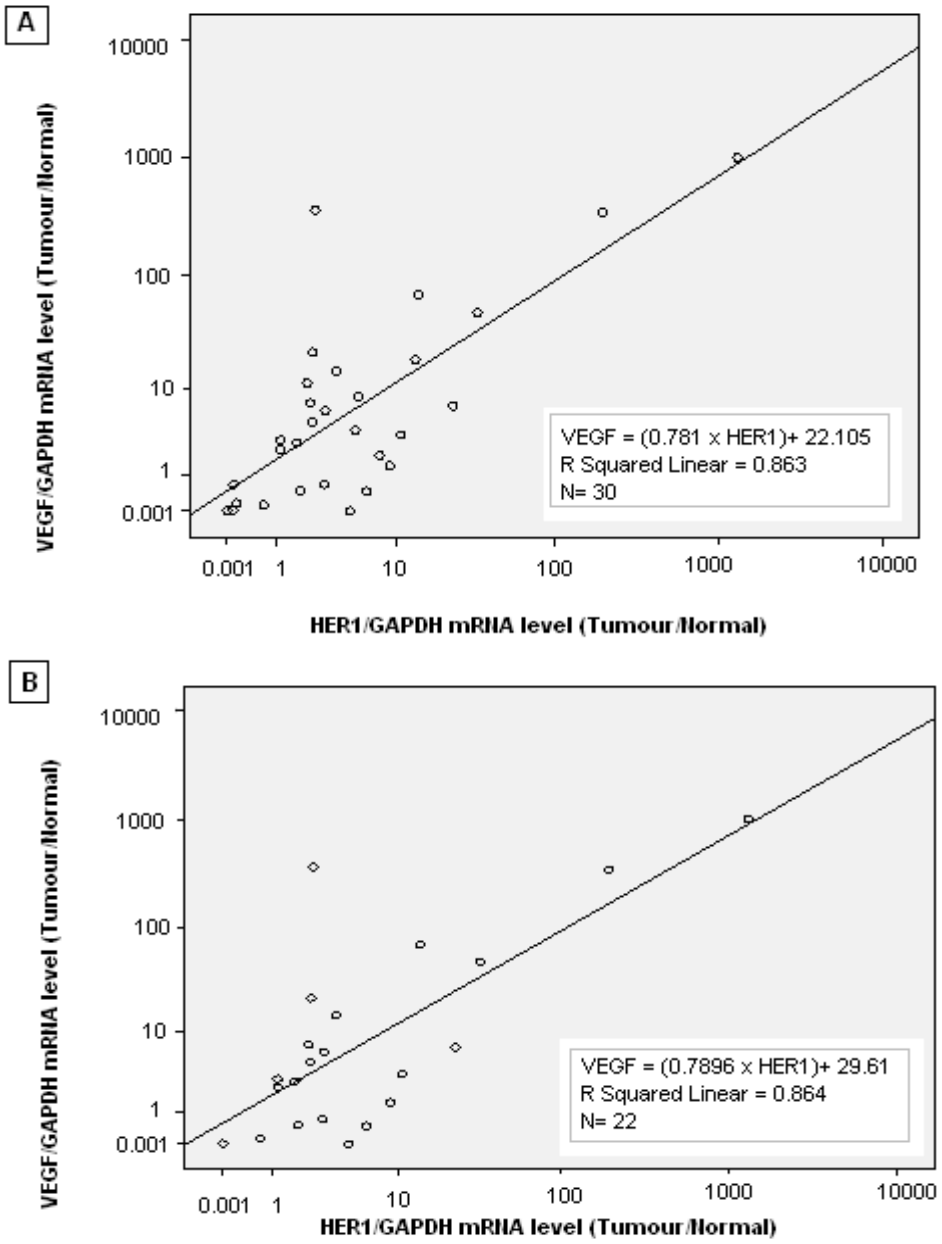

Figure 3.21. Correlation between the mRNA levels of *HER1*/*GAPDH* and *VEGF*/*GAPDH* in Groups A and B.

HER1 expression was associated with *MMP2* expression by a factor of 24.9% ($R^2 = 0.249$) in group A and 88.8% ($R^2 = 0.888$) in group B (Figure 3.22).

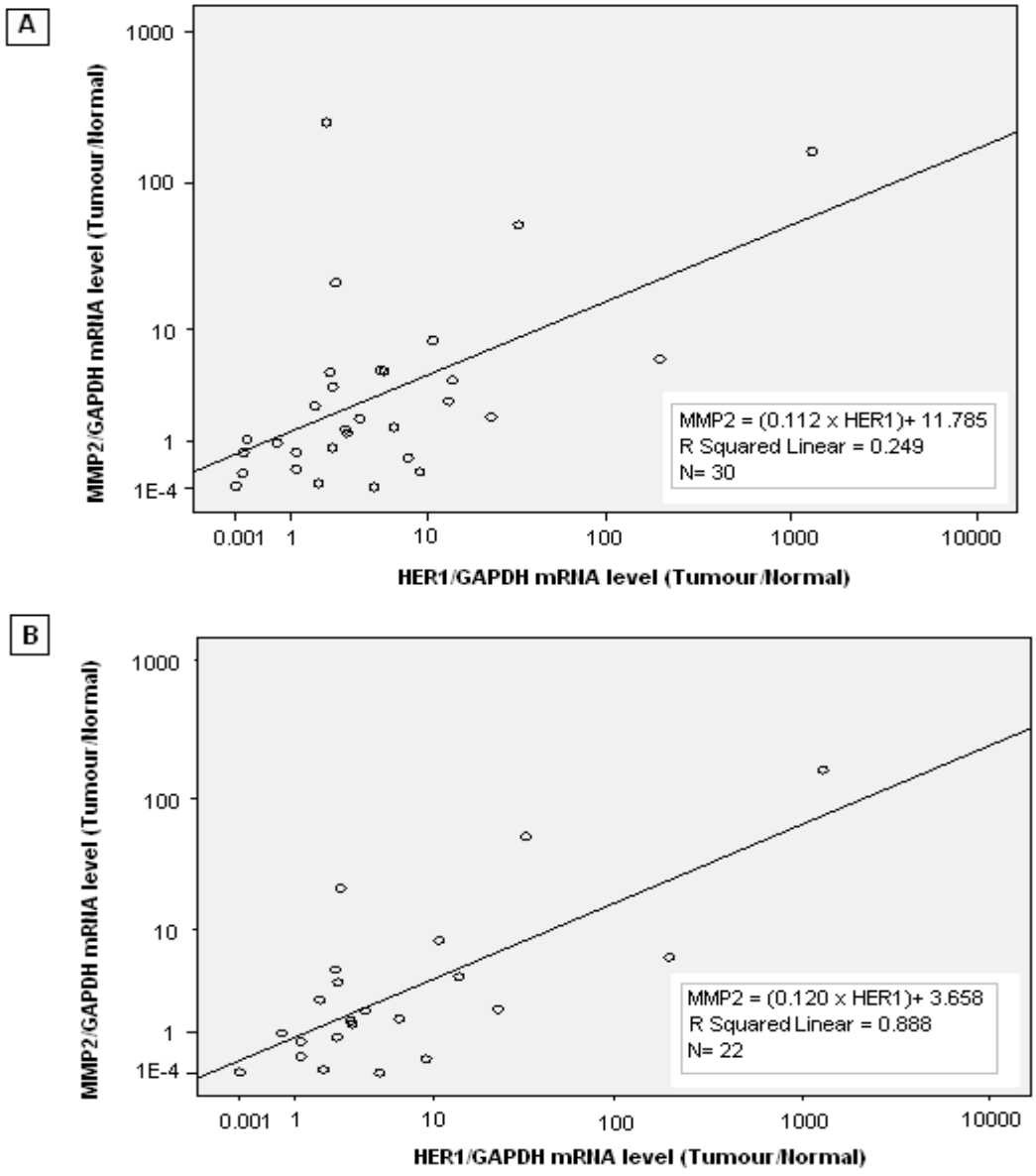

Figure 3.22. Correlation between the mRNA levels of *HER1*/*GAPDH* and *MMP2*/*GAPDH* in Groups A and B.

The increase in correlation between *HER1* and *MMP2* gene expression in group B was most likely due to the removal of discordant samples from group A. The discordant samples in group A presented outliers and did not fall into the normal trends of distribution of the gene expression values. This distribution pattern was also observed between the expression of *VEGF* and *MMP2* genes (Figure 3.20).

Chapter 4: Discussion

4.1 Introduction

Squamous cell carcinoma of the oesophagus is one of the most common malignancies worldwide with marked variations in geographical and ethnic distribution (Holmes and Vaughan, 2007). In South Africa, OSCC was reported to be the most commonly occurring cancer in Black individuals for the period between 1996 and 2000 (www.mrc.ac.za; Sammon, 2007). Clearly an understanding of the pathogenesis of OSCC, including underlying molecular changes, is required to develop and implement appropriate diagnostic and therapeutic interventions.

The current study was therefore carried out to evaluate whether changes in gene expression contribute to tumourigenesis in squamous cells of the oesophagus by assessing the relative gene expression of four well-described oesophageal cancer related genes, namely *VEGF*, *HER1*, *HER2* and *MMP2*, in a cohort of oesophageal cancer patients from the KZN region. Real time PCR technology was used to assess gene expression, as it is a reliable and rapid means of detecting and quantifying gene copy numbers. Additionally, this study aimed to evaluate a novel real time PCR probe detection system, namely the UPL system, by comparing it to the existing SYBR Green I dye fluorescence system. Relative gene expression was deduced by two different quantification methods, namely the standard curve method and the Pfaffl model, allowing for a comparison between data analysis methods.

Relationships between gene expression data and patient/tumour characteristics were also assessed, as well as relationships between clinicopathological factors, and between the expressions of the various genes. Finally, the study critiqued the impact of specimen sampling on the outcome of the investigation.

4.2 Comparison between the SYBR Green I method and UPL detection systems in real time PCR

Real time PCR technology has been used widely in both diagnostics and gene expression analysis. Several detection systems for use with real time PCR are available, ranging from simple intercalating dye systems to newer probe based systems (Bonetta, 2005). This study assessed the detection abilities of SYBR Green I, a standard fluorescent dye sytem and UPL, a hydrolysis probe based system.

Overall the differences between the two systems based on *VEGF* gene expression were found to be statistically insignificant. There was however, a significant difference between the two detection systems when comparing the *VEGF* expression values in normal and tumour oesophageal tissue (Table 3.4). Although the tests performed in this study concluded that both systems were similar in their detection abilities, it was found that the SYBR Green I system showed a constant pattern of overestimation of gene expression when compared to the UPL system. The SYBR Green I system overestimated the frequency of up and down regulation by 7% in group A and 14% in group B (Table 3.3). It also overestimated fold change values calculated using the Pfaffl model, by factors of 2 and 3, in groups A and B, respectively (Figure 3.14).

The overestimation of gene expression may be due to the inherent properties of the intercalating dye system which can cause false positive values. With SYBR Green I assays, the intercalating dye labels all PCR amplified double stranded DNA, including non specific products and primer dimers. In contrast, the UPL detection system is probe based and relies on the sequence specific detection of a desired PCR product by labeled probes.

The SYBR Green I system also reported lower CP values for normal and tumour oesophageal tissue (Appendix H) compared with the UPL system. This resulted in the detection of an increased concentration of PCR product. Similar results were reported in several UPL functionality studies (Horst and Peterhänsel, 2007; Mauritzen et al., 2005). Furthermore, the differential *VEGF* gene expression between normal and tumour oesophageal tissue as detected with the SYBR Green I system was significantly different in groups A and B, but only of borderline significance when detected with the UPL system. This statistical significance seen with the SYBR Green I system may be due to the overestimation in gene expression values of normal and tumour oesophageal tissue, whereas the more specific UPL system detected a smaller difference between the tissue types. These observations are in agreement with other studies comparing SYBR Green I and UPL/ probe based assays, in which a more reliable performance was observed with the UPL/ probe systems (Horst and Peterhänsel, 2007; Leucht and Bally-Cuif, 2007; Newby et al, 2003).

In a comparison of the laboratory usage of the two detection systems, the UPL system proved to be more user friendly and cost effective. Primers and probes designed by the probe finder software required very little user input and worked efficiently.

In addition, the UPL system can be used without any optimisation of PCR conditions, although for the purposes of this study, amplicons created using the SYBR Green I system were used to construct standard curves for the UPL system, and therefore optimisation was required. In contrast, the SYBR Green I system was time consuming as optimisation of PCR conditions was required for each gene to eliminate non specific amplification products such as primer dimers. This also resulted in increased costs. An infrequent limitation observed with the UPL system was probe degeneration at later cycles (cycle 36 onwards) when a sharp increase in the fluorescence of all samples, including the negative control was observed. Despite this, overall, the UPL system demonstrated more stability at later cycles than the SYBR Green I system. This is also in agreement with a study by Horst and Peterhänsel, (2007).

Conclusion

Real time PCR is a versatile technology that allows for the accurate measurement of gene expression. It is relatively simple to perform and provides reliable results. In this study, the evaluation of gene expression using real time PCR demonstrated that the UPL detection system simplified the real time PCR assays. While the results obtained were similar to those generated using SYBR Green I, overall the UPL system appeared to be more specific and reliable.

4.3 Comparison of real time PCR quantification methods

The choice of a reliable quantification method for use in real time PCR is critical for the accurate determination of gene expression. The real time PCR quantification methods used in this study, namely the standard curve method and the Pfaffl model, showed similar results in their evaluation. In a comparison of the gene expression fold change values between the two different methods of quantification, the fold change factors ranged from 0.2 to 1.9. The fold change values generated by the Pfaffl model were generally higher than those obtained using the standard curve model. This may be attributed to the efficiency correction used in the Pfaffl model and suggests that the standard curve model underestimated the degree of gene expression as a result of the underestimation of the actual efficiency of reactions. Relative gene expression with the Pfaffl model is reported to be more accurate since it determines whether there is a significant difference between samples and controls, while taking into account issues such as reaction efficiency and reference gene normalisation by using randomisation techniques (Pfaffl, 2002).

Studies have shown that small differences in the PCR efficiency can result in more than a ten fold variation in the calculation of sample amount. Efficiency correction is therefore essential for gene expression investigations using real time PCR (Roche Diagnostics, 2001). The calculation of gene expression with the Pfaffl model using the incorporated REST database was simple and efficient to use since statistical tests, normalisation with housekeeping gene and the efficiency of reactions were all incorporated into a single spreadsheet. Efficiency curves were also easier to create than standard curves, since the need for the creation of amplicons using the SYBR Green I step was eliminated.

Conclusion

The Pfaffl model with incorporated REST software provides a simple and efficient mathematical model for data analysis. In contrast to complex, time consuming quantification models based on standard curves, the Pfaffl model produces rapid and reproducible relative gene expression quantification.

4.4 Relative expressions of the *VEGF*, *HER1*, *HER2* and *MMP2* genes

Individually almost all oesophageal tumours in this study demonstrated the upregulation of the *VEGF*, *HER1*, *HER2* and *MMP2* genes irrespective of the detection system used, or the method of analysis. All genes were significantly upregulated in both groups A and B, with the exception of *HER1* in group B, when using the UPL system with the Pfaffl model (Figure 3.14). With use of the standard curve method, only *VEGF* expression using SYBR Green I and *HER1* expression using UPL, demonstrated statistically significant upregulation (Figure 3.17, 3.18). In terms of the amount of upregulation, expression of the *VEGF* was found to be upregulated by the highest factor using the standard curve method, whereas the *HER2* gene displayed the highest degree of upregulation with the Pfaffl model. The *MMP2* gene demonstrated the least amount of upregulation as calculated by both models. With respect to the frequency of upregulation in the study population, overexpression of *HER1* was more common in individual patients compared to *VEGF*. All other genes demonstrated high frequencies of upregulation in the majority of individuals.

The findings of this study suggest that *VEGF*, *HER1*, *HER2* and *MMP2* are related to the growth and metastases of oesophageal carcinoma due to their increased expression in tumours. Oesophageal tumours require increased proliferation, sustained angiogenesis and the ability to invade through the ECM, in order to expand locally and spread to distant sites. The increased expression of *HER1*, *HER2*, *VEGF* and *MMP2* support these properties of cancer cells. Most patients in this study have advanced OSCC (Table 3.5), suggesting that the overexpression of these genes is important for the progression of the disease. The results of this study are consistent with reports on other studies in which overexpression of the *VEGF*, *HER1*, *HER2* and *MMP2* genes have been associated with advanced OSCC (Martinez et al, 2003).

This the first study however, to report on the gene expression of *VEGF*, *HER1*, *HER2* and *MMP2* in oesophageal tumours in South African individuals. Since OSCC demonstrates a marked variation with regard to ethnicity, there is an obvious need to conduct studies of this nature in different ethnic groups and populations.

Conclusion and future perspectives

The genes for *VEGF*, *HER1*, *HER2* and *MMP2* are widely reported to be influential for the growth and development of oesophageal tumours (Martinez et al, 2003). This study establishes the overexpression of these genes in oesophageal tumours of a South African population. Further studies investigating the exact roles and mechanisms of these genes in the progression of OSCC need to be conducted with a particular focus on high incidence populations, such as the Black South African population.

4.5 Correlation of gene inter-relationships

In this study, regression analyses of mRNA transcript levels revealed a strong correlation between the *VEGF*, *HER1* and *MMP2* genes (Table 3.12), suggesting a possible association between the transcription of these genes. It has been postulated that the VEGF and HER1 pathways are related with respect to tumour induced angiogenesis (Tabernero, 2007). Several studies have reported that tumour associated endothelial cells activate HER1, which in turn induces VEGF expression in cell culture models (Ellis, 2004; Kim, et al., 2003; Perrotte, et al., 1999). It has also been suggested that the HER1 pathway modulates angiogenesis in tumours by upregulating VEGF and/or other components of the angiogenic cascade, including the MMPs (Perrotte, et al., 1999). Figure 4.1 below, modified from Tabernero, (2007), illustrates the hypothesis governing the initiation of the angiogenic process, following the release of VEGF by tumour cells initiates the angiogenic process.

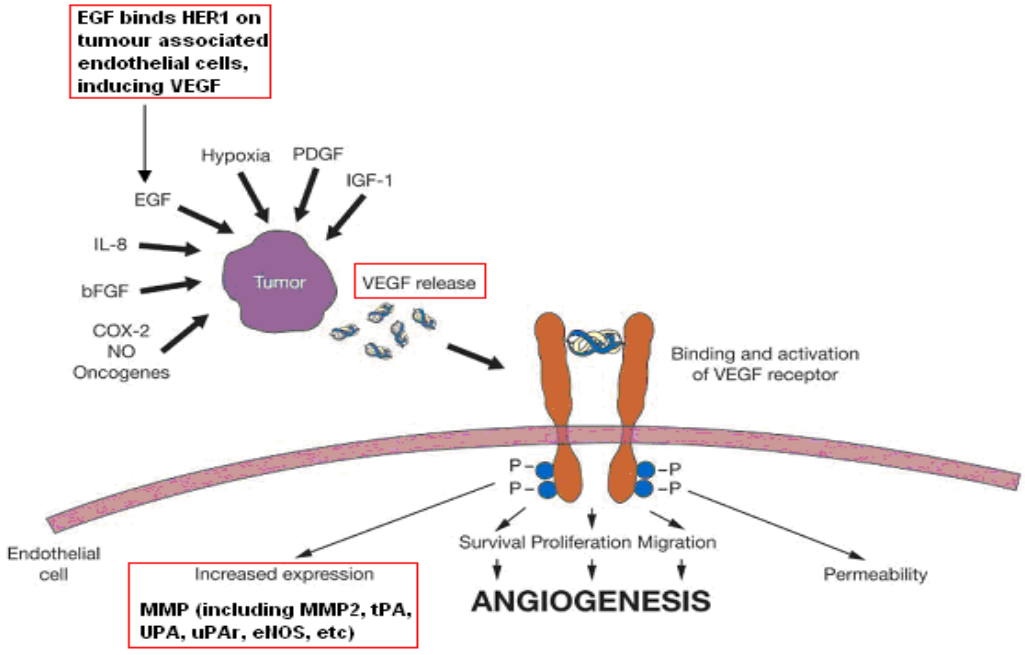

Figure 4.1 Features that promote tumour induced angiogenesis.

Expression of *VEGF* is driven by many factors including the expression of oncogenes such as *HER1*, *HER2* and *ras*, and other factors, such as hypoxia. The binding of VEGF to its receptor results in the activation of intracellular signalling pathways that are involved in endothelial cell proliferation and migration (Tabernero, 2007). Endothelial cell activation results in the secretion of matrix metalloproteinases, urokinase plasminogen activator and receptor which degrade the ECM, and allows proliferating cells to migrate towards the tumour cells. Pathologic angiogenesis is essential for the tumour as it provides means for its growth and dissemination (metastases). Other studies have reported that the blockage of HER1 by inhibitors resulted in the down regulation of pro-angiogenic mediators, including VEGF (Ellis, 2004). This allowed continued tumour angiogenesis and growth, but at a much reduced level, suggesting that inhibition of HER1 alone cannot completely block VEGF production because its expression is regulated by many other factors. Thus, the observed gene inter-relationship correlations demonstrated in this study supports previous reports linking *VEGF*, *HER1* and *MMP2* gene expression.

Conclusion and future perspectives

Associations between *VEGF*, *HER1* and *MMP2* are clearly evident in this study although further confirmation is essential. Such studies may provide clues to molecular events related to the carcinogenesis of OSCC and suggest possible therapeutic targets. The overexpression of VEGF, EGF and their receptors *(HER1, HER2)* and MMPs observed in many human neoplasms supports the postulate discussed above. The use of inhibitory agents to several of these gene products has produced promising results and a multi-targeted therapeutic approach to cancer aimed at targeting different molecular agents has proved to be more successful than targeting a single agent (Tabernero, 2007).

4.6 Histological assessment of tissue sampling method

The retrospective assessment of sampling methods is useful to verify that the tissue used was accurately classified. This contributes to ensuring that the results obtained are reliable and reproducible. Retrospective analysis provides the potential for improvement in the methodological approach in future studies. It is essential that the starting material used for any study is of satisfactory quality and is obtained using standardised and ethically sound laboratory practices.

As was clear from the retrospective histological assessment of the samples used in this study, the quality of some of the tissue provided was poor with an insufficient amount of squamous cells present for reliable investigation. Approximately 11% of 'tumour' samples had a low percentage of tumour cells while 26% of 'normal' samples contained tumour cells within the sample. The quantitative gene expression calculated from these samples cannot therefore be an accurate representation of expression status. One possible reason for these discrepancies could be that the bulk of the normal or tumour tissue in these samples had been excised previously for other purposes. In order not to confound the study results, data analyses were subsequently performed on two groups, with (Group A) and without (Group B) the discordantly classified samples.

Furthermore, in gene expression studies it is important to ensure that the 'normal' tissue is free of dysplastic areas because these areas are known to be associated with inflammation (Lu et al, 2006). Inflammation is defined as the local physiological response to tissue injury (Underwood, 2000) and results in the stimulation of several genes, including *VEGF*, *HER1*, *HER2* and *MMPs*.

Several studies have reported the overexpression of the *MMP2* gene in areas of cellular dysplasia (Coussens and Werb, 2002; Samantaray et al., 2004; Underwood, 2000). Clearly the estimation of gene expression levels from ambiguous samples would be inaccurate. In this study, dysplasias were evident in several 'normal' oesophageal samples (Appendix I: Samples 1, 11 and 45), Appendix J: Figure J.12). These inaccurately classified samples were excluded from group B.

The relative gene expression data generated with the standard curve model in group A (comprising of all samples) showed many outlying results for both normal and tumour oesophageal tissue (Figures 3.17, 3.18). Following the removal of the discordant samples from group B, these outliers disappeared and the gene expression data assumed a normal pattern of distribution. Similar observations were noted for gene association correlations using linear regression (Table 3.12 and Figures 3.20, 3.21, 3.22). With respect to the histopathological correlation with gene expression, several differences were observed between groups A and B. These differences could however also have been attributed to the smaller sample size in group B which diminished the statistical power of the test.

The assignation of normal and tumour oesophageal tissue based on visual inspection of the surgical specimen alone, can clearly result in misclassification, as observed in this study. Fresh or frozen normal, dysplastic and tumour tissue that is classified by a pathologist is frequently favoured in gene expression studies, as the yield and quality of RNA is good, although limited availability of fresh tissue could be restrictive.

Studies have reported that a good quality of tissue sample is ensured when using formalin-fixed paraffin-embedded (FFPE) methods since it is possible to choose adequately representative regions of sample type (Chen et al., 2007; Cronin et al., 2004; Gloghini et al., 2004; Godfrey et al., 2000). Although the process of formalin fixation may contribute to RNA degradation, recent technical developments now allow the isolation of high quality RNA from FFPE samples for use in real time PCR and gene array experiments (Chen et al., 2007; Cronin et al., 2004; Gloghini et al., 2004; Godfrey et al., 2000).

Conclusion and future perspectives

The retrospective assessment of experimental sampling methods carried out in this study highlights the important role of optimal sampling and laboratory practice in research. Additionally, it also demonstrates the need for effective team work, as well as discipline specific expertise and accountability in inter-and multidisciplinary research. Based on the observations made in this study, it is recommended that gene expression studies should utilise formalin-fixed paraffin-embedded (FFPE) tissues as they are readily available, and are accurately and comprehensively classified.

4.7 Correlation of gene expression to clinicopathological profile

The present study cohort comprised mostly Black African patients, reflecting the local demographic public sector hospital admissions. Cancer of the oesophagus is characterised by a 2:1 male: female prevalence (Blot, 1994), but in this study cohort there were more females than males. This preponderance of females is most likely related to the small sample population. The inclusion of patients in early and intermediate stage of OSCC is desirable to allow the comparison of gene expression with disease progression.

In this study however, most patients presented with an advanced disease stage in which tumours had already spread to the adventitia at the time of diagnosis. It is not always possible to include patients with different disease stages in short term studies that utilise frozen sample tissue for analysis. Analysis of gene expression in relation to clinical or phenotypic variations may indicate biologically meaningful changes at a transcriptional level. Such studies such may provide evidence for associations between upregulated genes and carcinogenesis, or between gene expression and clinical factors.

In this study, all male patients displayed significant overexpression of *VEGF* gene ($p = 0.012$ (A), $p = 0.044$ (B)). In group A, all Black patients displayed significant overexpression of *VEGF* gene ($p = 0.044$). This suggests gender and race may have an influence on *VEGF* expression. The upregulation of *HER2* was also significantly associated with race in group A ($p = 0.015$), at least, suggesting a possible association between race and *HER2* expression in OSCC. Furthermore, gender was significantly associated with race when evaluating prognostic factors (Table 3.11). Overexpression of *VEGF* in this study, as evaluated using the SYBR Green I system, in group A, was also significantly correlated with depth of tumour invasion. Most tumours that had invaded the adventitia displayed significant *VEGF* overexpression ($p = 0.046$). As discussed previously in Chapter 1, *VEGF* is a key regulator of angiogenesis and provides the growing tumour with the necessary vascular development required for both local growth and distant metastasis (Ciardiello et al., 2006, Folkman, 2003). An association between increased VEGF protein expression in squamous cell carcinoma and an increased depth of tumour invasion, tumour stage, lymph node and distant metastases and a poorer survival has been reported (Vallböhmer and Lenz, 2006).

These findings suggest the possibility that the advanced oesophageal carcinomas investigated in this study employed similar angiogenic pathways for their local growth and spread.

Other genes that are involved in the spread of tumours are MMPs, which are directly involved in tumour invasion by means of ECM degradation and the maintenance of the tumour microenvironment. Matrix Metalloproteinase 2 has been suggested to be involved in the early events of malignant transformation in several cancers, including oesophageal, cervical, oral and lung cancers (Samantaray et al., 2004). Increased MMP2 protein expression in OSCC has been associated with increased depth of tumour invasion, tumour stage, vascular/lymphatic vessel invasion and poorer survival (Vallböhmer and Lenz, 2006). However, several other studies have reported no significant association between MMP2 protein expression and lymphatic node invasion (Koyama et al, 2000; Samantaray et al., 2004).

In this study, group A of oesophageal tumours demonstrated a significant association of *MMP2* gene overexpression in patients without lymphatic node invasion ($p= 0.030$). This could be explained by the reported involvement of MMPs in the critical events of tumour evolution at earlier stages, such as tumour promotion, modulation of the growth of the primary tumour and angiogenesis (Samantaray et al., 2004). The overall absence of a correlation of MMP2 overexpression with tumour invasion and other signs of advanced disease in this and other studies, suggests the role of MMP2 in early tumour development.

Growth factor receptors such as HER1 and HER2 are also directly involved in neoplastic transformation and involved in the regulation of cellular proliferation and differentiation (Ciardiello et al, 2006).

Reports of increased HER1 and HER2 protein expression have been linked to an increased local recurrence, depth of tumour invasion, lymph node metastasis and a poorer survival in OSCC (Dreilich et al., 2006; Vallböhmer and Lenz, 2006). In this study however, no significant associations of *HER1* and *HER2* overexpression with clinicopathological factors were observed.

Another factor that is essential for tumour growth is the rate of cell proliferation. The division of cells occurs by the process of mitosis, which is part of the cell cycle and defined by the appearance of cytologically detectable chromosomes (Čemerikić-Martinović et al, 1998) (Appendix J: Figure J.1). In group B of oesophageal tumours in this study, the mitotic rate of the tumour was significantly associated with the size of the tumour ($p = 0.043$), as well as lymph node metastasis ($p = 0.044$). This suggests that the mitotic index of a tumour may be linked in some manner to the rate of local tumour growth, as well as distant spread. Cancer cells frequently exhibit a higher mitotic index than the corresponding normal cell population, and higher frequencies of cellular proliferation have been reported to be associated with a poor prognosis (Underwood, 2000). In group B, larger tumours were significantly associated with an increased presence of necrosis ($p = 0.043$) (Appendix J: Figure J.3). Necrotic areas are capable of stimulating angiogenic factors that promote the growth and movement of endothelial cells, thus providing the tumour with vasculature (Ribatti and Vacca, 2008). A study by Ikpatt et al, (2002) in breast cancer patients also reported a correlation of necrosis with the size of the tumours and suggested that necrosis was associated with progressive and advanced disease. Thus the results from this study together with others, suggest that in oesophageal tumours, necrosis may be a means by which tumours increase vasculature for growth purposes.

Another factor that is reported to influence the growth of tumours is perinuerial invasion (PNI). This occurs when cancer cells invade the perineurium (Appendix J, Figure J.7) and is reported to be a crucial route for the local spread of gastric tumours associated with poor prognosis (Duraker et al, 2003). Perineurial invasion was reported to be closely related to local recurrence of OSCC in patients and was classified as an important prognostic factor for the disease (Tanaka et al., 1998). In this study, PNI was not associated with any clinicopathologic factors except for the female gender in group A ($p = 0.041$). This observation could however be due to the higher number of female participants in this study.

The majority of oesophageal carcinomas in this study were moderately differentiated and it was observed that increased anaplasia was significantly associated with increased depth of tumour invasion in group A ($p= 0.015$). The degree of differentiation of tumours is clinically useful as it is associated with prognosis and may influence therapeutic choices (Underwood, 2000). Poorly differentiated cells may be anaplastic and lack similarity to surrounding normal cells (Underwood, 2000). Poorly differentiated tumours are reported to have high mitotic rates indicating rapid and aggressive growth compared to well or moderately differentiated tumours (Underwood, 2000).

The TNM status of oesophageal tumours in this study was not analysed in relation to gene expression data as information on the metastasic status of the tumour was unavailable or incomplete. The combination of the TNM classification and VEGF expression has been reported to be a possible means of devising therapy using angiogenesis inhibitors (Shih et al., 2000). Gene expression data were however not correlated with patient survival in this study due to the unavailability of accurate patient survival statistics.

Conclusion and future perspectives

The overexpression of *VEGF* in this study was influenced by gender and race, as well as by an increased depth of tumour invasion. Overexpression of *HER2* was influenced by race only, while overexpression of the *MMP2* gene was related to patients who did not have lymphatic node metastasis. Clinically, large tumour size was associated with an increased mitotic rate and an elevated amount of necrosis. Anaplasia was frequently observed with an increased depth of tumour invasion and perineurial invasion was influenced by gender. Further scientific evidence confirming these correlations are essential, as are larger prospective studies to confirm the relationship between gene expression levels and prognosis.

Studies such as the current one are useful in identifying new molecular and prognostic markers for OSCC. The prevention and early diagnosis of OSCC is as important as treatment of the disease. The pathophysiological and clinical aspects of tumours need to be studied in combination to gain perspective and insight into the multi-faceted nature of the disease. To successfully devise and perform such studies, strong interdisciplinary co-operation is required to cover every aspect, including comprehensive clinical follow up to ensure availability of all necessary data.

Appendices

Appendix A: Reagents required for RNA extraction

1. Diethyl pyrocarbonate water

250µl Diethyl pyrocarbonate (DEPC) (0.001mmol/l) (Catalogue number: 150902, ICN Biochemicals Inc.) was added to 250ml of distilled water in a fume cupboard and incubated overnight at 37˚C. The solution was autoclaved twice before use.

2. Ethanol (75%)

Absolute ethanol (Merck Ltd, Poole, UK) was diluted with 75% DEPC water and stored at -20˚C

Appendix B: Reagents required for gel electrophoresis

1. Tris-Borate/EDTA (TBE) Buffer

9.3g EDTA (31.8mmol/l), 55g Boric acid (889.5mmol/l) and 108g Tris base (891.8mmol/l) were dissolved in 1000ml of sterile water, filtered and then stored.

2. Ethidium Bromide Dye

100mg of Ethidium bromide (0.25mmol/l) was dissolved in 1ml of sterile water. The tube was covered with aluminium foil and stored at room temperature.

3. Bromophenol Blue dye

The solution consisted of 50% glycerol, 0.02% bromophenol blue and 0.02% xylene cyanol.

4. **10x MOPS** (3-[N-Morpholino] propanesulfonic acid) (Catalogue no. M-1254, (Sigma, Germany).

41.9g of MOPs (200mmol/l), 4.1g of sodium acetate (50mmol/l) and 3.7g of EDTA (10mmol/l) were added to a one litre flask and the pH was adjusted to 7 using a ph meter. DEPC water was added to bring the volume up to one litre.

Appendix C: RNA isolation using TRIZOL method

50-100mg of normal or tumour oesophageal tissue was thoroughly homogenised in 1ml Trizol reagent and passed through a 21 gauge needle to disrupt the cells. The homogenate was centrifuged at 12000 gravitational force (g) for 10 minutes at 4°C before 200µl of chloroform was added. This mixture was shaken vigorously for 30 seconds and incubated at room temperature for 5 minutes before centrifugation at 12000g for 15 minutes at 4°C. The supernatant which contained the total RNA was transferred to a clean 1.5ml eppendorf tube and mixed with equal volume of 60% ethanol for subsequent RNA purification (Perou et al., 1999).

Appendix D: RNA purification using Aurum Total RNA mini kit

700µl of 60% ethanol was added to the RNA, mixed and allowed to stand for 1 minute. The elution solution was placed in a water bath at 70̊C. A RNA binding column was inserted into a 2ml capless tube containing the binding column. The lysate was transferred on to the column. The tube was centrifuged for 1 minute at room temperature and the filtrate was discarded. All centrifugations were carried out at 12000g. 700µl of low stringency wash solution was added to the RNA binding column, centrifuged for 1 minute and the filtrate discarded. 75µl of DNase dilution solution was added to 5µl of reconstituted DNAse. 1.80µl of this solution was added to the RNA binding column and incubated at room temperature for 25 minutes. The column was then centrifuged for 30 seconds and the filtrate discarded. 700µl of high stringency wash solution was added to the column which was then centrifuged for 30 seconds and the filtrate was discarded. 700µl of low stringency wash solution was added to the column and centrifuged for 30 seconds. The filtrate was discarded and the column was centrifuged for an additional minute. The RNA binding column was placed into a sterile 1.5 ml capped tube and 80µl of 70˚C elution solution was placed on the membrane stack, allowed to incubate for 1 minute and then centrifuged for 2 minutes in order to elute out pure RNA (Biorad package insert).

Appendix E: Agarose gel electrophoresis protocol

A 2% agarose gel was prepared by dissolving 1.4g agarose in 70ml TBE buffer (x1) (Appendix B) in a 200ml conical flask. The solution was heated in a microwave until all the agarose had dissolved. After cooling, 3.5µl of ethidium bromide was added (Appendix B). The gel was then poured into a casting tray with a comb in place, and allowed to set for 45 minutes at room temperature. The comb was then gently removed and the tray was submerged in an electrophoretic tank containing TBE buffer (x1). 5µl of RNA sample was added to 2µl of bromophenol blue loading dye and the mixture was loaded into wells. Electrophoresis was carried out at 90V for 1 hour at room temperature (Maniatis et al., 1989). The RNA was then visualised and photographed using the Chemidoc UV transilluminator (Biorad).

Appendix F: Denaturing gel electrophoresis

All gel trays, combs and rigs were wiped clean with RNase Zap (Ambion, USA) and rinsed with DEPC treated water before use (Appendix A). A 1% (w/v) agarose gel was prepared by adding 0.5g agarose, 5ml MOPS (10 x) (Appendix B) and 37.5ml DEPC water to a 200ml Erlenmeyer flask. This mixture was heated in a microwave until the agarose had dissolved. After cooling, 3.5 ml formaldehyde (37%) (Appendix B) was added to the solution in a fume cupboard. The solution was poured into a casting tray and allowed to set for 30 minutes. The gel was then placed onto the gel rig and 200ml of MOPS (1x) (Appendix B) was gently poured in, ensuring that the gel was completely covered. The RNA samples were prepared by adding 5ug of total RNA to 2µl of loading buffer (5x), 1µl ethidium bromide (Appendix B) and 10µl water in eppendorf tubes. The RNA samples were spun briefly in a microcentrifuge. The samples were heated at 65°C for 10 minutes then left to chill on ice for 2 minutes and spun in a microcentrifuge briefly. The samples were then loaded into the wells of the gel. Electrophoresis was carried out at 80V for 40 minutes at room temperature (University of Pretoria laboratory manual, 2006). The gel was visualised and photographed using the Chemidoc UV transilluminator (Biorad).

Appendix G (i): Gene sequences designed using BLAST at NCBI

VEGF

GCTGCTCTACCTCCACCATGCCAAGTGGTCCCAGGCTGCACCCATGGCAG
AAGGAGGAGGGCAGAATCATCACGAAGTGGTGAAGTTCATGGATGTCTAT
CAGCGCAGCTACTGCCATCCAATCGAGACCCTGGTGGACATCTTCCAGGA
GTACCCTGATGAGATCGAGTACATCTTCAAGCCATCCTGTGTGCCCCTGA
TGCGATGCGGGGGCTGCTCCAATGACGAGGGCCTGGAGTGTGTGCCCACT
GAGGAGTCCAACATCACCATGCAGATTATGCGGATCAAACCTCACCAAGG
CCAGCACATAGGAGAGATGAGCTTCCTACAGCACAACAAATGTGAATGCA
GACCAAAGAAAGATAGAGCAAGACAAGAAAA

MMP2

CCACACGCACCGAGCCAGCGACCCCCGGGCGACGCGCGGGGCCAGGGAGC
GCTACGATGGAGGCGCTAATGGCCCGGGGCGCGCTCACGGGTCCCCTGAG
GGCGCTCTGTCTCCTGGGCTGCCTGCTGAGCCACGCCGCCGCCGCGCCGT
CGCCCATCATCAAGTTCCCCGGCGATGTCGCCCCCAAAACGGACAAAGAG
TTGGCAGTGCAATACCTGAACACCTTCTATGGCTGCCCCAAGGAGAGCTG
CAACCTGTTTGTGCTGAAGGACACACTAAAGAAGATGCAGAAGTTCTTTG
GACTGCCCCAGACAGGTGATCTTGACCAGAATACCATCGAGACCATGCGG
AAGCCACGCTGCGGCAACCCAGATGTGGCCAACTACAACTTCTTCCCTCG
CAAGCCCAAGTGGGACAAGAACCAGATCACATACAGGATCATTGGCTACA
CACCTGATCTGGACCCAGAGACAGTGGATGATGCCTTTGCTCGTGCCTTC
CAAGTCTGGAGCGATGTGACCCCACTGCGGTTTTCTCGAATCCATGATGG
AGAGGCAGACATCATGATCAACTTTGGCCGCTGGGAGCATGGCGATGGAT
ACCCCTTTGACGGTAAGGACGGACTCCTGGCTCATGCCTTCGCCCCAGGC
ACTGGTGTTGGGGGAGACTCCCATTTTGATGACGATGAGCTATGGACCTT
GGGAGAA

HER1

CTCCGTCCAGTATTGATCGGGAGAGCCGGAGCGAGCTCTTCGGGGAGCAG
CGATGCGACCCTCCGGGACGGCCGGGGCAGCGCTCCTGGCGCTGCTGGCT
GCGCTCTGCCCGGCGAGTCGGGCTCTGGAGGAAAAGAAAGTTTGCCAAGG
CACGAGTAACAAGCTCACGCAGTTGGGCACTTTTGAAGATCATTTTCTCA
GCCTCCAGAGGATGTTCAATAACTGTGAGGTGGTCCTTGGGAATTTGGAA
ATTACCTATGTGCAGAGGAATTATGATCTTTCCTTCTTAAAGACCATCCA
GGAGGTGGCTGGTTATGTCCTCATTGCCCTCAACACAGTGGAGCGAATTC
CTTTGGAAAACCTGCAGATCATCAGAGGAAATATGTACTACGAAAATTCC
TATGCCTTAGCAGTCTTATCTAACTATGATGCAAATAAAACCGGACTGAA
GGAGCTGCCCATGAGAAATTTACAGGAAATCCTGCATGGCGCCGTGCGGT
TCAGCAACAACCCTGCCCTGTGCAACGTGGAGAGCATCCAGTGGCGGGAC
ATAGTCAGCAGTGACTTTCTCAGCAACATGTCGATGGACTTCCAGAACCA
CCTGGGCAGCTGCCAAAAGTGTGATCCA

HER2

TGATGGGGAGAATGTGAAAATTCCAGTGGCCATCAAAGTGTTGAGGGAAA
ACACATCCCCCAAAGCCAACAAAGAAATCTTAGACGAAGCATACGTGATG
GCTGGTGTGGGCTCCCCATATGTCTCCCGCCTTCTGGGCATCTGCCTGAC
ATCCACGGTGCAGCTGGTGACACAGCTTATGCCCTATGGCTGCCTCTTAG
ACCATGTCCGGGAAAACCGCGGACGCCTGGGCTCCCAGGACCTGCTGAAC
TGGTGTATGCAGATTGCCAAGGGGATGAGCTACCTGGAGGATGTGCGGCT
CGTACACAGGGACTTGGCCGCTCGGAACGTGCTGGTCAAGAGTCCCAACC
ATGTCAAAATTACAGACTTCGGGCTGGCTCGGCTGCTGGACATTGACGAG
ACAGAGTACCATGCAGATGGGGGCAAGGTGCCCATCAAGTGGATGGCGCT
GGAGTCCATTCTCCGCCGGCGGTTCACCCACCAGAGTGATGTGTGGAGTT
ATGGTGTGACTGTGTGGGAGCTGATGACTTTTGGGGCCAAACCTTACGAT
GGGAT

GAPDH

ATCAATGGAAATCCCATCACCATCTTCCAGGAGCGATCCCTCCAAATCAAGTGGGGC
GATGCTGGCGCTGAGTACGTCGTGGAGTCCACTGGCGTCTTCACCACCATGGAGAAGGCT
GGGGCTCATTTGCAGGGGGGAGCCAAAAGGGTCATCATCTCTGCCCCCTCTGCTGATGCC
CCCATGTTCGTCATGGGTGTGAACCATGAGAAGTATGACAACAGCCTCAAGATCATCAGC
AATGCCTCCTGCACCACCAACTGCTTAGCACCCCTGGCCAAGGTCATCCATGACAACTTT
GGTATCGTGGAAGGACTCATGACCACAGTCCATGCCATCATTGCCACCCAGAAGACTGT

Appendix G (ii): UPL primers and probes

Probes and primers were designed by Roche Diagnostics using the UPL design software (www.probelibrary.com).

Genes	**UPL probes number**
VEGF	9 (cat.No. 04685075001)
MMP2	43 (cat. No. 04688031001)
HER1	83 (cat.no. 04689062001)
HER2	46 (cat. No. 04688066001)
GAPDH	45 (cat.No. 04688058001)

	Oligonucleotide primer sequence (5'-3')	**No. of bases**	**GC content (%)**	**Primer Tm (˚C)**
Gene-***VEGF***				
Forward	AGT GTG TGC CCA CTG AGG A	19	57.9	58.8
Reverse	GGT GAG GTT TGA TCC GCA TA	20	50.0	57.3
Gene- ***MMP2***				
Forward	TTG GCA GTG CAA TAC CTG AA	20	45.0	55.3
Reverse	CTT CAG CAC AAA CAG GTT GC	20	50	57.3
Gene- ***HER1***				
Forward	TCT TTC CTT CTT AAA GAC CAT CCA	24	37.5	57.6
Reverse	GTG TTG AGG GCA ATG AGG AC	20	55.0	59.4
Gene- ***HER2***				
Forward	GGT GCA GCT GGT GAC ACA	18	61.1	58.2
Reverse	TTT TCC CGG ACA TGG TCT AA	20	45.0	55.3
Gene- ***GAPDH***				
Forward	TCC ACT GGC GTC TTC ACC	18	61.1	58.2
Reverse	GGC AGA GAT GAT GAC CCT TTT	21	47.6	57.9

Appendix H: Crossing point values for *VEGF* gene expression with UPL and SYBR Green I systems

Patients	CP Normal UPL	CP Normal SYBR	CP Tumour UPL	CP Tumour SYBR
1	33.66	25.69	38.00	33.60
2	33.65	26.63	30.39	24.58
3	35.16	28.91	34.16	27.47
4	36.64	26.53	32.80	27.56
5	34.10	27.30	32.09	26.78
6	30.83	25.16	30.96	25.86
7	32.16	26.53	33.57	29.14
8	33.79	26.51	34.63	27.78
9	36.01	30.66	30.98	25.11
10	35.57	29.12	30.88	26.25
11	31.28	25.83	27.95	23.72
12	32.97	29.41	29.22	24.90
13	28.88	24.04	27.64	24.65
14	32.33	30.02	31.53	27.56
15	29.53	26.25	28.31	25.06
16	28.66	23.71	24.92	22.57
17	28.33	24.77	28.85	26.18
18	29.82	26.71	26.38	23.71
19	30.34	25.58	26.80	23.65
20	28.90	25.78	28.97	25.68
21	27.38	24.50	29.17	29.02
22	36.63	37.48	13.80	0.00
23	26.89	25.94	26.10	29.30
24	31.16	31.01	28.34	24.29
25	28.53	27.28	27.97	26.76
26	28.53	26.30	33.66	34.13
27	30.33	30.79	24.61	26.31
28	26.35	27.48	26.89	28.20
29	27.05	26.24	28.28	29.50
30	29.89	31.18	24.68	26.78

Appendix I: Histological assessment of 19 pairs of oesophageal squamous cell carcinoma

Sample #	Clinical Type	Histological type
1*	Normal	Normal epithelia, dysplastic, tumour present; MIB1 marker to show dysplasia (Figure 3.15. A)
2*	Tumour	Pulled tissue, AE13 marker, no visible tumour
3	Normal	Normal epithelia, eosinophils present, oesophagitis
4	Tumour	Moderately differentiated tumour, keratinization
5	Normal	Normal epithelia, no tumour present
6	Tumour	Moderately differentiated tumour (70%), keratinization
7	Normal	Normal muscle, no epithelia present
8	Tumour	Moderately differentiated tumour, food particles present
9*	Normal	Not good specimen, tumour present: epithelial markers AE13 (Figure 3.16. A)
10	Tumour	Tumour present
11*	Normal	Normal dysplastic epithelia, Invasive tumour present
12	Tumour	Moderately differentiated tumour
15*	Normal	Normal epithelia, degenerated tissue suspicious for carcinoma
16	Tumour	Tumour present
17	Normal	Normal smooth muscle and fibrocollagenous tissue, no epithelium present
18	Tumour	Moderately differentiated tumour, very small amount. Foreign material present
19*	Normal	Tumour in normal tissue. AE13 marker to confirm epithelial tissue
20	Tumour	Moderately differentiated tumour (60%)
21	Normal	Normal skeletal muscle confirmed by AE13 epithelial marker
22	Tumour	Moderately differentiated tumour
23	Normal	Normal epithelia
24	Tumour	Moderately differentiated tumour (60%), dyplastic and invasive
27	Normal	Normal epithelia
28*	Tumour	Freezer artifact- degenerated tissue
33	Normal	Normal epithelia, good specimen, no tumour present
34	Tumour	Tumour present, not good enough specimen to grade differentiation
37	Normal	Skeletal & smooth muscle, fibrocollagenous tissue. No tumour present
38	Tumour	Tumour present, confirmed by marker, very little tumour (approx. 10 cells) of poor quality
41	Normal	Skeletal muscle, AE13 marker to check for epithelial cells
42	Tumour	No visible tumour. AE13 marker to check for epithelial cells.
43*	Normal	Freezer artifact- degenerated tissue
44	Tumour	Freezer artifact- degenerated tissue, some remnants of tumour (Figure 3.16. B)
45*	Normal	Normal epithelia, tumour present (Figure 3.15. B)
46	Tumour	Moderately differentiated tumour (70%)
51	Normal	Smooth muscle, no epithelia present. No tumour present
52	Tumour	Poorly differentiated tumour
59	Normal	Fibro fatty tissue
60	Tumour	Moderately differentiated tumour. many apoptotic and mitotic figures

* = removed samples in pairs, numbers: 1+2, 9+10, 11+12, 15+16, 19+20, 27+28, 43+44, 45+46

Appendix J: Histopathological analyses of OSCC

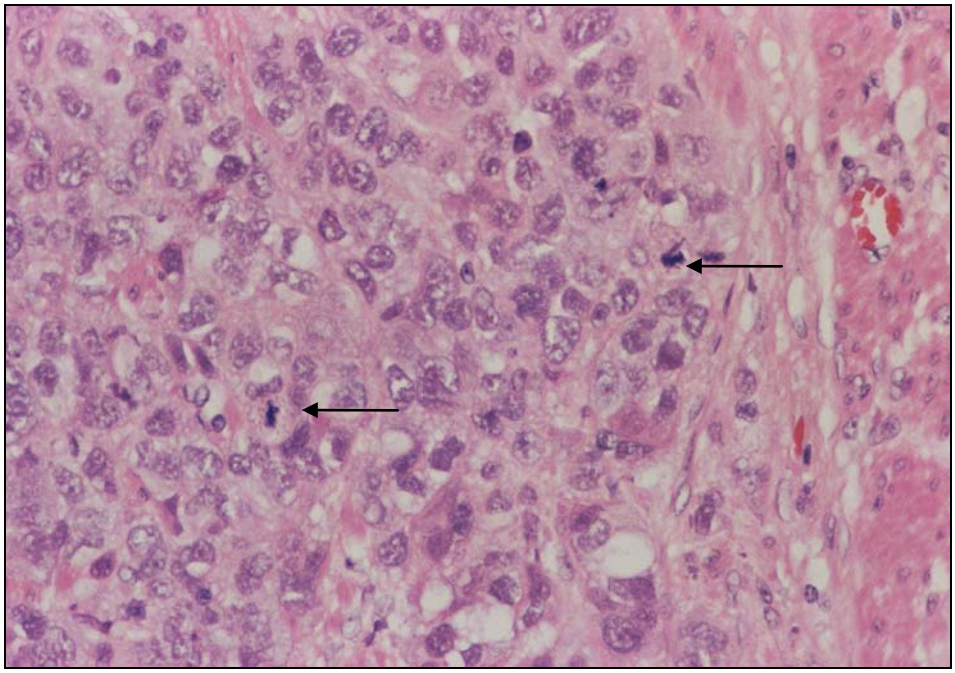

Figure J.1. Pleomorphic cells and mitotic figures present within squamous cell carcinoma of the oesophagus (arrow) (H&E stain: original magnification, x 480).

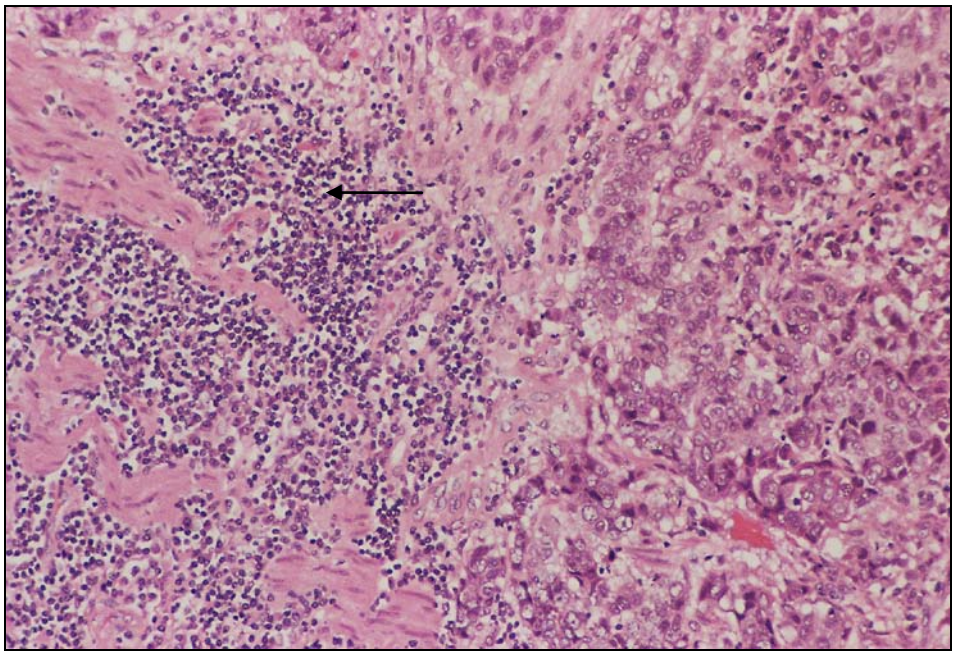

Figure J.2. The host lymphocytic response of squamous cell carcinoma of the oesophagus (arrow) (H&E stain: original magnification, x 240).

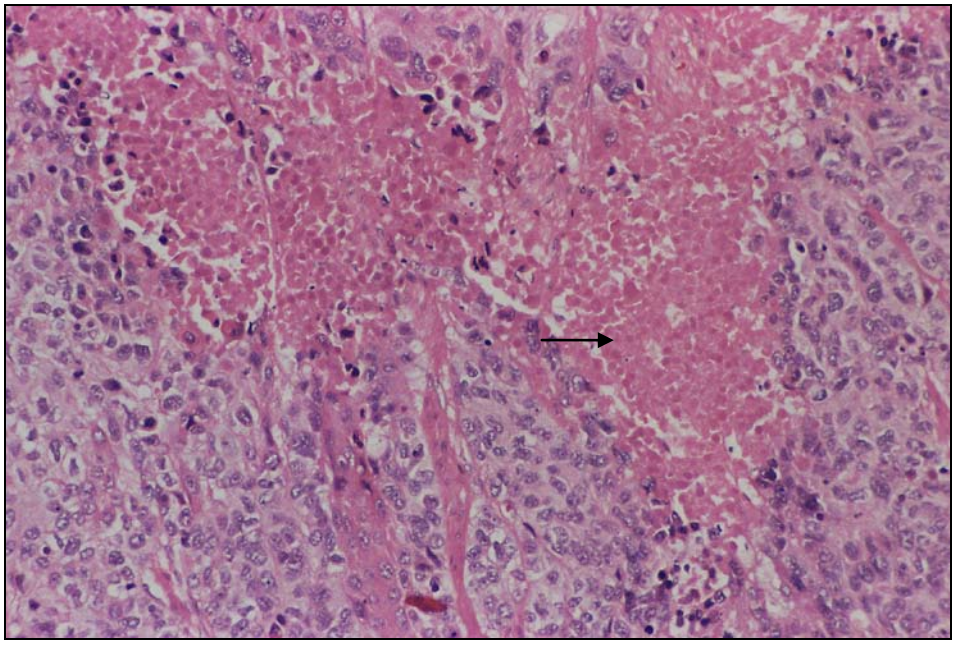

Figure J.3. Confluent necrosis within squamous cell carcinoma of the oesophagus (arrow) (H&E stain: original magnification, x 480).

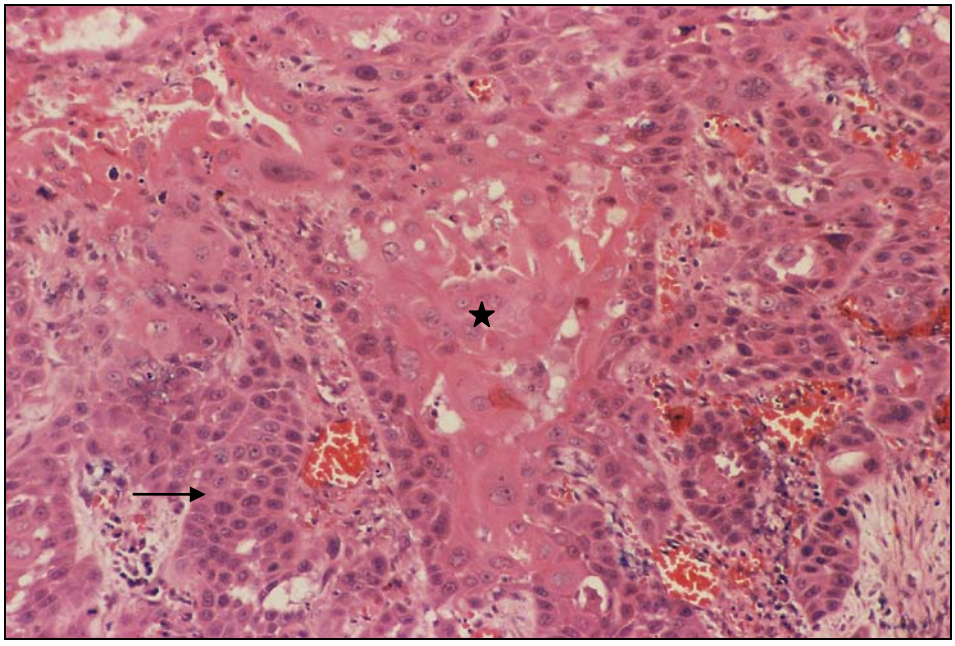

Figure J.4. Squamous cell carcinoma of the oesophagus presenting abundant keratinization and indicating, a well differentiated component (*) and peripheral moderate differentiation (arrow) (H&E stain: original magnification, x 240).

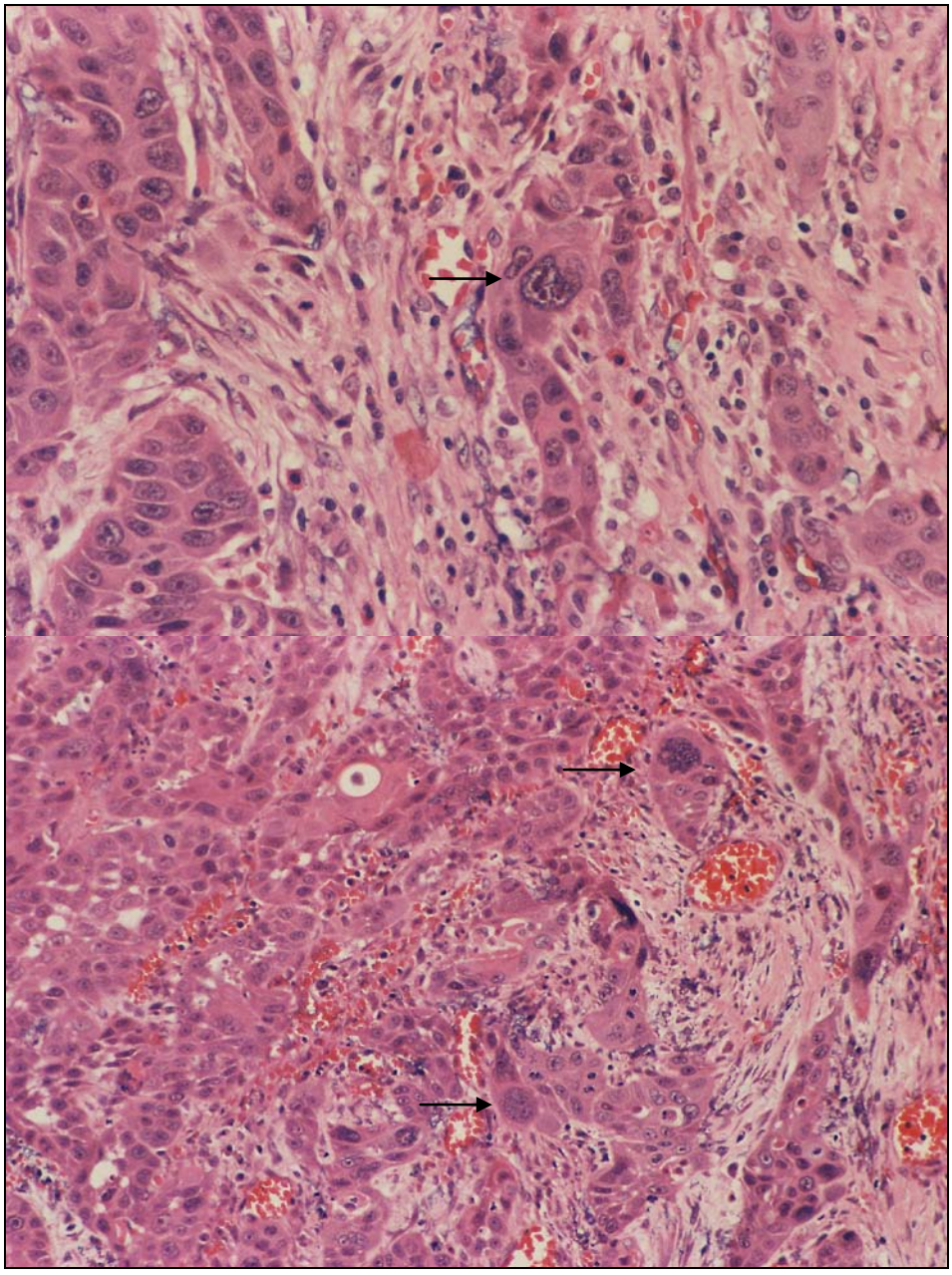

Figure J.5. Anaplasia within squamous cell carcinoma of the oesophagus (arrow) (H&E stain: original magnification, x 480, x 120).

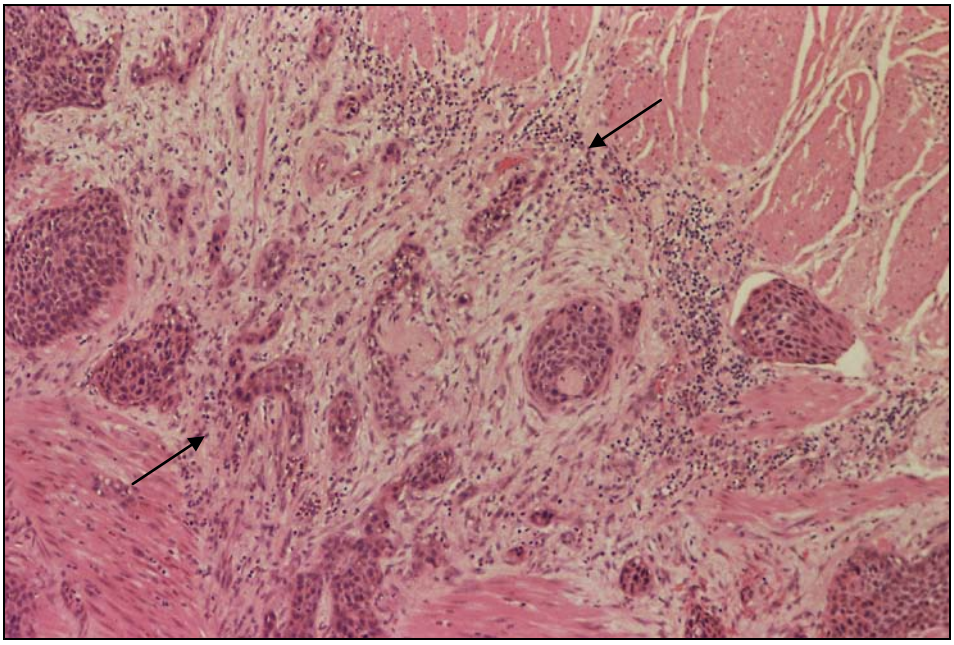

Figure J.6. Myenteric plexus invasion by tumour cells within OSCC (arrow) (H&E stain: original magnification, x 120).

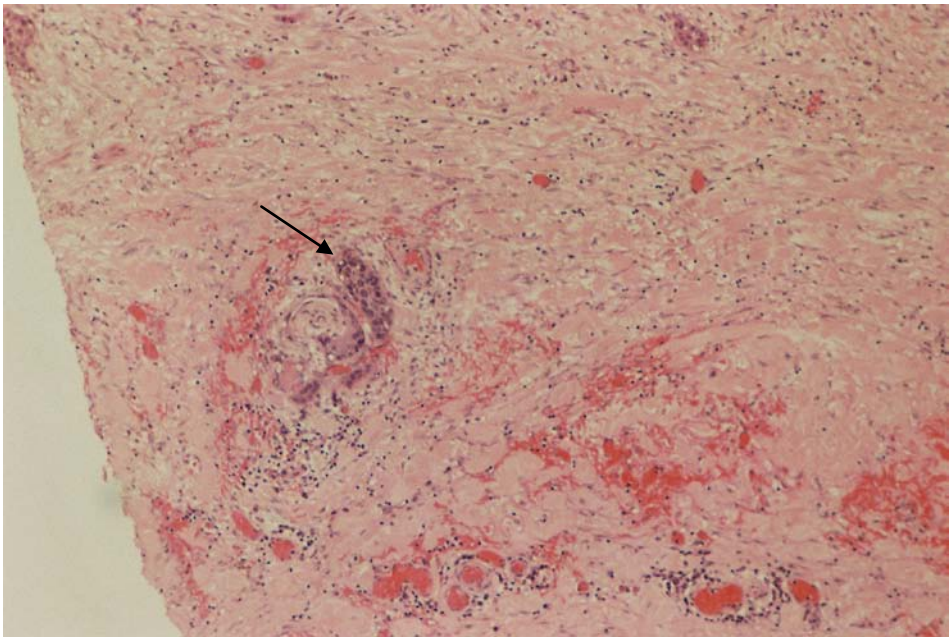

Figure J.7. Perineurial invasion by tumour cells in OSCC (arrow) (H&E stain: original magnification, x 120).

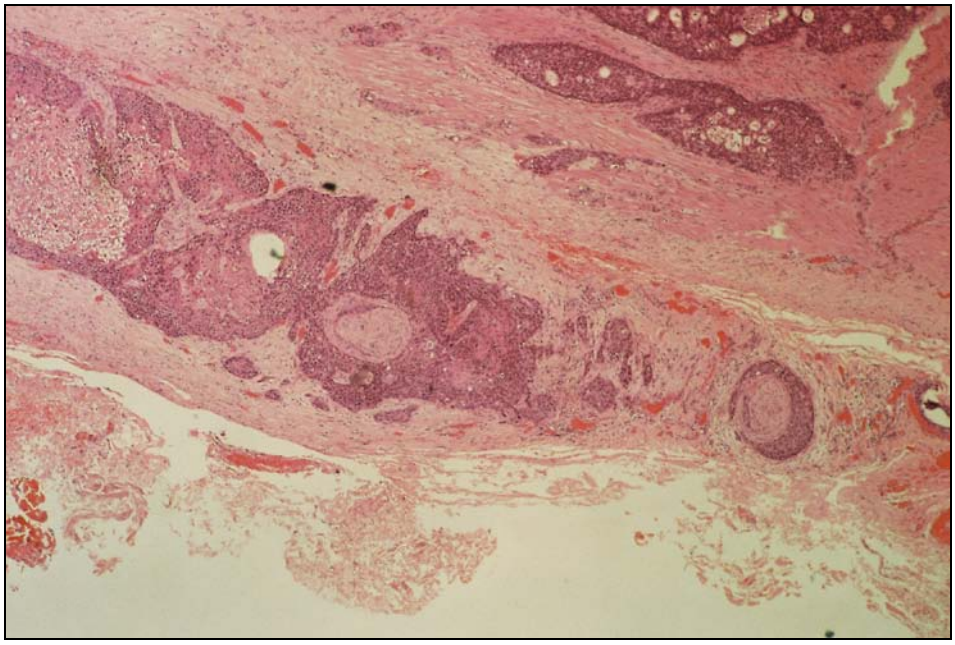

Figure J.8. Invasion of the perineurium by tumour cells within adventitial oesophageal tissue (H&E stain: original magnification, x 120).

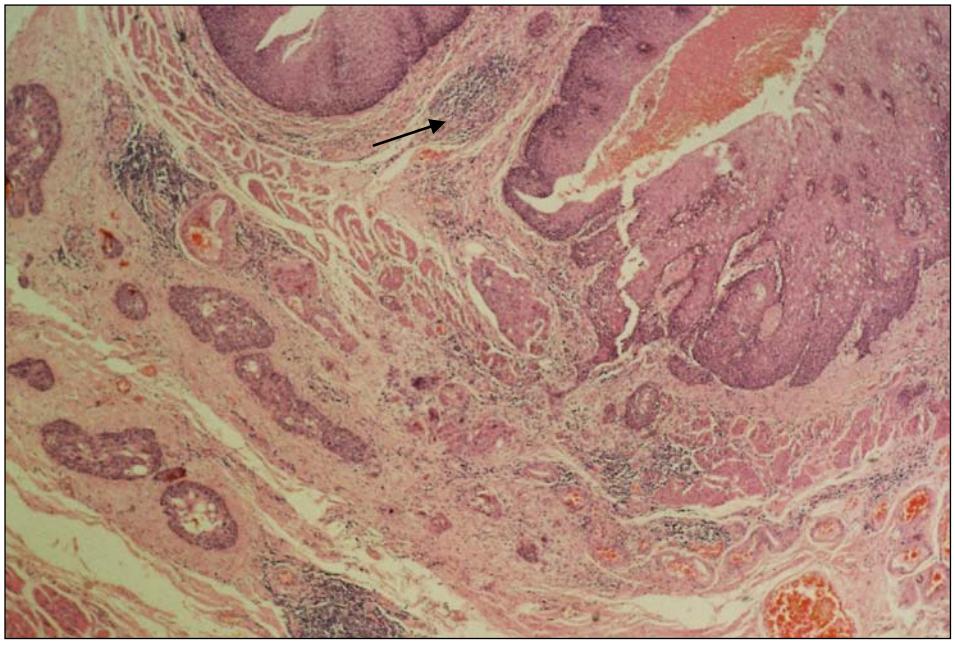

Figure J.9. Normal oesophageal squamous epithelium overlying submucosal tumour infiltration (arrow) (H&E stain: original magnification, x 120).

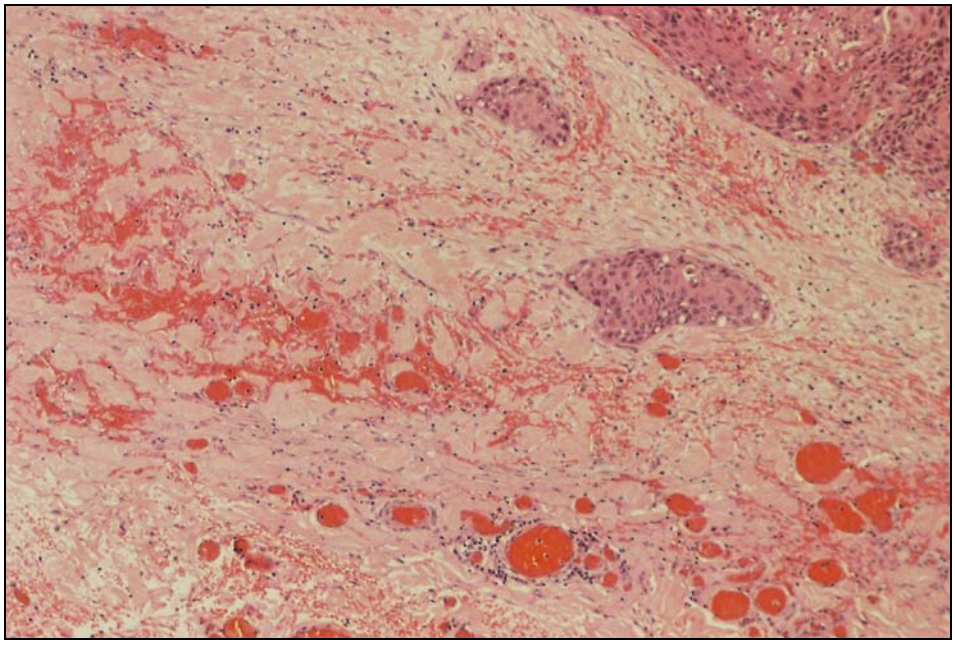

Figure J.10. Tumour infiltration on the serosal surface of oesophageal tissue (H&E stain: original magnification, x 120).

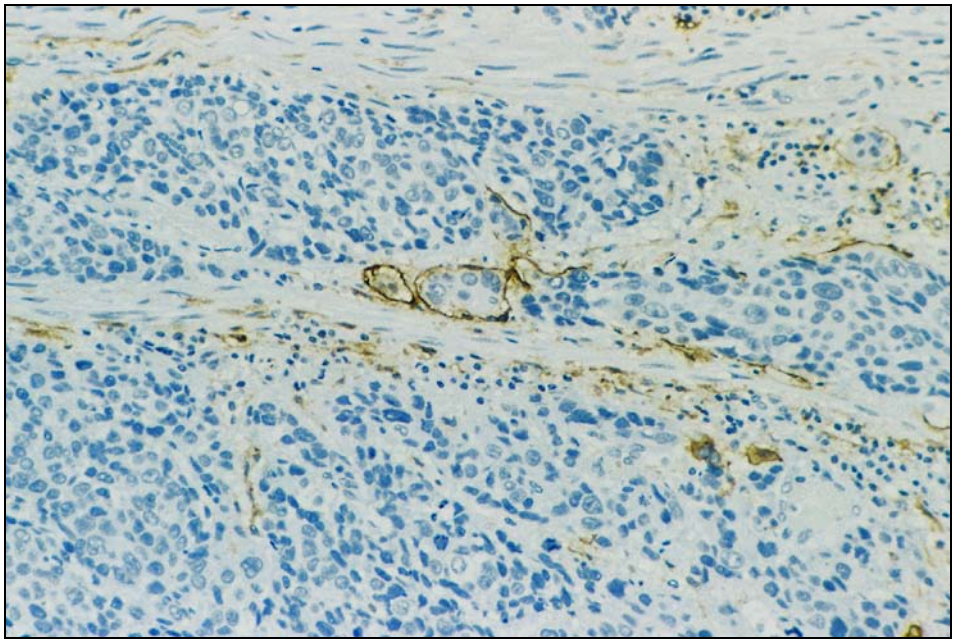

Figure J.11. Immunohistochemical D240 stain confirming tumour cells within lymphatic vessels of oesophageal tissue (original magnification, x 240).

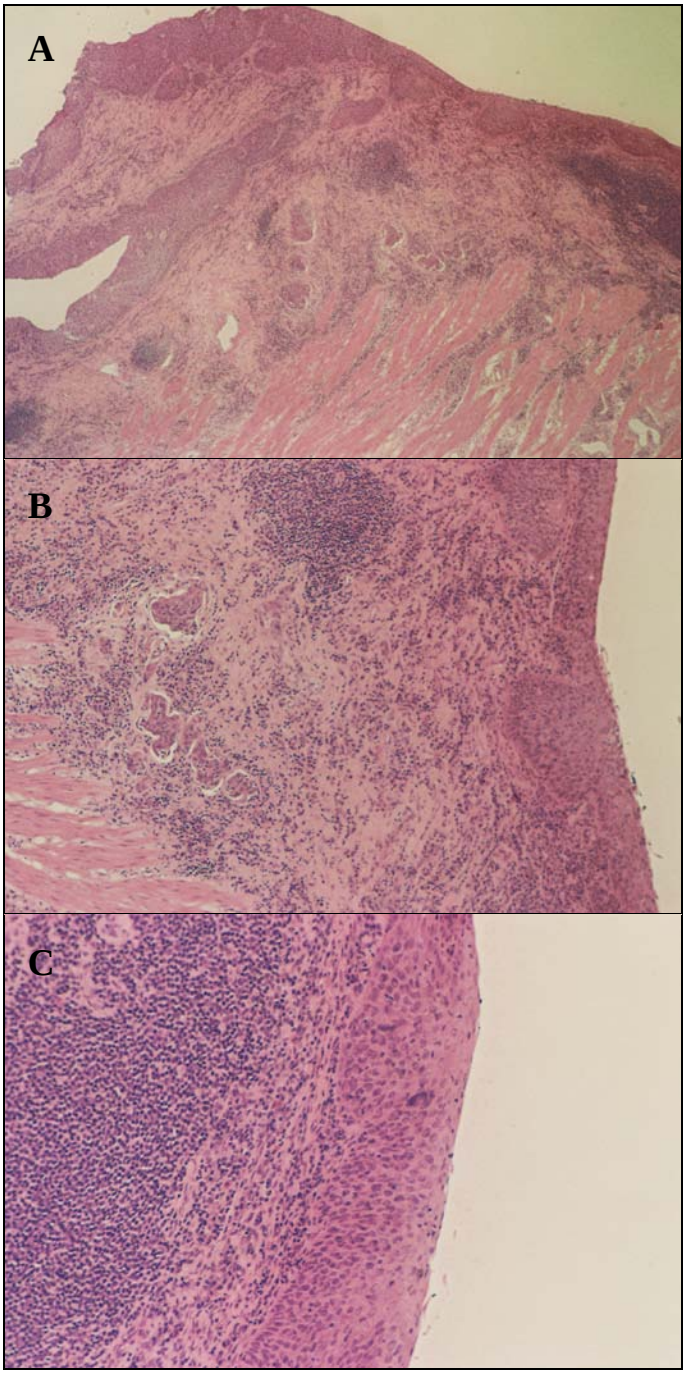

Figure J.12. A, Surface dysplasia in OSCC with tumour infiltration of subepithelial lymphatic channels. **B,** Tumour cells within lymphatics in OSCC. **C,** Dysplastic epithelia of OSCC. (Frozen samples, H&E stain: original magnification, x 24).

References:

Adams, J., Carder, P.J., Downey, S., Forbes, M.A., Maclennan, K., Allgar, V., Kaufman, S., Hallam, S., Bicknell, R., Walker, J.J., Cairnduff, F., Selby P.J., Perren T.J., Lansdown, M., Banks, R.E. (2000). Vascular endothelial growth factor (VEGF) in breast cancer: comparison of plasma, serum, and tissue VEGF and microvessel density and effects of tamoxifen. *Cancer Res*, 60, 2898-2905.

Andl, C.D., Mizushima, T., Nakagawa, H., Oyama, K., Harada, H., Chruma, K., Herlyn, M., Rustgi, A.K. (2003). Epidermal Growth Factor Receptor mediates increased cell proliferation, migration, and aggregation in esophageal keratinocytes in vitro and in vivo. *J Biol Chem*, 278, 1824-30.

Aoki, T., Nakagawa, Y., Tsuchida, A., Kasuya, K., Kitamura, K., Inoue, K., Ozawa, T., Koyanagi, Y., Itoi, T. (2002). Expression of cyclooxygenase-2 and vascular endothelial growth factor in pancreatic tumours. *Oncol Rep*, 9, 761-5.

Arteaga, C.L. (2001). The epidermal growth factor receptor: from mutant oncogene in nonhuman cancers to therapeutic target in human neoplasia. *J Clin Oncol*, 19, 32S-40S.

Baker, A.H., Edwards, D.R., Murphy, G. (2002). Metalloproteinase inhibitors: biological actions and therapeutic opportunities. *J Cell Sci*, 115, 3719-27.

Bancroft J.D., Cook H.C. (2002). Manual of histological techniques and their diagnostic application. Churchill Livingstone, Longman group UK.

Baselga, J., Tripathy, D., Mendelsohn, J., Baughman, S., Benz, C.C., Dantis, L., Sklarin, N.T., Seidman A.D., Hudis, C.A., Moore, J., Rosenn, P.P., Twadell, T., Henderson, I.C., Norton, L. (1996). Phase II study of weekly intravenous recombinant humanized anti-p185HER2 monoclonal antibody in patients with HER2/neu- overexpressing metastatic breast cancer. *J Clin Oncol*, 14, 737-44.

Becker, J.W., Marcy, A.I., Rokosz, L.L., Axel, M.G., Burbaum, J.J., Fitzgerald, P.M., Cameron, P.M., Esser, C.K., Hagmann, W.K., Hermes, J.D., et al. (1995). Stromelysin-1: three-dimensional structure of the inhibited catalytic domain and of the C-truncated proenzyme. *Protein Sci*, 4, 1966-76.

Bertram, J.S. (2001). The molecular biology of cancer. *Mol Aspects Med*, 21, 167-223.

Birkedal-Hansen, H., Moore, W.G., Bodden, M.K., Windsor, L.J., Birkedal-Hansen, B., DeCarlo, A., Engler, J.A. (1993). Matrix metalloproteinases: a review. *Crit Rev Oral Biol Med,* 4, 197-250.

Bleiberg, H., Conroy, T., Paillot, B., Lacave, A.J., Blijham, G., Jacob, J.H., Bedenne, L., Namer, M., De Besi, P., Gay, F., Collette, L., Sahmoud T. (1997). Randomised phase II study of cisplatin and 5-fluorouracil (5-FU) versus cisplatin alone in advanced squamous cell oesophageal cancer. *Eur J Cancer,* 33, 1216-20.

Blot, W.J. (1994). Esophageal cancer trends and risk factors. *Semin Oncol,* 21, 403-10.

Blot, W.J., McLaughlin, J.K. (1999). The changing epidemiology of esophageal cancer. *Semin Oncol,* 26, 2-8.

Bode, W., Gomis-Ruth, F. X. and Stacker, W. (1993). Astacins, serralysins, snake venom and matrix metalloproteinases exhibit identical zincbinding environments (HEXXHXXGXXH and Met-turn) and topologies and should be grouped into a common family, the ‘metzincins’, *FEBS Lett.* 331, 134-140.

Bonneta, L. (2005). Prime time for real-time PCR. *Nat Methods,* 2, 305-312.

Borre, M., Nerstrøm, B., Overgaard, J. (2000). Association between immunohistochemical expression of vascular endothelial growth factor (VEGF), VEGF-expressing neuroendocrine-differentiated tumour cells, and outcome in prostrate cancer patients subjected to watchful waiting. *Clin Cancer Res,* 6, 1882-90.

Brabender, J., Danenberg, K.D., Metzger, R., Schneider, P.M., Park, J., Salonga, D., Hölscher, A.H., Danenberg, P.V. (2001). Epidermal growth factor receptor and HER2-neu mRNA expression in non-small cell lung cancer Is correlated with survival. *Clin Cancer Res,* 7, 1850-5.

Bradshaw, E., Schonland, M. (1969). Oesophageal and lung cancers in Natal African males in relation to certain socio-economic factors. An analysis of 484 interviews. *Br J Cancer,* 23, 275-84.

Bramhall, S.R., Stamp, G.W., Dunn, J., Lemoine, N.R., Neoptolemos, J.P. (1996). Expression of of collagenase (MMP2), stromelysin (MMP3) and tissue inhibitor of the metalloproteinases (TIMP1) in pancreatic and ampullary disease. *Br J Cancer,* 73, 972-8.

Brem, S., Brem, H., Folkman, J., Finkelstein, D., Patz, A. (1976) Prolonged tumour dormancy by prevention of neovascularization in the vitreous. *Cancer Res* 36, 2807-12.

Brown, P.D. (1999). Clinical studies with matrix metalloproteinase inhibitors. *APMIS*, 107, 174-180.

Bustin, S.A. (2000). Absolute quantification of mRNA using real-time reverse transcription polymerase chain reaction assays. *J Molec Endocrinol*, 25, 169-193.

Caldeira, S., de Villiers, E.M., Tommasino, M. (2000). Human papillomavirus E7 proteins stimulate proliferation independently of their ability to associate with retinoblastoma protein. *Oncogene*, 19, 821-6.

Cao, R., Bråkenhielm, E., Li, X., Pietras, K., Widenfalk, J., Ostman, A., Eriksson U., Cao, Y. (2002). Angiogenesis stimulated by PDGF-CC, a novel member in the PDGF family, involves activation of PDGFR-alphaalpha and -alphabeta receptors. *FASEB J*, 16, 1575-83.

Carpenter, G. (2000). The EGF receptor: a nexus for trafficking and signalling. *Bioessays*, 22, 697-707.

Carraway, K.L.3rd, Weber, J.L., Unger, M.J., Ledesma, J., Yu, N., Gassman, M., Lai, C. (1997). Neuregulin-2, a new ligand of ErbB3/ErbB4-receptor tyrosine kinases. *Nature*, 387, 512-6.

Cascinu, S., Staccioli, M.P., Gasparini, G., Giordani, P., Catalano, V., Ghiselli, R., Rossi, C., Baldelli, A.M., Graziano, F., Saba, V., Muretto, P., Catalano, G. (2000). Expression of vascular endothelial growth factor can predict event-free survival in stage II colon cancer. *Clin Cancer Res*, 6, 2803-7.

Čemerikić-Martinović, V., Trpinac, D., Ercegovac M. (1998). Correlations between mitotic and apoptotic indices, number of interphase NORs, and histological grading in squamous cell lung cancer. *Microsc Res Tech*, 40, 408-417.

Chang, F., Syräjnen, S., Shen, Q., Cintorino, M., Santopietro, R., Tosi, P., Syräjnen, K. (2000). Human papillomavirus involvement in esophageal carcinogenesis in the high-incidence are of China. A study of 700 cases by screening and type-specific in situ hybridization. *Scand J Gastroenterol*, 35, 123-30.

Chang, F., Syräjnen, S., Wang, L., Syrjänen, K. (1992). Infectious agents in the etiology of esophageal cancer. *Gastroenterology*, 103, 1336-48.

Chang, H., Riese, D.J., 2nd, Gilbert, W., Stern, D.F., McMahan, U.J. (1997). Ligands for the ErbB-family receptors encoded by a neuregulin-like gene. *Nature*, 387, 509-12.

Chang-Claude, J., Becher, H., Blettner, M., Qiu, S., Yang, G., Wahrendorf, J. (1997). Familial aggregation of oesophageal cancer in a high incidence area in China. *Int J Epidemiol*, 26, 1159-65.

Chen, J., Byrne, G.E., Lossos, I.S. (2007). Optimization of RNA extraction from formalin-fixed, paraffin-embedded lymphoid tissues. *Diagn Mol Pathol*, 16, 61-72

Chen, L.Q., Hu, C.Y., Ghadirian, P., Duranceau, A. (1999). Early detection of esophageal squamous cell carcinoma and its effect on therapy: an overview. *Dis Esophagus*, 12, 161-167.

Chetty, R., Simelane, S. (1999). p53 and cyclin A protein expression in squamous carcinoma of the oesophagus. *Pathol Oncol Res*, 5, 193-6.

Chiang, P.W., Beer, D.G., Wei, W.L., Orringer, M.B., Kurnit, D.M. (1999). Detection of erbB-2 amplifications in tumours and sera from esophageal carcinoma patients. *Clin Cancer Res*, 5, 1381-6.

Chiu, S.T., Hsieh, F.J., Chen, S.W., Chen, C.L., Shu, H.F., Hung, L. (2005). Clinicopathologic correlation of up-regulated genes identified using cDNA microarray and real-time reverse transcription-PCR in human colorectal cancer. *Cancer Epidemiol Biomarkers Prev*, 14, 437-43.

Ciardiello, F., Bianco, R., Damiano, V., Fontanini, G., Caputo, R., Pomatico, G., De Placido, S., Bianco, A.R., Mendelsohn, J., Tortora, G. (2000). Antiangiogenic and antitumour activity of anti-epidermal growth factor receptor C225 monoclonal antibody in combination with vascular endothelial growth factor antisense oligonucleotide in human GEO colon cancer cells. *Clin Cancer Res*, 6, 3739-47.

Ciardiello, F., Troiani, T., Bianco, R., Orditura, M., Morgillo, F., Martinelli, E., Morelli, M.P., Cascone, T., Tortora, G. (2006). Interaction between the epidermal growth factor receptor (EGFR) and the vascular endothelial growth factor (VEGF) pathways: a rational approach for multi-target anticancer therapy. *Ann Oncol*, 17, vii109-vii114.

Citri, A., Skaria, K.B., Yarden, Y. (2003). The deaf and the dumb: the biology of ErbB-2 and ErbB-3. *Exp Cell Res*, 284, 54-65.

Cobleigh, M.A., Vogel, C.L., Tripathy, D., Robert, N.J., Scholl, S., Fehrenbacher, L., Wolter, J.M., Paton, V., Shak, S., Lieberman, G., Slamon, D.J. (1999). Multinational study of the efficacy and safety of humanized anti-HER2 monoclonal antibody in woman who have HER2-overexpressing metastatic breast cancer that has progresses after chemotherapy for metastatic disease. *J Clin Oncol*, 17, 2639-48.

Cornelius, L.A., Nehring, L.C., Harding, E., Bolanowski, M., Welgus, H.G., Kobayashi, D.K., Pierce, R.A., Shapiro, S.D. (1998). Matrix metalloproteinases generate angiostatin: effects on neovascularization. *J Immunol*, 161, 6845-52.

Costa, C., Soares, R., Reis-Filho, J.S., Leitão, D., Amendoeira, I., Schmitt, F.C. (2002). Cyclo-oxygenase 2 expression is associated with angiogenesis and lymph node metastasis in human breast cancer. *J Clin Pathol*, 55, 429-34.

Coussens, L., Yang-Feng, T.L., Liao, Y.C., Chen, E., Gray, A., McGrath, J., Seeburg, P.H., Libermann, T.A., Schlessinger, J., Francke, U., et al. (1985). Tyrosine kinase receptor with extensive homology to EGF receptor shares chromosomal location with neu oncogene. *Science*, 230, 1132-9.

Coussens, L.M., Werb, Z. (2002). Inflammation and cancer. *Nature*, 420, 860-867.

Crew, K.D., Neugut, A.I. (2004). Epidemiology of upper gastrointestinal malignancies. *Semin Oncol*, 31, 450-64.

Cronin, M., Pho, M., Dutta, D., Stephans, J.C., Shak, S., Kiefer, M.C., Esteban, J.M., Baker, J.B. (2004). Measurement of gene expression in archival paraffin-embedded tissues: development and performance of a 92-gene reverse transcriptase-polymerase chain reaction assay. *AM J Pathol*, 164, 35-42.

Damjanov, I., Linder, J., Eds. (1996). Anderson's Pathology. 10th ed. pp.1647-59, Mosby-Year Book. Missouri (USA).

Deryugina, E.I., Luo, G.X., Reisfeld, R.A., Bourdon, M.A., Strongin, A. (1997). Tumour cell invasion through matrigel is regulated by activated matrix metalloproteinase-2. *Anticancer Res*, 17, 3201-10.

Dlamini, Z., Bhoola, K. (2005). Esophageal cancer in African blacks of Kwazulu Natal, South Africa: an epidemiological brief. *Ethn Dis*, 15, 786-9.

Doll, R. (1969). The geographical distribution of cancer. *Br J Cancer*, 23, 1-8.

Dreilich, M., Wanders, A., Brattström, D., Bergström, S., Hesselius, P., Wagenius, G., Bergqvist, M. (2006). HER-2 overexpression (3+) in patients with squamous cell esophageal carcinoma correlates with poorer survival. *Dis Esophagus*, 19, 224-31.

Duraker, N., Şişman, S., Günay, C. (2003). The significance of perineural invasion as a prognostic factor in patients with gastric carcinoma. *Surg Today*, 33, 95-100.

Duranceau, A. (1998). Epidemiologic trends and etiologic factors of esophageal carcinoma in International ternds in general thoracic surgery: esophageal cancer, 4, 3-15.

Dvorak, H.F. (2002). Vascular permeability factor/vascular endothelial growth factor: a critical cytokine in tumour angiogenesis and a potential target for diagnosis and therapy. *J Clin Oncol*, 20, 4368-80.

Dvorak, H.F. (2003). Rous-Whipple Award Lecture. How tumours make bad blood vessels and stroma. *Am J Pathol*, 162, 1747-57.

Dvorak, H.F. (2005). Angiogenesis: update 2005. *J Thromb Haemost*, 3, 1835-42.

Egeblad, M., Werb, Z. (2002). New functions for the matrix metalloproteinases in cancer progression. *Nat Rev Cancer*, 2, 161-74.

Ekstrand, A.J., Longo, N., Hamid, M.L., Olson, J.J., Liu, L., Collins, V.P., James, C.D. (1994). Functional characterization of an EGF receptor with a truncated extracellular domain expressed in glioblastomas with EGFR gene amplification. *Oncogene,* 9, 2313-20.

Ellis, F.H. Jr., Watkins, E.Jr., Krasna, M.J., Heatley, G.J., Balogh, K. (1993). Staging of carcinoma of the esophagus and cardia: a comparison of different staging criteria. *J Surg Oncol,* 52, 231-5.

Ellis, L.M. (2004). Epidermal growth factor receptor in tumour angiogenesis. *Hemotol Oncol Clin North Am,* 18, 1007-21.

Ellis, L.M., Liu, W., Fan, F., Reinmuth, N., Shaheen, R.M., Jung, Y.D., Ahmad, S. (2001). Role of angiogenesis inhibitors in cancer treatment. *Oncology,* 15, 39-46.

Enzinger, P.C., Mayer, R.J. (2003). Esophageal cancer. *New Engl J Med,* 349, 2241-52.

Evan, G., Littlewood, T. (1998). A matter of life and cell death. *Science,* 281, 1317-22.

Fang, J., Shing, Y., Wiederschain, D., Yan, L., Butterfield, C., Jackson, G., Harper, J., Tamavakopoulos, G., Moses, M.A. (1999). Matrix metalloproteinase-2 is required for the switch to the angiogenic phenotype in a tumour model. *Proc Natl Acad Sci U S A,* 97, 3884-9.

Fendly, B.M., Winget, M., Hudziak, R.M., Lipari, M.T., Napier, M.A., Ullrich, A. (1990). Characterization of murine monoclonal antibodies reactive to either the human epidermal growth factor receptor or HER2/neu gene product. *Cancer Res,* 50, 1550-8.

Ferguson, A., Kingstone, K. (1996). Coeliac disease and malignancies. *Acta Pediatr Suppl,* 412, 78-81.

Ferrara, N., Davis-Smyth, T. (1997). The biology of vascular endothelial growth factor. *Endocr Rev,* 18, 4-25.

Ferrara, N., Henzel, W.J. (1989). Pituitary follicular cells secrete a novel heparin-binding growth factor specific for vascular endothelial cells. *Biochem Biophys Res Commun,* 161, 851-8.

Ferrara, N., Houck, K., Jakeman, L., Leung, D.W. (1992). Molecular and biological properties of the vascular endothelial growth factor family of proteins. *Endocr Rev,* 13, 18-32.

Fishman, D.A., Bafetti, L.M, Stack, M.S. (1996). Membrane-type matrix metalloproteinase expression and matrix metalloproteinase-2 activation in primary human ovarian epithelial carcinoma cells. *Invasion Metastasis*, 16, 150-159.

Folkman, J. (1971). Tumour angiogenesis: therapeutic implications. *New Engl J Med*, 285, 1182-6.

Folkman, J. (2003). Angiogenesis and apoptosis. *Semin Cancer Biol,* 13, 159-67.

Fong, G.H., Rossant, J., Gertsenstein, M., Breitman, M.L. (1995). Role of the Flt-1 receptor tyrosine kinase in regulating the assembly of vascular endothelium. *Nature*, 376, 66-70.

Frederick, L., Wang, X.Y., Eley, G., James, C.D. (2000). Diversity and frequency of epidermal growth factor receptor mutations in human glioblastomas. *Cancer Res*, 60, 1383-7.

Freitag, L., Telkof, E., Steveling, H., Donovan, T.J., Stamatis, G. (1996). Management of malignant esophagotracheal fistulas with airway stenting and double stenting. *Chest*, 110, 1155-60.

Garcia de Palazzo, I.E., Adams, G.P., Sundareshan, P., Wong, A.J., Testa, J.R., Bigner, D.D., Weiner, L.M. (1993). Expression of mutated epidermal growth factor receptor by non-small cell lung carcinomas. *Cancer Res,* 53, 3217-20.

Gately, S. (2000). The contributions of cyclooxygenase-2 to tumour angiogenesis. *Cancer Metastasis Rev*, 19, 19-27.

Gianneli, G., Falk-Marzillier, J., Schiraldi, O., Stetler-Stevenson, W.G., Quaranta, V. (1997). Induction of cell migration by matrix metalloproteinase-2 cleavage of laminin-5. *Science*, 277, 225-8.

Gloghini, A., Canal, B., Klein, U., Dal Maso, L., Perin, T., Dalla-Farvera, R., Carbone, A. (2004). RT-PCR analysis of RNA extracted from Bouin-fixed and paraffin-embedded lymphoid tissues. *J Mol Diagn*, 6, 290-96.

Godfrey, T.E., Kim, S.H., Chavira, M., Ruff, D.W., Warren, R.S., Gray, J.W., Jensen, R.H. (2000). Quantitative mRNA expression analysis from formalin-fixed paraffin embedded tissues using 5' nuclease quantitative reverse transcription-polymerase chain reaction. *J Mol Diagn*, 2(2), 84-91

Graus-Porta, D., Beerli, R.R., Daly, J.M., Hynes, N.E. (1997). ErbB-2, the preferred heterodimerization partner of all ErbB receptors, is a mediator of lateral signaling. *EMBO J*, 16, 1647-55.

Greene, F.L., Page, D.L., Fleming, I.D., Fritz, A., Balch, C.M., Haller, D.G., Morrow, M. (2002). AJCC cancer staging manual, 6th edn., Springer-Verlag, New York (USA).

Guanrei, Y., He, H., Sungliang, Q., Yuming, C. (1982), Endoscopic diagnosis of 115 cases of early esophageal carcinoma. *Endoscopy*, 14, 157.

Gullick, W.J. (1990). The role of the epidermal growth factor receptor and the c-erbB-2 protein in breast cancer. *Int J Cancer*, 5, 55-61.

Guy, P.M., Platko, J.V., Cantley, L.C., Cerione, R.A., Carraway, K.L.3rd (1994). Insect cell-expressed p180 erbB3 possesses an impaired tyrosine kinase activity. *Proc Natl Acad Sci U S A*, 91, 8132-36.

Hanahan, D., Weinberg, R.A. (2000). The hallmarks of cancer. *Cell*, 100, 57-70.

Hanawa, M., Suzuki, S., Dobashi, Y., Yamane, T., Kono, K., Enomoto, N., Ooi, A. (2006). EGFR protein overexpression and gene amplification in squamous cell carcinomas of the esophagus. *Int J Cancer*, 118, 1173-80.

Hashimoto, Y., Ito, T., Inoue, H., Okumura, T., Tanaka, E., Tsunoda, S., Higashiyama, M., Watanabe, G., Imamura, M., Shimada, Y. (2005). Prognostic significance of Fascin overexpression in human esophageal squamous cell carcinoma. *Clin Cancer Res*, 11, 2597-2605.

Hermanek, P., Sobin, L.H. (1987). UICC International Union against Cancer: TNM classification of malignant tumours. pp.40-42. Springer-Verlag, Berlin (Germany).

Hertoghs, K.M.L., Ellis, J.H., Catchpole, I.R. (2003). Use of locked nucleic acid oligonucleotides to add functionality to plasmid DNA. Nucleic acids research., 31, 5817-30.

Hicklin, D.J., Ellis, L.M. (2005). Role of the vascular endothelial growth factor pathway in tumour growth and angiogenesis. *J Clin Oncol*, 23, 1011-27.

Higginson, J., Oettle, A.G. (1960). Cancer incidence in the Bantu and "Cape coloured" races of South Africa: report of a cancer survey in the Transvaal (1953-55). *J Natl Cancer Inst*, 24, 589-671.

Hirai, T., Kuwahara, M., Yoshida, K., Kagawa, Y., Hihara, J., Yamashita, Y., Toge, T. (1998). Clinical results of transhiatal esophagectomy for carcinoma of the lower thoracic esophagus according to biological markers. *Dis Esophagus*, 11, 221-5.

Hiratsuka, S., Maru, Y., Okada, A., Seiki, M., Noda, T., Shibuya, M. (2001). Involvement of Flt-1 tyrosine kinase (vascular endothelial growth factor receptor-1) in pathological angiogenesis. *Cancer Res*, 61, 1207-13.

Hoekstra, R., Eskens, F.A., Verweij, J. (2001). Matrix metalloproteinase inhibitors: current developments and future perspectives. *Oncologist*, 6, 415-27.

Hoffman, D., Hecht, S.S., Ornam, R.M., Wynder, E.L., Tso, T.C. (1976). Chemical studies on tobacco smoke. XLII. Nitrosonornicotine: presence in tobacco, formation and carcinogenecity. *IARC Sci Publ*, 307-320.

Holmes, R.S., Vaughan, T.L. (2007). Epidemiology and pathogenesis of esophageal cancer. *Semin Radiat Oncol*, 17, 2-9.

Holmgren, l., O'Reilly, M.S., Folkman, J. (1995). Dormancy of micro-metastases: balanced proliferation and apoptosis in the presence of angiogenesis suppression. *Nat Med*, 1, 149-53.

Horst, I., Peterhänsel, C. (2007). Quantification of Zea mays mRNAs by Real-Time PCR using the Universal Probe Library. *Biochemica*, 1, 8-10.

Iihara, K., Shiozaki, H., Tahara, H., Kobayashi, K., Inoue, M., Tamura, S., Miyata, M., Oka, H., Doki, Y., Mori, T. (1993). Prognostic significance of transforming growth factor-alpha in human esophageal carcinoma. Implication for the autocrine proliferation. *Cancer*, 71, 2902-9.

Ikpatt, O., Ndoma-Egba, R., Collan, Y. (2002). Prognostic value of necrosis in Nigerian breast cancer. *Adv Clin Path*, 6 , 31-7.

Inada, S., Koto, T., Futami, K., Arima, S., Iwashita, A. (1999). Evaluation of malignancy and the prognosis of esophageal cancer based on an immunohistochemical study (p53, E-cadherin, epidermal growth factor receptor). *Surg Today*. 29, 493-503.

Isaacson, C. (1982). Pathology of a Black African population. *Current Top Pathol*, 72, 1-152

Itoh, T., Tanioka, M., Yoshida, H., Yoshioka, T., Nishimoto, H., Itohara, S. (1998). Reduced angiogenesis and tumour progression in gelatinase A-deficient mice. *Cancer Res*, 58, 1048-51.

Iwase, H., Itoh, Y., Kuzushima, T., Yamashita, H., Itawa, H., Toyama, T., Hara, Y., Kobayashi, S. (1997). Simultaneous quantitative analyses of c-erbB-2 protein, epidermal growth factor receptor, cathepsin D, and hormone receptors in breast cancer. *Cancer Detect Prev*, 21, 29-35.

Jiang, W., Zhang, Y.J., Kahn, S.M., Hollstein, M.C., Santella, R.M., Lu, S.H, Harris, C.C., Montesano, R., Weinstein, I.B. (1993). Altered expression of the cyclin D1 and retinoblastoma genes in human esophageal cancer. *Proc Natl Acad Sci U S A*, 90, 9026-30.

JSED (Japanese Society for Esophageal Diseases) (1999). In: Guidelines for the clinical and pathologic studies on carcinoma of the esophagus [in Japanese]. 9th ed. Kanehara and Co., Tokyo (Japan).

Kainz, P. (2000). The PCR plateau phase- towards an understanding of its limitations. *Biochem Biophys Acta*, 1494, 23-27.

Kaipainen, A., Korhonen, J., Mustonen, T., van Hinsbergh, V.W., Fang, G.H., Dumont, D., Breitman, M., Alitalo, K. (1995). Expression of the fms-like tyrosine kinase 4 gene becomes restricted to lymphatic endothelium during development. *Proc Natl Acad Sci U S A*, 92, 3566-70.

Kato, H., Tachimori, Y., Mizobuchi, S., Igaki, H., Ochiai, A. (1993). Cervical, mediastinal, and abdominal lymph node dissection (three-field dissection) for superficial carcinoma of the thoracic oesophagus. *Cancer*, 72, 2879-82.

Kaya, M., Wada, T., Akatsuka, T., Kawaguchi, S., Nagoya, S., Shindoh, M., Higashino, F., Mezawa, F., Okada, F., Ishii, S. (2000). Vascular endothelial growth factor expression in untreated osteosarcoma is predictive of pulmonary metastasis and poor prognosis. *Clin Cancer Res*, 6, 572-77.

Keck, P.J., Hauser, S.D., Krivi, G., Sanzo, K., Warren, T., Feder, J., Connolly, D.T. (1989). Vascular permeability factor, an endothelial cell mitogen related to PDGF. *Science,* 246, 1309-12.

Kedar, D., Baker, C.H., Killion, J.J., Dinney, C.P., Fidler, I.J. (2002). Blockade of the epidermal growth factor receptor signaling inhibits angiogenesis leading to regression of human renal cell carcinoma growing orthotopically in nude mice. *Clin Cancer Res*, 8, 3592-600.

Kim, S.J., Uehara, H., Karashima, T., Shephard, D.L., Killion, J.J., Fidler I.J. (2003). Blockade of epidermal growth factor receptor signaling in tumour cells and tumour-associated endothelial cells for therapy of androgen-independent human prostrate cancer growing in the bone of nude mice. *Clin Cancer Res*, 9, 1200-10.

Klapper, L.N., Kirschbaum, M.H., Sela, M., Yarden, Y. (2000). Biochemical and clinical implications of the ErbB/HER signaling network of growth factor receptors. *Adv Cancer Res*, 77, 25-79.

Kleeff, J., Freiss, H., Liao, Q., Büchler, M.W. (2002). Immunohistochemical presentation in non-malignant and malignant Barret's epithelium. *Dis Esophagus* 15, 10-15.

Koshikawa, N., Gianelli, G., Cirulli, V., Miyazaki, K., Quaranta, V. (2000). Role of cell surface metalloprotease MT1-MMP in epithelial cell migration over laminin-5. *J Cell Biol,* 148, 615-24.

Koyama, H., Iwata, H., Kuwabara, Y., Iwase, H., Kobayashi, S., Fujii, Y. (2000). Gelatinolytic activity of matrix metalloproteinase-2 and -9 in oesophageal carcinoma; a study using in situ zymography. *Eur J Cancer* 36, 2164-70.

Kumar, V., Cotran, R.S., Robbins, S.L. Eds. (2003). Robbins: Basic Pathology. pp.165-209. Saunders, Philadelphia, (USA).

Lam, A.K. (2000). Molecular biology of esophageal squamous cell carcinoma. *Crit Rev Oncol Hematol*, 33, 71-90.

Lam, K.Y., Loke S.L., Chen, W.Z., Cheung, K.N. (1995). Expression of p53 in oesophageal squamous cell carcinoma in Hong Kong chinese. *Eur J Surg Oncol*, 21, 242-7.

Lam, K.Y., Tin, L., Ma L. (1998). C-erbB-2 protein expression in oesophageal squamous epithelium from Oesophageal squamous cell carcinomas, with special reference to histological grade of carcinoma and pre-invasive lesions. *Eur J Surg Oncol*, 24, 431-5.

Larsson, L.G., Sandström, A., Westling, P. (1975). Relationship of Plummer-Vinson disease to cancer of the upper alimentary tract in Sweden. *Cancer Res* 35, 3308-16.

Leucht, C., Bally-Cuif, L. (2007). The universal probe library- a versatile tool for quantitative expression analysis in the Zebrafish. *Biochemica*, 2, 16-18.

Leung, D.W., Cachianes, G., Kuang, W.J, Goeddel, D.V., Ferrara, N. (1989). Vascular endothelial growth factor is a secreted angiogenic mitogen. *Science* 246(4935), 1306-1309.

Levine, A.J. (1997). p53, the cellular gatekeeper for growth and division. *Cell* 88, 323-31.

Li, H., Lindenmeyer, F., Grenet, C., Opolon, P., Menashi, S., Soria, C., Yeh, P., Perricaudet, M., Lu, H. (2001). AdTIMP-2 inhibits tumour growth, angiogenesis, and metastasis, and prolongs survival in mice. *Hum Gene Ther*, 12, 515-26.

Lin, C.R., Chen, W.S., Kruiger, W., Stolarsky, L.S., Weber, W., Evans, R.M., Verma, I.M., Gill, G.N., Rosenfeld, M.G. (1984). Expression cloning of human EGF receptor complementary DNA: gene amplification and three related messenger RNA products in A431 cells. *Science*, 224, 843-8.

Lin, D.X., Tang, Y.M., Peng, Q., Lu, S.X., Ambrosone, C.B., Kadlubar, F.F. (1998). Susceptibility to esophageal cancer and genetic polymorphisms in glutathione S-transferases T1, P1 and M1 and cytochrome P450 2E1. *Cancer Epidemiol Biomarkers Prev* 7, 1013-8.

Liu, W., Saint, D.A. (2002). A new quantitative method of real time reverse transcription polymerase chain reaction assay based on simulation of polymerase chain reaction kinetics. *Annals Biochem*, 302, 52-9

Livak, K.J., Schmittgen, T.D. (2001). Analysis of relative gene expression data using real-time quantitative PCR and the 2(-Delta Delta CT) method. *Methods*, 25, 402-408.

Lonardo, .F, Di Marco, E., King, C.R., Pierce, J.H., Segatto, O., Aaronson, S.A., Di Fiore, P.P. (1990). The normal erbB-2 product is an atypical receptor-like tyrosine kinase with constitutive activity in the absence of ligand. *New Biol*, 2, 992-1003.

Loncaster, J.A., Cooper, R.A., Logue, J.P., Davidson, S.E., Hunter, R.D., West, C.M. (2000). Vascular endothelial growth factor (VEGF) expression is a prognostic factor for radiotherapy outcome in advanced carcinoma of the cervix. *Br J Cancer*, 83, 620-5.

Lu, H., Ouyang, W., Huang, C. (2006). Inflammation, a key event in cancer development. *Mol Cancer Res*, 4, 221-233.

Lu, S.H., Chui, S.X., Yang, W.X., Hu, X.N., Guo, L.P., Li, F.M. (1991). Relevance of N-nitrosamines to esophageal cancer in China. *IARC Sci Publ*, 105, 11-7

Mandard, A.M., Chasle, J., Marnay, J., Villedieu, B., Bianco, C., Roussel, A., Elie, H., Vernhes, J.C. (1981). Autopsy findings in 111 cases of esophageal cancer. *Cancer*, 48, 329-35.

Maniatis, T., Fritsch, E. F., Sambrook, J. (1989). Molecular Cloning: A Laboratory Manual. pp. 6.3, Cold Spring Harbor Laboratory Press, New York.

Mantovani, F., Banks, L. (1999). The interaction between p53 and papillomaviruses. *Semin Cancer Biol*, 9, 387-395.

Marasas, W.F. (2001). Discovery and occurrence of the fumonisins: a historical perspective. *Environ Health Perspect*, 109(Suppl 2), 239-43.

Marger, R.S., Marger, D. (1993). Carcinoma of the esophagus and tylosis. A lethal genetic combination. *Cancer*, 72(1), 17-9.

Martinez, J.D., Parker, M. T., Fultz, K.E., Ignatenko, N.A., Gerner, E.W. Ed: Abraham, D.J. (2003). Molecular biology of cancer Burger's Medicinal Chemistry and Drug Discovery: Volume 5: chemotherapeutic agents. 6th ed. pp.1-50. John Wiley and Sons, New York (USA).

Mauritz, R.P., Mauritzen, P., Pfundheller, H.M., Tolstrup, N., Lomholt, C. (2005). Universal probe library set: one transcriptome-one kit. *Biochemica*, 2, 22-24.

Mauritzen, P., Nielsen, P.S., Jacobsen, N., Noerholm, M., Lomholt, C., Pfundhellar, H.M., Ramsing, N.B., Kaupinen, S., Tolstrup, N. (2004). The Probe Library (TM)- expression profiling 99% of all human genes using only 90 dual labeled real-time PCR probes. *Biotechniques*, 37, 492-495.

Mauritzen, P., Noerholm, M., Nielsen, P.S., Jacobson, N., Lomholt, C., Pfundhellar H.M., Tolstrup, N. (2005). Probelibrary: a new method for faster design and execution of real-time PCR. *Nature methods*, 2, 313-6

McGee, J. O. D., Isaacson, P.G., Wright N.A., Eds. (1992). Oxford Textbook of Pathology: Volume 2a: Pathology of Systems. pp. 1133-4. Oxford University Press, Oxford (UK).

Merendino, K.A., Mark, V.H. (1952). An analysis of 100 cases of squamous cell carcinoma. *Cancer*, 52-61.

Meuer, S., Witwer, C.T., Nakagawara, K., Eds. (2001). Rapid cycle real-time PCR: methods and applications, pp. 1-7. Springer Verlag, Heidelberg

Mineta, H., Miura, K., Ogino, T., Takebayashi, S., Misawa, K., Uede, Y., Suzuki, I., Dictor, M., Borg, A., Wennerberg, J. (2000). Prognostic value of vascular endothelial growth factor (VEGF) in head and neck squamous cell carcinoma. *Br J Cancer*, 83(6), 775-81.

Morrisson, T.B., Weiss, J.J., Wittwer, C.T. (1998). Quantification of low-copy transcripts by continuous Sybr Green 1 monitoring during amplification. *Biotechniques*, 954-962.

Moscatello, D.K., Holgado-Madruga, M, Godwin, A.K., Ramirez, G., Gunn, G., Zoltick, P.W., Biegel, J.A., Hayes, R.L., Wong, A.J. (1995). Frequent expression of a mutant epridermal growth factor receptor in multiple human tumours. *Cancer Res* 55, 5536-9.

Moscatello, D.K., Montgomery, R.B., Sundareshan, P., McDanel, H., Wong, M.Y., Wong, A.J. (1996). Transformational and altered signal transduction by a naturally occuring mutant EGF receptor. *Oncogene*, 13, 85-96.

MRC (2001). Our Research: Burden of Disease Research Unit. Medical Research Council of South Africa. [online] Available at http://www.mrc.ac.za.bod/faqcancer.htm (Accessed on 10/01/2005).

Muller, Y.A, Li, B., Christinger, H.W., Wells, J.A., Cunningham, B.C., de Vos, A.M. (1997). Vascular endothelial growth factor: crystal structure and functional mapping of the kinase domain receptor binding site. *Proc Natl Acad Sci U S A*, 94, 7192-7.

Mullis, K.B. (1990). The unusual origin of the polymerase chain reaction. *Sci Am*, 262, 56-61

Mullis, K.B., Faloona, F.A. (1987). Specific synthesis of DNA in vitro via a polymerase-catalyzed chain reaction. *Methods enzymol*, 155, 335-350.

Muňoz, N., Hayashi, M., Bang, L.J., Wahrendorf, J., Crespi, M., Bosh, F.X. (1987). Effect of riboflavin, retinol, and zinc on micronuclei of buccal mucosa and of esophagus: a randomised double-blind intervention study in China. *J Natl Cancer Inst*, 79, 687-91.

Nagase, H., Woessner, J.F. Jr. (1999). Matrix metalloproteinases. *J Biol Chem* 274, 21491-4.

Nakamura, T., Nekarda, H., Hoelscher, A.H., Bollschweiler, E., Harbeck, N., Becker, K., Siewert, J.R., Harbeck, N. (1994). Prognostic value of DNA ploidy and c-ErbB-2 oncoprotein overexpression in adenocarcinoma of Barret's oesophagus. *Cancer*, 73, 1785-94.

Nebel, O.T., Fornes, M.F., Castell, D.O. (1976). Symptomatic gastrooesophageal reflux: incidence and precipitating factors. *Am J Dig Dis*, 21, 953-6.

Nelson, A.R., Fingleton, B., Rothenberg, M.L., Matrisian, L.M. (2000). Matrix Metalloproteinases: biological activity and clinical implications. *J Clin Oncol*, 18, 1135-49.

Newby, D.T., Hadfield, T.L., Roberto, F.F. (2003). Real-Time PCR detection of *Brucella abortus*: a comparitive study of SYBR Green I, 5'-exonuclease and hybridization probe assays. *Appl Environ Microbiol*, 69, 4753-4759.

Nicholson, R.I., Gee, J., Harper, M.E. (2001). EGFR and cancer prognosis. *Eur J Cancer*, 37, S9-15.

Normanno, N., Bianco, C., Strizzi, L., Mancino, M., Maiello, M.R., De Luca, A., Caponigro, F., Salomon, D.S. (2005). The ErbB receptors and their ligands in cancer: an overview. *Curr Drug Targets*, 6, 243-57.

Norrby, K. (1997). Angiogenesis: new aspects relating to its initiation and control. *Acta Pathologica, Microbiologica et Immunologica Scandinavica*, 105, 417-37.

Nowell, P.C. (1976). The clonal evolution of tumour cell populations. *Science*, 194, 23-8.

Oh, J., Takahashi, R., Kondo, S., Mizoguchi, A., Adachi, E., Sasahara, R.M., Nishimura, S., Imamura, Y., Kitayama, H., Alexander, D.B., Ide, C., Horan, T.P., Arakawa, T., Yoshida H., Nishikawa, S., Itoh, Y., Seiki, M., Itohara, S., Takahashi, C., Noda, M. (2001). The membrane-anchored MMP inhibitor RECK is a key regulator of extracellular matrix integrity and angiogenesis. *Cell*, 107, 789-800.

Ohtani, H. (1998). Stromal reaction in cancer tissue: pathophysiologic significance of the expression of matrix-degrading enzymes in relation to matrix turnover and immune/inflammatory reactions. *Pathol Int*, 48, 1-9.

Olayioye, M.A., Neve, R.M., Lane, H.A, Hynes, N.E. (2000). The ErbB signaling network: receptor heterodimerization in development and cancer. *EMBO J*, 199, 3159-3167

Olsen, T.A., Mohanraj, D., Carson, L.F., Ramakrishnan, S. (1994). Vascular permeability factor gene expression in normal and neoplastic human ovaries. *Cancer Res*, 54, 276-280.

Parkin, D.M., Läärä, E., Muir, C.S. (1988). Estimates of the worldwide frequency of sixteen major cancers in 1980. *Int J Cancer*, 41, 184-97.

Pepper, M.S., Montesano, R., Mandriota, S.J., Orci, L., Vassali, J.D. (1996). Angiogenesis: a paradigm for balanced extracellular proteolysis during cell migration and morphogenesis. *Enzyme Protein*, 49, 138-162.

Perou, C.M., Jeffrey, S.S., van deRijn, M., Rees, C.A., Eisen, M.B., Ross, D.T., Pergamenschikov, A., Williams, C.F., Zhu, S.X., Lee, J.C., Lashkari, D., Shalon, D., Brown, P.O., Botstein D. (1999). Distinctive gene expression patterns in human mammary epithelial cells and breast cancers. *Proc Natl Acad U S A*, 96, 9212-7.

Perrotte, P., Matsumoto, T., Inoue, K., Kuniyasu, H., Eve, B.Y., Hicklin, D.J., Radinsky R., Dinney, C.P. (1999). Anti-epidermal growth factor receptor antibody C225 inhibits angiogenesis in human transitional cell carcinoma growing orthotopically in nude mice. *Clin Cancer Res*, 5, 257-65.

Peters, K.G., De Vries, C., Williams, L.T. (1993). Vascular endothelial growth factor receptor expression during embryogenesis and tissue repair suggests a role in endothelial differentiation and blood vessel growth. *Proc Natl Acad Sci U S A* 90, 8915-8919.

Pfaffl, M.W., Horgan, G.W., Dempfle, L. (2002). Relative expression software tool (REST) for group-wise comparison and statistical analysis of relative expression results in real-time PCR. *Nucleic Acids Research*, 30, 1-10.

Plouët, J., Schilling, J., Gospodarowicz, D. (1989). Isolation and characterization of a newly identified endothelial cell mitogen produced by AtT20 cells. *EMBO J*, 8, 3801-6.

Prenzel, N., Fischer, O.M., Streit, S., Hart, S., Ullrich, A. (2001). The epidermal growth factor receptor family as a central element for cellular signal transduction and diversification. *Endocr Relat Cancer*, 8, 11-31.

Rafii, S., Lyden, D. (2003). Therapeutic stem and progenitor cell transplantation for organ vascularization and regeneration. *Nat Med*, 9, 702-712.

Rak, J., Kerbel, R.S. (2001). Ras regulation of vascular endothelial growth factor and angiogenesis. *Methods Enzymol*, 333, 267-83.

Ramakers, C., Ruijter, J.M., Deprez, R.H., Moorman, A.F. (2003). Assumption free analysis of quantitative real time polymerase chain reaction (PCR) data. *Neurosci Lett*, 339, 62-66.

Rasmussen, R., Quantification on the Lightcycler. In Meuer, S., Wittwer, C., Nakagawara, K.I., ed. (2001). Rapid Cycle Real Time PCR: Methods and Applications. pp. 21-34, Springer, Heidelberg.

Ravdin, P.C., Chamness, G.C. (1995). The c-erbb-2 proto-oncogene as a prognostic and predictive marker in breast cancer: a paradigm for the development of other macromolecular markers--a review. *Gene*, 159, 19-27.

Ribatti, D., Vacca, A. (2008). The role of microenvironment in tumour angiogenesis. *Genes Nutr*, 3, 29-34.

Ribeiro, U. Jr., Posner, M.C., Safatale-Ribeiro, A.V., Reynolds, J.C. (1996). Risk factors for squamous cell carcinoma of the oesophagus. *Br J Surg*, 83, 1174-1185.

Robinson, C.J., Stringer, S.E. (2001). The splice variants of vascular endothelail growth factor (VEGF) and their receptors. *J Cell Sci*, 114, 853-65.

Roche Applied Science, Technical Note No. LC 10/update (2003). Overview of lightcycler quantification methods. pp. 1-16. Mannheim, Germany. Roche Diagnostics GmbH.

Roche Diagnostics (2001). Lightcycler relative quantification software.

Roche Molecular Biochemicals ME (2000). Lightcycler operator's manual: version 3.5. Mannheim, Germany, Roche Diagnostics GmbH.

Roncalli, M., Bosari, S., Marchetti, A., Buttitta, F., Bossi, P., Graziani, D., Peracchia, A., Bonavina, L., Viale, G., Coggi, G. (1998). Cell cycle-related gene abnormalities and product expression in esophageal carcinoma. *Lab Invest*, 78, 1049-57.

Rose, E.F. (1973). Esophageal cancer in the Transkei: 1955-69. *J Natl Cancer Inst*, 51, 7-16.

Sadava, D.E. (1993). Cell biology. pp.444-454. Jones and Bartlett, Boston (USA).

Salomon, D.S., Brandt, R., Ciardiello, F., Normanno, N. (1995). Epidermal growth factor-related peptides and their receptors in human malignancies. *Crit Rev Oncol Hematol*, 19, 183-232.

Samantaray, S., Sharma, R., Chattopadhyaya, T.K., Datta Gupta, S., Ralhan, R. (2004). Increased expression of MMP-2 and MMP-9 in esophageal squamous cell carcinoma. *J Cancer Res Clin Oncol*, 130, 37-44.

Sammon, A.M. (1992). A case-control study of diet and social factors in cancer of the esophagus in Transkei. *Cancer*, 69, 860-5.

Sammon, A.M. (2007). Carcinogens and endemic squamous cancer of the oesophagus in Transkei, South Africa. Environmental initiation is the dominant factor; tobacco or other carcinogens of low potency or concentration are sufficient for carcinogenesis in the predisposed mucosa. *Med Hypotheses*, 69, 125-31.

Schonland, M., Bradshaw, E. (1969). Oesophageal Cancer in Natal Bantu: a review of 516 cases. *S Afr Med J*, 43, 1028-1031.

Segal, I., Reinach, S.G., de Beer, M. (1988). Factors associated with oesophageal cancer in Soweto, South Africa. *Br J Cancer*, 58, 681-6.

Senger, D.R., Galli, SJ, Dvorak, A.M., Peruzzi, C.A., Harvey, V.S., Dvorak, H.F. (1983). Tumour cells secrete a vascular permeability factor that promotes accumulation of ascites fluid. *Science*, 219, 983-5.

Shen, G.H., Ghazizadeh, M., Kawanami, O., Shimizu, H., Jin, E., Araki, T., Sugisaki, Y. (2000). Prognostic significance of vascular endothelial growth factor expression in human ovarian carcinoma. *Br J Cancer*, 83, 196-203.

Shibuya, M., Yamagushi, S., Yamane, A., Ikeda, T., Tojo, A., Matsushime, H., Sato, M. (1990). Nucleotide sequence and expression of a novel human receptor-type kinase (flt) closely related to the fms family. *Oncogene*, 5, 519-24.

Shih, C.H., Ozawa, S., Ando, N., Ueda, M., Kitajima, M. (2000). Vascular endothelial growth factor expression predicts outcome and lymph node metastasis in squamous cell carcinoma of the esophagus. *Clin Cancer Res*, 6, 1161-8.

Shima, I., Sasaguri, Y., Kusukawa, J., Yamana, H., Fujita, H., Kakegawa, T., Morimatsu, M. (1992). Production of matrix metalloproteinase-2 and metalloproteinase-3 related to malignant behaviour of esophageal carcinoma. A clinicopathologic study. *Cancer*, 70:2747-53.

Sieg, D.J., Hauck, C.R., Ilic, D., Klingbeil, C.K., Schaefer, E., Damsky, C.H, Schlaepfer, D.D. (2000). FAK integrates growth-factor and integrin signals to promote cell migration. *Nat Cell Biol*, 2, 249-256.

Sitas, F. (1992). National Cancer Registry of South Africa: Incidence of Histologically Diagnosed Cancer in South Africa, 1988. South African Institute for Medical Research, Johannesburg.

Slaton, J.W., Inoue, K., Perrotte, P., El-Naggar, A.K., Swanson, D.A., Fidler, I.J. et al. (2001). Expression levels of genes that regulate metastasis and angiogenesis correlate with advanced pathological stage of renal cell carcinoma. *Am J Pathol* 158:735-43.

Stamenkovic I. (2000). Matrix metalloproteinases in tumour invasion and metastasis. *Semin Cancer Biol*, 10, 415-33.

Stamenkovic I. (2003). Extracellular matrix remodelling: the role of matrix metalloproteinases. *J Pathol*, 200, 448-64.

Stearns, M., Stearns, M.E. (1996). Evidence for increased activated metalloproteinase 2 (MMP-2a) expression associated with human prostrate cancer progression. *Oncol Res*, 8, 69-75.

Stein, H.J., Brücher, B.L., Sendler, A., Siewert, J.R. (2001) .Esophageal cancer: patient evaluation and pre-treatment staging. *Surg Oncol*, 10, 103-111.

Stoner, G.D., Gupta, A. (2001). Etiology and chemoprevention of squamous cell carcinoma. *Carcinogenesis*, 22, 1737-46.

Strongin, A.Y., Collier, I., Bannikov, G., Marmer, B.L., Grant, G.A., Goldberg, G.I. (1995). Mechanism of cell surface activation of 72-kDa type IV collagenase. Isolation of the activated form of the membrane metalloprotease. *J Biol Chem*, 270, 5331-8.

Sugimachi, K., Ikebe, M., Kitamura, K., Toh, Y., Matsuda, H., Kuwano, H. (1993). Long-term results of esophagectomy for early esophageal carcinoma. *Hepatogastroenterology*, 40, 203-6.

Syrjänen, K. (2002). HPV infections and oesophageal cancer. *J Clin Pathol*, 55, 721-8.

Tabernero, J. (2007). The role of VEGF and EGFR inhibition: Implications for combining anti-VEGF and anti-EGFR agents. *Mol Cancer Res*, 5, 203-220.

Tabone, M.D., Landman-Parker, J., Arcil, B., Coudert, M.C., Gerota, I., Benbunan, M., Leverger, G., Dosquet, C. (2001). Are basic fibroblast growth factor and vascular endothelial growth factor prognostic indicators in pediatric patients with malignant solid tumours? *Clin Cancer Res*, 7, 538-43.

Takagi, I., Karasawa, K. (1982). Growth of squamous cell oesophageal carcinoma observed by serial esophagographies. *J Surg Oncol*, 21, 57-60.

Talvensaari-Mattila, A., Pääkkö, P., Höyhtyä, M., Blanco-Sequeiros, G., Turpeenniemi-Hujanen, T. (1998). Matrix Metalloproteinase-2 immunoreactive protein: a marker for aggressiveness in breast carcinoma. *Cancer*, 83, 1153-62.

Tanaka, A., Matsumura, E., Yosikawa, H., Toshihiro, U., Machidera, N., Kubo, R., Okuno, K., Koh, K., Watatani, M., Yasutomi, M. (1998). An evaluation of neural invasion in esophageal cancer. *Jpn J Surg*, 28, 873-878.

Tischer, E., Mitchell, R., Hartman, T., Silva, M., Gospodarowicz, D., Fiddes, J.C., Abraham, J.A. (1991). The human gene for vascular endothelial growth factor. Multiple protein forms are encoded through alternative exon splicing. *J Biol Chem*, 266, 11947-54.

Tokuraku, M., Sato, H., Murakami, S., Okada, Y., Watanabe, Y., Seiki, M. (1995). Activation of the precursor of gelatinase A/72 kDa type IV collagenase/MMP-2 in lung carcinomas correlates with the expression of membrane-type matrix metalloproteinase (MT-MMP) and with lymph node metastasis. *Int J Cancer*, 64, 355-9.

Tsujii, M., Kawano, S., Tsuji, S., Sawaoka, H., Hori, M., DuBois, R.N. (1998). Cyclo-oxygenase regulates angiogenesis induced by colon cancer cells. *Cell*, 3, 705-16.

Tuyns, A. J., Pequignot, G., and Abbatucci, J. S. (1979). Oesophageal cancer and alcohol consumption: importance of type of beverage. *Int J Cancer* 23, 443-447.

Tzahar, E., Waterman, H., Chen, X., Levkowitz, G., Karunagaran, D., Lavi, S., Ratzkin, B.J., Yarden, Y. (1996). A hierarchical network of interreceptor interactions determines signal transduction by Neu differentiation factor/neuregulin and epidermal growth factor. *Mol Cell Biol*, 6, 5276-87.

Underwood, J.C.E. (2000). General and surgical pathology. 3rd edn. Chapter 10-11, pp. 202-262, Churchill Livingstone, UK.

University of Pretoria (2006). Microarray laboratory training workshop. pp7-21.

Valasek, M.A., Repa, J.J. (2005). The power of real time PCR. *Advan Physiol Educ*, 21, 151-159.

Vallböhmer, D., Lenz, H.-J. (2006). Predictive and prognostic molecular markers in outcome of esophageal cancer. *Dis Esophagus*, 19, 425-432.

van Heerden, W.F., van Rensburg, E.J., Hemmer, J., Raubenheimer, E.J., Englebrecht, S. (1998). Correlation between p53 gene mutation, p53 protein labeling and PCNA expression in oral squamous cell carcinomas. *Anticancer Res*, 18, 237-40.

van Rensburg, S.J. (1981). Epidemiologic and dietary evidence for a specific nutritional predisposition to esophageal cancer. *J Natl Cancer Inst*, 67, 243-51.

van Rensburg, S.J., Bradshaw, E.S., Bradshaw, D., Rose, E.F. (1985) Oesophageal cancer in Zulu men, South Africa: a case-control study. *Br J Cancer*, 51, 399-405.

Vincenti, V., Cassano, C., Rocchi, M., Persico, G. (1996). Assignment of the vascular endothelial growth factor gene to human chromosome 6p21.3. *Circulation*, 93, 1493-5.

Visse, R., Nagase, H. (2003). Matrix metalloproteinases and tissue inhibitors of metalloproteinases: structure, function and biochemistry. *Circ Res*, 92, 827-39.

Vu, T.H., Werb, Z. (2000). Matrix metalloproteinases: effectors of development and normal physiology. *Genes Dev*, 14, 2123-33.

Watanabe, H., Jass, J.R., Sobin L.H. Eds. (1990). Histological typing of oesophageal and gastric tumours. 2nd ed. Springer-Verlag, Berlin (Germany).

Weinberg, R.A. (1994). Oncogenes and tumour Suppressor Genes. *CA Cancer J Clin*, 44, 160-170.

Whitaker, J.A., Bishop, R. (1979). Scleroderma with carcinoma of the esophagus. Case report. *Am J Gastroenterol*, 71, 496-500.

WHO (World health Organization) (1997), World Health Report 1997: Conquering suffering, Enriching humanity (World Health Report). World health organization, Geneva (Switzerland).

Wikstrand, C.J., Hale, L.P., Batra, S.K., Hill, M.L., Humphrey, P.A., Kurpad, S.N., McLendon, R.E., Moscatello, D., Pegram, C.N., Reist, C.J., et al. (1995). Monoclonal antibodies against EGFRvIII are tumour specific and react with breast and lung carcinomas and malignant gliomas. *Cancer Res*, 55 3140-8.

Wittwer, C.T., Hermann, M.G., Moss, A.A., Rasmussen, R.P. (1977). Continuous fluorescence monitoring of rapid cycle DNA amplification. *Biotechniques*, 22, 130-138.

Wong, L.M., Medrano, J.F. (2005). Real-time PCR for mRNA quantitation. *Biotechniques*, 39, 75-85.

www.mrc.ac.za/promec/cancerresults.pdf. Accessed on 02/03/2008.

www.ncbi.nlm.nih.gov/.../probe/doc/TechPCR.shtml. Accessed on 04/02/2008.

www.probelibrary.com. Accessed on 02/09/2005.

Xia, W., Lau, Y.K., Zhang, H.Z., Xiao, F.Y., Johnston, D.A., Liu, A.R., Li, L., Katz, R.L., Hung, M.C. (1999) Combination of EGFR, HER-2/neu, and HER-3 is a stronger predictor for the outcome of oral squamous cell carcinoma than any individual family members. *Clin Cancer Res*, 5:4164-74.

Xu, J., Rodriguez, D., Petitclerc, E., Kim, J.J., Hangai, M., Moon, Y.S., Davis, G.E., Brooks, P.C. (2001). Proteolytic exposure of a cryptic site within collagen type IV is required for angiogenesis and tumour growth in vivo. *J Cell Biol*, 154, 1069-79.

Yamada, I., Izumi, Y., Kawano, T., Yoshino, N., Tetsumura, A., Kumagai, J., Shibuya, H. (2006). Esophageal Carcinoma: evaluation with high-resolution three dimensional constructive interference in steady state MR imaging in vitro. *J Magn Reson Imaging*, 24, 1326-32.

Yang, C.S. (1980). Research on esophageal cancer in China: a review. *Cancer Res*, 40, 2633-44.

Yang, W., Klos, K., Yang, Y., Smith, T.L., Shi, D., Yu, D. (2002). ErbB2 overexpression correlates with increased expression of vascular endothelial growth factors A, C and D in human breast carcinoma. *Cancer*, 94, 2855-61.

Yarden Y. (2001) Biology of HER2 and its importance in breast cancer. *Oncology*, 61, 1-13.

Yarden, Y. (2001). The EGFR family and its ligands in human cancer. signalling mechanisms and therapeutic opportunities. *Eur J Cancer*, 37, S3-8.

Yoshizawa, T., Yamashita, A., Luo, Y. (1994). Fumonisin occurrence in corn from high- and low-risk areas for human esophageal cancer in China. *Appl Environ Microbiol*, 60, 1626-9.

Yu, C., Zhou, Y., Miao, X., Xiong, P., Tan, W., Lin, D. (2004). Functional haplotypes in the promoter of matrix metalloproteinase-2 predict risk of the occurrence and metastasis in esophageal cancer. *Cancer Res*, 64, 7622-8.

Yu, J., Shannon, W.D., Watson, M.A., McLeod, H.L. (2005). Gene expression profiling of the Irinotecan pathway in colorectal cancer. *Clin Cancer Res*, 11, 2053-2062.

Yu, M.C., Garabrant, D.H., Peters, J.M., Mack, T.M. (1988). Tobacco, alcohol, diet, occupation, and carcinoma of the esophagus. *Cancer Res*, 48, 3843-8.

Yudoh, K., Kanamori, M., Ohmori, K., Yasuda, T., Aoki, M., Kimura, T. (2001). Concentration of vascular endothelial growth factor in the tumour tissue as a prognostic factor of soft tissue sarcomas. *Br J Cancer*, 84, 1610-5.

Zhang, D., Sliwkowski, M.X., Mark, M., Frantz, G., Akita, R., Sun, Y., Hillan K., Crowley, C., Brush, J., Godowski, P.J. (1997). Neuregulin-3 (NRG-3): a novel neural tissue-enriched protein that binds and activates ErbB4. *Proc Natl Acad Sci U S A*, 94, 9562-7.

zur Hausen, H. (1999). Immortalization of human cells and their malignant conversion by high risk human papillomavirus genotypes. *Semin Cancer Biol*, 9, 405-11.